JAAVSO

Volume 39
Number 2
2011

The Journal of the American Association of Variable Star Observers

Light Curve of the Eccentric Eclipsing Binary GSC 3152-1202

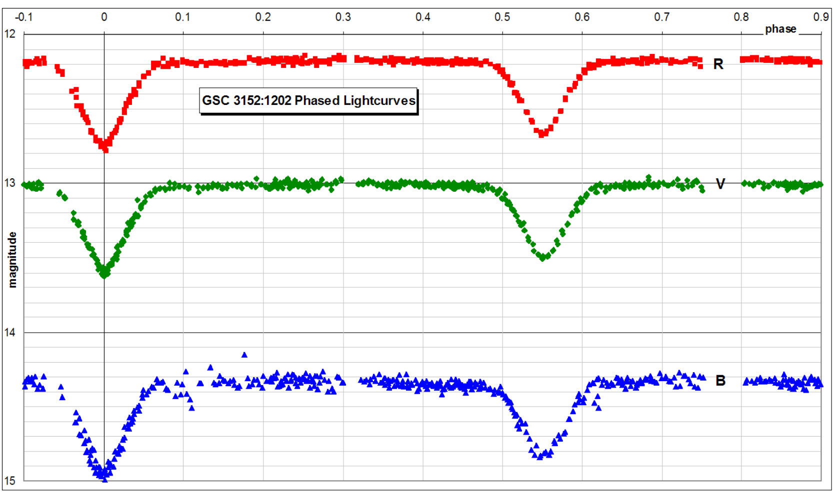

Light curve of GSC 3152:1202 in B-, V-, and R-bands.

see page 170

Also in this issue...

- The Ross Variable Stars Revisited
- δ Scuti Behavior Detected in HD 349422
- Recent Minima of 146 EB Stars

Complete table of contents inside...

THE AMERICAN ASSOCIATION OF VARIABLE STAR OBSERVERS
FOUNDED 1911

49 Bay State Road
Cambridge, MA 02138
U. S. A.

ISSN 0271-9053

JAAVSO

The Journal of
The American Association
of Variable Star Observers

Volume 39
Number 2
2011

49 Bay State Road
Cambridge, MA 02138
U. S. A.

ISSN 0271-9053

The *Journal of the American Association of Variable Star Observers* is a refereed scientific journal published by the American Association of Variable Star Observers, 49 Bay State Road, Cambridge, Massachusetts 02138, USA. The *Journal* is made available to all AAVSO members and subscribers.

In order to speed the dissemination of scientific results, selected papers that have been refereed and accepted for publication in the *Journal* will be posted on the internet at the *eJAAVSO* website as soon as they have been typeset and edited. These electronic representations of the *JAAVSO* articles are automatically indexed and included in the NASA Astrophysics Data System (ADS). *eJAAVSO* papers may be referenced as *J. Amer. Assoc. Var. Star Obs., in press,* until they appear in the concatonated electronic issue of *JAAVSO*. The *Journal* cannot supply reprints of papers.

Page Charges

Unsolicited papers by non-Members will be assessed a charge of $15 per published page.

Instructions for Submissions

The *Journal* welcomes papers from all persons concerned with the study of variable stars and topics specifically related to variability. All manuscripts should be written in a style designed to provide clear expositions of the topic. Contributors are strongly encouraged to submit digitized text in MS WORD, LATEX+POSTSCRIPT, or plain-text format. Manuscripts may be mailed electronically to journal@aavso.org or submitted by postal mail to *JAAVSO*, 49 Bay State Road, Cambridge, MA 02138, USA.

Manuscripts must be submitted according to the following guidelines, or they will be returned to the author for correction:

Manuscripts must be:
1) original, unpublished material;
2) written in English;
3) accompanied by an abstract of no more than 100 words.
4) not more than 2,500–3,000 words in length (10–12 pages double-spaced).

Figures for publication must:
1) be camera-ready or in a high-contrast, high-resolution, standard digitized image format;
2) have all coordinates labeled with division marks on all four sides;
3) be accompanied by a caption that clearly explains all symbols and significance, so that the reader can understand the figure without reference to the text.

Maximum published figure space is 4.5" by 7". When submitting original figures, be sure to allow for reduction in size by making all symbols and letters sufficiently large.

Photographs and halftone images will be considered for publication if they directly illustrate the text.

Tables should be:
1) provided separate from the main body of the text;
2) numbered sequentially and referred to by Arabic number in the text, e.g., Table 1.

References:
1) References should relate directly to the text.
2) References should be keyed into the text with the author's last name and the year of publication, e.g., (Smith 1974; Jones 1974) or Smith (1974) and Jones (1974).
3) In the case of three or more joint authors, the text reference should be written as follows: (Smith *et al.* 1976).
4) All references must be listed at the end of the text in alphabetical order by the author's last name and the year of publication, according to the following format:
   Brown, J., and Green, E. B. 1974, *Astrophys. J.*, **200**, 765.
   Thomas, K. 1982, *Phys. Report*, **33**, 96.
5) Abbreviations used in references should be based on recent issues of the Journal or the listing provided at the beginning of *Astronomy and Astrophysics Abstracts* (Springer-Verlag).

Miscellaneous:
1) Equations should be written on a separate line and given a sequential Arabic number in parentheses near the right-hand margin. Equations should be referred to in the text as, e.g., equation (1).
2) Magnitude will be assumed to be visual unless otherwise specified.
3) Manuscripts may be submitted to referees for review without obligation of publication.

Journal of the American Association of Variable Star Observers
Volume 39, Number 2, 2011

A Message From the Editor

John R. Percy
Department of Astronomy and Astrophysics, University of Toronto, Toronto, ON M5S 3H4, Canada; john.percy@utoronto.ca

Happy Birthday, AAVSO! The year 2011 has been a very special one for the AAVSO, being the hundredth anniversary of its founding, as a small group of enthusiastic variable star observers, in 1911.

The AAVSO centennial was marked in several ways, notably by the publication of its official history, *Advancing Variable Star Astronomy*, by Drs. Tom Williams and Michael Saladyga, by a joint meeting with the American Astronomical Society (AAS) in Boston in May, and by an extended Centennial Fall Meeting in Woburn in October. The invited history and science papers from these meetings, and the abstracts of contributed papers, will be published in a special issue of the *JAAVSO*, to be published in June 2012. This issue will also include a set of invited short reviews of the state of variable star science in 2011, including how AAVSO observations have contributed.

The centennial year has also been a year of continued scientific and educational progress for the AAVSO, as you will learn from the Director's Reports which are found on the AAVSO website. Among other things, 2011 marked the culmination of the Citizen Sky project, which was focussed on the 2009–2011 eclipse of epsilon Aurigae. This exemplary project attracted, trained, and mentored many new observers, who were motivated by the opportunity to help solve the mysteries of this bright binary star system. Another special issue of the *JAAVSO*, in 2012, will be devoted to papers arising from this project.

Other papers submitted to the *JAAVSO* in 2011 and 2012 will continue to be published in regular issues. As usual, all papers will be made available on-line as soon as they have been received, reviewed, edited, and formatted.

At this time, I would like to thank Drs. Aaron Price, Matt Templeton, and Tom Williams for their work in organizing the Citizen Sky, science, and history papers for these special issues, and Dr. Michael Saladyga and his colleagues at AAVSO Headquarters for doing most of the real work in producing the *JAAVSO*. We recognize that AAVSO staff have gone far beyond the call of duty to organize these Centennial events; they have been much appreciated, both scientifically and socially. Thanks also to the *JAAVSO* Editorial Board for their ongoing advice, to the anonymous referees for their work in maintaining the high standards of the *JAAVSO*, to the authors for sharing their research and scholarship with us, and to you the readers for making it all worthwhile.

Enjoy!

δ Scuti Behavior Detected in HD 349422

Garrison Turner
Ronald Kaitchuck
Department of Physics and Astronomy, Ball State University, Muncie, IN 47306; ghturner@bsu.edu

Received February 9, 2011; revised June 13, 2011; accepted June 16, 2011

Abstract Evidence for variability in the star HD 349422 is presented. Low-amplitude variations seen in the Bessel B and Bessel V filters are presented for three nights on two different telescopes. A period of 0.0400 day in the B and 0.0413 day in the V filters, respectively, were determined. These periods agree within the determined uncertainty. The spectral type from the literature is given as F0. It is therefore proposed that due to the period and spectral type that HD349422 is a member of the δ Scuti family.

1. Introduction

HD 349422 has magnitudes of 9.19 in the B and 8.90 in the V bands, with coordinates R.A. 18^{h} 50^{m} 50.2671^{s}, Dec. +20° 52' 16.479" (2000). The HD catalogue spectral type is given as F0 (Nesterov *et al.* 1995). The star was first noticed to be variable when observing the eclipsing binary AD Her as part of a survey of eclipsing binaries. HD 349422 was used as the comparison star and the variability was noticed. The light curves generated from subsequent observations suggest amplitude of about 0.012 magnitude in both the B and V filters. δ Scuti stars are generally low-amplitude, short-period variables with spectral types ranging from A to F. Periods range between 0.02 and about 0.3 day. Amplitudes can either be large (> 0.30 magnitude) or small, usually on the order of tens of a millimag. The first class represents a minority of δ Scuti variables, referred to as High Amplitude δ Scuti stars, or HADS. The second class represents the majority of δ Scuti stars. They are found at the intersection of the main sequence and the instability strip. Breger (2000) estimates that between 1/3 and 1/2 of all stars at this intersection show variability between 0.003 and 0.010 magnitude. The detection of new δ Scuti stars should increase rapidly over the next years as high-precision photometric campaigns increase, especially with projects such as Kepler and CoRot. Percy (2007) and Templeton (2004) provide general overviews of δ Scuti stars. For a detailed description on the current status of δ Scuti stars see Breger (2000).

2. Observations

Observations of HD 349422 were done with two different telescopes.

All data were reduced using IRAF (Tody 1993) for bias, dark, and flat-field correction, while AIP4WIN (Berry and Burnell 2006) was used to perform the differential photometry. As AIP4WIN processes each image, a photometric error is assigned to each measurement. The errors for the variable and comparison star are obtained by a calculation involving camera gain, camera read noise, dark current, and the sky background. These errors were then added in quadrature to obtain the errors for each delta magnitude.

Table 1 summarizes the dates, amplitudes of variability in each filter, and the average errors for the differential measurements. The quoted amplitudes are measured with the half-amplitude method.

The first data set was collected with a 0.6-meter Cassegrain telescope and an Apogee Alta CCD camera located at Cerro Tololo, Chile, operated by the SARA consortium (http://astro.fit.edu/sara/sara.html). The focal ratio of the telescope is *f*/13.5, giving a plate scale of 0.6 arc sec per pixel. The first set of observations was taken in the B with exposures ranging between ten and twenty seconds on the night of June 28, 2010 (UT). The observations on this night spanned a total of four hours with mean photometric error of about 0.0015 magnitude. The comparison star used for these observations was HD 349426 (R.A. 18^h 50^m 13.317^s Dec +20° 45' 01.634" (2000)) with a field star (R.A. 18^h 50^m 18.53^s Dec +20° 45' 30" (2000)) serving as the check star. The standard deviations for the variable-comp delta mag data and the check-comp delta mag data were 0.008 and 0.004 magnitude, respectively.

The second set of observations was collected over two nights at the Ball State University observatory using a 0.4-meter Schmidt-Cassegrain telescope with an SBIG ST-10 CCD camera on August 26 and 27, 2010 (UT) (the observations spanned two hours on the 26th and three and 3½ hours on the 27th). The *f*/6 focal ratio gave a plate scale of 0.58 arc sec per pixel. These observations were done in the V with exposures of fifty seconds. Due to a larger field of view with the second set, a brighter comparison star was available. This allowed better signal-to-noise ratios per exposure. The mean photometric errors were 0.0014 and 0.0016, respectively. Choosing a second comparison star this way ensures the variability was due to the suspected variable and not the original comparison star. It is becoming increasingly important for the photometry technique to ensure comparison stars are not low-amplitude variables. This is becoming more difficult with better CCD technology. This is the reason many new δ Scuti and γ Doradus stars are being found (this case is a good example). The comparison star for this set of observations was HD 349418 (R.A. 18^h 51^m 42.86^s Dec +20° 52' 23.0" (2000)), while HD 349420 served as the check star (R.A. 18^h 51^m 04.92^s Dec +20° 48' 14.8" (2000)).

3. Light curves

Figures 1 and 2 show the differential light curves of HD 349422 for the night of June 28, 2010 (UT), in the B filter and the night of August 26, 2010 (UT), in the V filter. The light curves show a variation of about 0.012 magnitude in both the B and the V filters. Periods were determined using the PERANSO software package (Vanmunster 2007) with the Lomb-Scargle method (Lomb 1976; Scargle 1982). Figures 3 and 4 show the power-spectra produced. The data were searched for periods between 0.01 and 0.3 day in both filters, giving 0.0400 + 0.0022 day in B and 0.0413 + 0.0007 day in V (with the twenty-four hour aliases in V), thus giving good agreement within the determined uncertainties. Figure 3 indicates a second peak in the B filter at 0.0300 day. This is a possible signature of multi-periodicity, yet it is unconfirmed at this time. This peak is also evident after pre-whitening, seen in Figure 5, which is a power-spectrum of the B data after removing the 0.0400 day period. Figure 4 shows a secondary peak in the V filter at 0.0286 day. Figure 6 shows the power-spectrum of the V data with the 0.0413 day peak removed. The 0.0286 day peak is not evident after removing the dominant period. However, further observations are encouraged to completely determine whether this object is multi-modal. Figure 7 shows the B-filter data phased onto the dominant period.

4. Conclusions

Due to the short periodicity determined for HD 349422 and given its spectral type, it is proposed that this object be included as a member of the δ Scuti family. The F0 spectral classification falls right into the δ Scuti range of spectral types. This object was observed with two different comparison stars due to observations being done using telescopes with different light-gathering powers and different fields of view. The determined periods for both filter sets gave agreement to within the given uncertainties. However, only a small number of complete cycles and short observational time spans were obtained. The dominant period, while in agreement between the B and V filters, is still rather uncertain. Further observations are encouraged to precisely determine the dominant period and whether other periods are photometrically detectable.

5. Acknowledgements

This work was funded by the Indiana Space Grant Consortium and telescope time was provided by the SARA consortium. We would also like to thank an anonymous referee for making several helpful comments.

References

Berry, R., and Burnell, J. 2006, "Astronomical Image Processing Software," provided with *The Handbook of Astronomical Image Processing*, Willmann-Bell, Richmond, VA.

Breger, M. 2000, in *Delta Scuti and Related Stars, Reference Handbook and Proceedings of the 6th Vienna Workshop in Astrophysics, held in Vienna, Austria, 4–7 August, 1999*, eds. M. Breger and M. Montgomery, ASP Conf. Ser. 210, Astron. Soc. Pacific, San Francisco, 3.

Lomb, N. R. 1976, *Astrophys. Space Sci.*, **39**, 447.

Nesterov, V. V., Kuzmin, A. V., Ashimbaeva, N. T., Volchkov, A. A., Roeser, S., and Bastian, U. 1995, *Astron. Astrophys., Suppl. Ser.*, **110**, 367.

Percy, J. R. 2007, *Understanding Variable Stars*, Cambridge Univ. Press, New York.

Scargle, J. D. 1982, *Astrophys. J.*, **263**, 835.

Templeton, M. 2004, www.aavso.org/vsots_delsct.

Tody, D. 1993, in *Astronomical Data Analysis Software and Systems II*, eds. R. J. Hanisch, R. J. V. Brissenden, and J. Barnes, ASP Conf. Ser., 52, Astron. Soc. Pacific, San Francisco,173.

Vanmunster, T., 2007, PERANSO period analysis software, http://www.peranso.com.

Table 1. Summary of observations for HD 349422.

Filter	*UT Date*	*HJD Range*	*Amplitude (mag)*	*Mean Error (mag)*
B	2010 June 28	2455375.6795 – 0.8455	0.012	0.0015
V	2010 August 26	2455434.71077 – 0.7929	0.012	0.0014
V	2010 August 27	2455435.5615 – 0.7020	0.012	0.0016

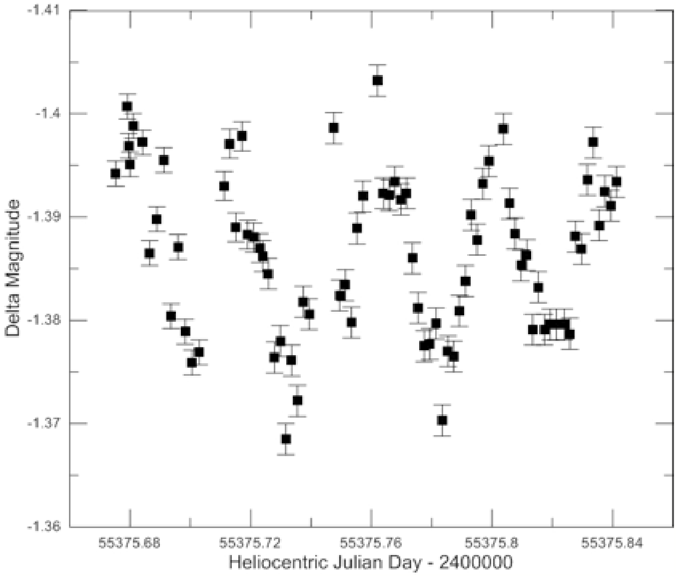

Figure 1. ΔB magnitudes of HD 349422 on the night of 2010 June 28 (UT).

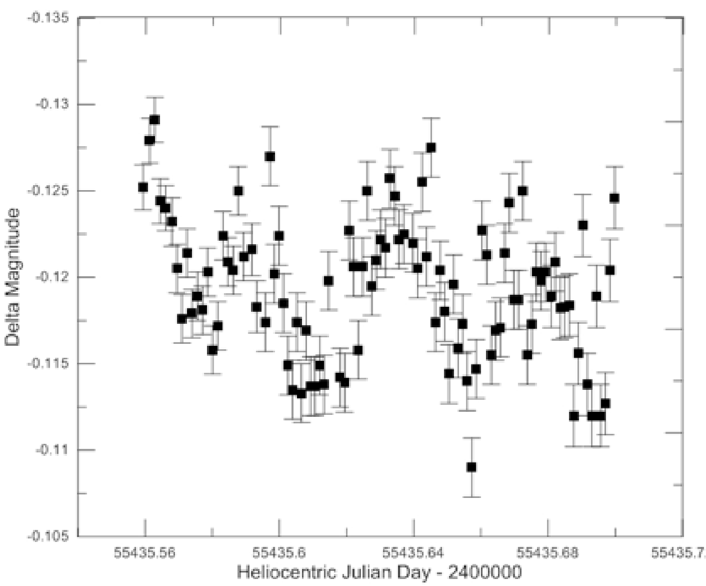

Figure 2. ΔV magnitudes of HD 349422 on the night of 2010 August 27 (UT).

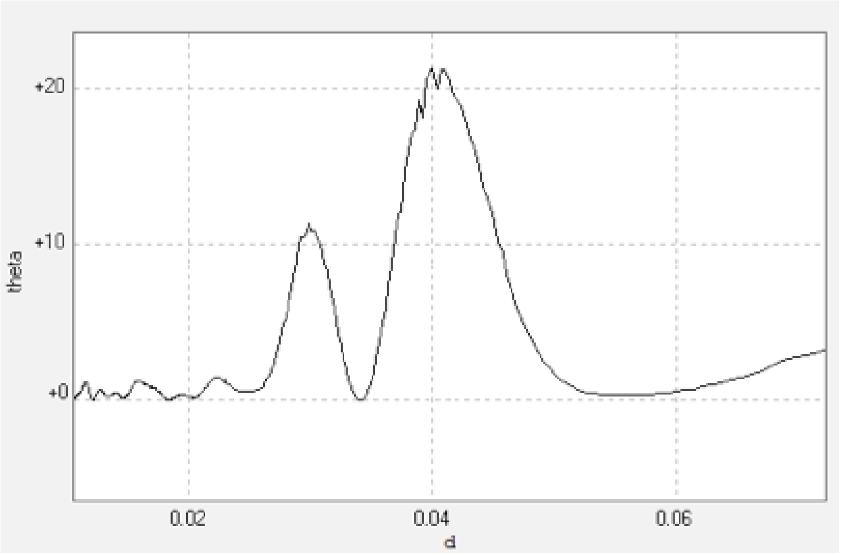

Figure 3. The power spectrum analysis of the differential B magnitudes of HD 349322 for 2010 June 28 (UT).

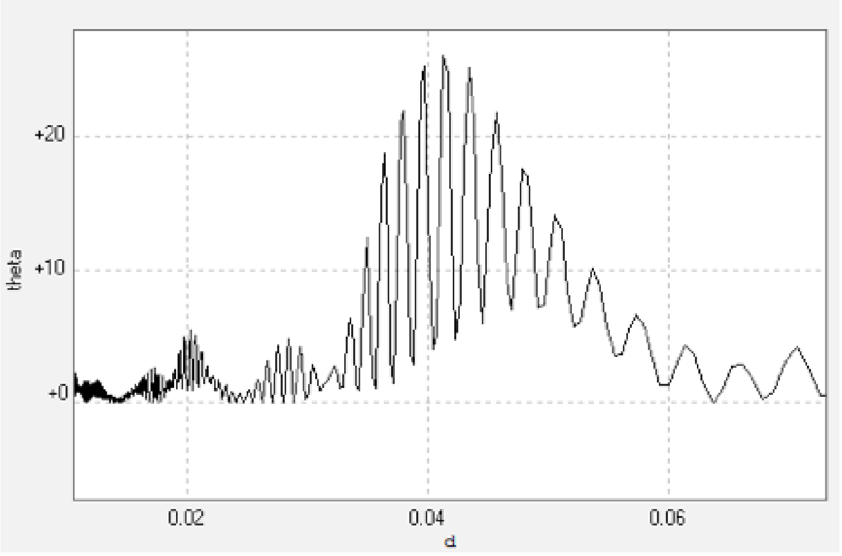

Figure 4. The power spectrum analysis of the differential V magnitudes of HD 349422 for the nights of 2010 August 26, 27 (UT).

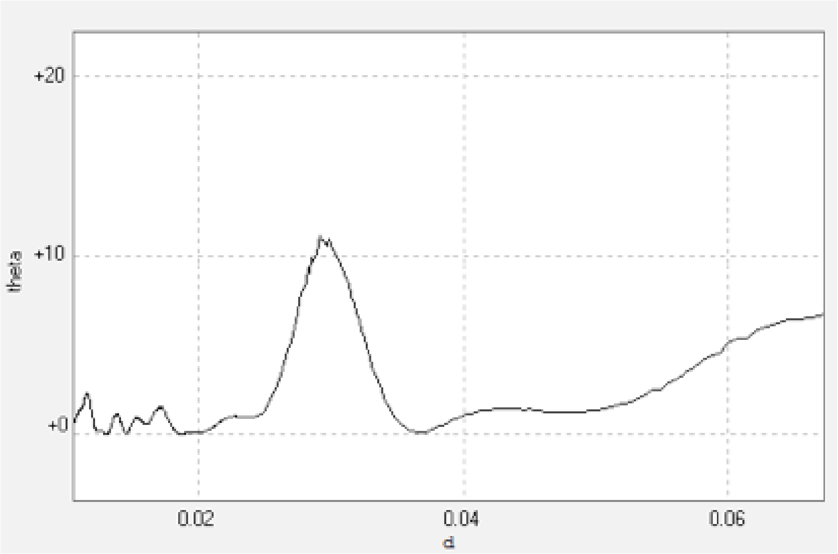

Figure 5. Results of period-searching the B data after removing the 0.0400 day period.

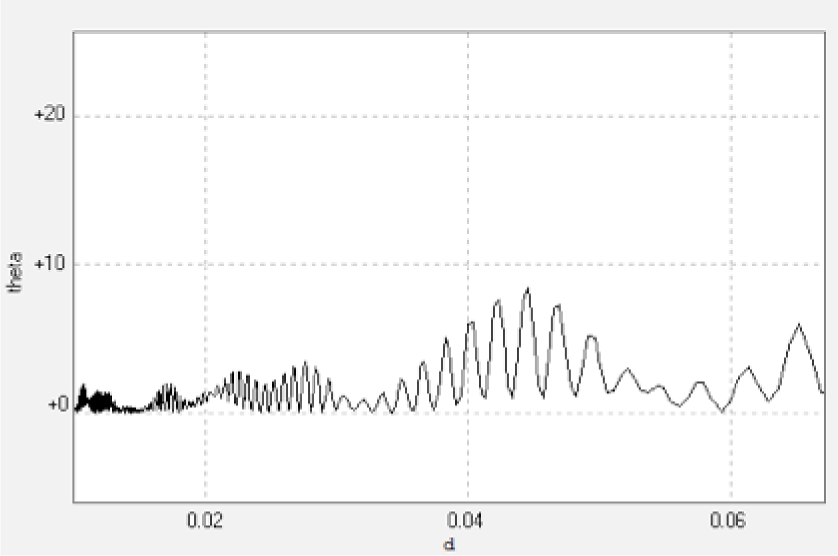

Figure 6. Results of period-searching the V data after removing the 0.0413 day period.

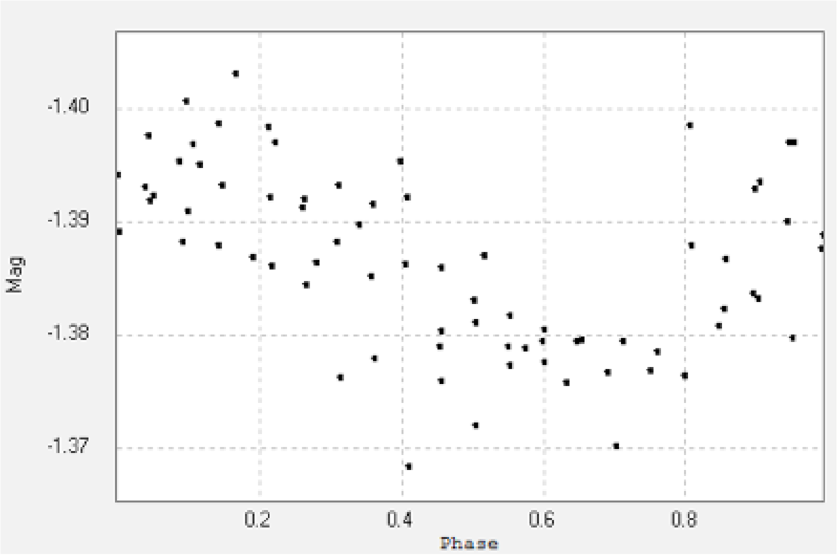

Figure 7. The differential B magnitudes of HD 349422 phased on the 0.0400 day period.

Periodicity Analysis of the Semiregular Variable Star EV Aquarii

Emil Terziev
John R. Percy
Department of Astronomy and Astrophysics, University of Toronto, Toronto, ON M5S 3H4, Canada; address correspondence to john.percy@utoronto.ca

Arne A. Henden
AAVSO, 49 Bay State Road, Cambridge, MA 02138; arne@aavso.org

Received May 5, 2011; revised September 8, 2011; accepted September 13, 2011

Abstract EV Aquarii is a variable star which was formerly misclassified as a cataclysmic variable, but photometric observations and colour indices have since indicated that it is most likely a semiregular M giant. The authors of this paper have used self-correlation analysis and Fourier analysis to determine the variability profile of the star. Data from the AAVSO International Database, the All-Sky Automated Survey, The Amateur Sky Survey, and co-author Arne Henden were used. The period of variation has been found to be 123.6 days ± 2.1 days. The amplitude of this variation is not constant; it changes with time between approximately 0.4 and 1.0 magnitude. There were no indications of a longer secondary period, though there has been observed an instance of a transient period of variation on a shorter timescale of about 40 days. There was no evidence found of periodic variation of the color differences.

1. Introduction

This paper arose as a result of a message, on the Citizen Sky distribution list, from co-author Henden, who is Director of the AAVSO. Over the course of his many years as an observer, he had accumulated a list of about forty projects which would be suitable for an experienced amateur astronomer or student. Co-author Terziev, who is an undergraduate Astronomy and Physics major, was looking for such a project. Since he had some experience in analyzing red semiregular variables, this project on EV Aquarii (R. A. $21^h\ 06^m\ 17.87^s$, Dec. +00° 52' 43.9" (J2000)) seemed promising. Henden's file on this star (Henden 2011) included over a decade of email correspondence and observations.

This variable was initially called CSV 5342 and a finding chart was published in 1971 (Tsesevich and Kazanasamas 1971). There followed a series of confusions that often arise in variable star research, including a rather small and complex finder chart that may have led to a misidentification and inclusion in the second edition of the *Catalog and Atlas of Cataclysmic Variables* (Downes *et al.* 1997). Finally in 1999, Henden obtained observations which confirmed that the star was a red (*B–V* = +1.5) variable with a small amplitude and a longish period. He also provided a comparison star sequence for other observers to use.

Several sources of observational data were used in order to determine the variability profile and calculate the period of the star. One set of observations came from the American Association of Variable Star Observers (AAVSO), containing both Visual and *V*-band measurements. Another was obtained from the All Sky Automated Survey (ASAS), and was imaged in the *V* band. Observations of *V–I* color indices from The Amateur Sky Survey (TASS) were also used. Finally, we used Henden's personal observations, which were of the *V*-band magnitude and of color indices. Figure 1 shows light curves constructed from these datasets.

2. Discussion

We used two methods to analyze the data. The first was standard Fourier analysis of the data to produce frequency spectra of each dataset, using Period04 (Lenz and Breger 2005). The second was self-correlation analysis, which involves calculating the average differences in magnitude between all pairs of points in the dataset, and grouping them into bins according to the separation in time between the points. Points that are separated by multiples of the period manifest as minima in a self-correlation diagram. For a more detailed description of self-correlation analysis, consult Percy and Mohammed (2004).

To determine the period, we combined all of the *V*-band datasets, and performed Fourier analysis of the *V*-band and Visual observations. The spectra are presented in Figure 2.

The frequency of the most prominent peak in the Fourier transforms of each band gave us estimates of the period of 123.5 days ± 3.6 days (*V* band) and 123.7 days ± 2.6 days (Visual). The errors in frequency were calculated as the Half Width Half Max of the main peak, expressed as percentage errors in terms of the frequency of maximum amplitude, and the same percentage errors were applied to the corresponding period lengths. We calculated an average period, weighing each of the values we obtained by the inverse of their error. The average period was 123.6 days ± 2.1 days. Note that there are additional peaks of considerable amplitude on either side of the main frequency. However, they are separated from the main frequency by approximately 0.0027 (1/365) cycle per day. They are, in all likelihood, 1 cycle per year aliases of the main frequency. The alias structure responsible for the additional peaks can be seen in the spectral windows included in the same figure. Additionally, the frequency of maximum amplitude is actually double-peaked in the transforms of both the *V* band and Visual data. The companion peaks are at periods of 131.2 days ± 3.4 days (*V* band) and 129.7 days ± 3.1 days (Visual).

It can be seen in the light curves (Figure 1) that, while the star remains mostly periodic over the span of the observations, the amplitude of the brightness variations is not constant in time, and neither is the median magnitude around which the brightness oscillates. This implies that there could possibly be a longer period which governs these factors. Typically, the longer (secondary) period would be of the order of 10 times the shorter period (Nicholls *et al.* 2009). However, there are no prominent peaks in the Fourier transforms (Figure 2) at such low frequencies. We also performed self-correlation analysis looking for such secondary periods, and found none (Figure 3).

Since the amplitude of variation does not appear constant (it varies between approximately 0.5 magnitude and 1.0 magnitude in the light curves), we split the data into intervals of about 1,000 days (based on observational gaps), and calculated the amplitude in each interval separately. We were unable to use the AAVSO Visual data for amplitude determination, since the spacing of observations left gaps in the self-correlation diagrams, making the extrema hard to distinguish. The self-correlation diagrams of the *V*-band data can be seen in Figure 4. The repeating minima show that the periodic component of variation is very coherent. It is also possible to determine the average observation error of each dataset using self-correlation. Extrapolating the delta magnitudes to a delta time of 0 day would give us an approximation for the measurement error. We discovered that the AAVSO *V*-band data were accurate to about 0.05 magnitude, the AAVSO Visual data to about 0.15 magnitude, the ASAS *V*-band data to about 0.07 magnitude, and Henden's *V*-band data to about 0.01 magnitude.

To determine the amplitude from a self-correlation diagram, we took the average value of the maxima in the diagram and subtracted the average value of the minima. This difference is approximately 0.9 of the full amplitude of variation of the star. The values for the amplitude we obtained are summarized in Table 1.

We created phase diagrams using the average period we calculated (Figure 5). Again, the data were split into intervals of about 1,000 days to avoid excessive amplitude changes within each interval. The phase diagrams of each segment of observations show amplitudes similar to those obtained from self-correlation.

It should be noted that we found an instance of EV Aqr exhibiting transient periodic behavior on a shorter timescale. Figure 6 presents a light curve of a single observation season lasting approximately 250 days. During this season, there is an obvious cyclic behavior with a period of about 40 days. The self-correlation diagram in the same figure confirms this. The shorter period cannot be found in either the previous or the next observation season, so it must have been short lived.

We used 2MASS multiband observations (Skrutskie *et al.* 2006) and Henden's data to determine the star's colors. From Henden's data, we determined that the star's approximate colors are: $U–B = +1.2$, $B–V = +1.5$, $V–R = +1.4$ and $R–I = +1.9$. The 2MASS observations with A-quality flags revealed that the average $J–K$ color is +0.7. These values are typical of stars of this type; it is almost certainly an M giant. Henden had also taken time series *B–V* data, and we used *V–I* data from TASS. In Figure 7, we have plotted a phase diagram of Henden's observations from JD 2451810 to 2452172, comprising about three cycles of the main period. The observations are phased to our calculated average period of 123.6 days. The *V–I* phase diagram (phased to the same period) is also shown. The *V–I* colors were observed between JD 2452870 and 2453322, which is a length of time equal to about 3.7 cycles of variation. As Figure 7 reveals, the color differences are most likely random and do not vary systematically like the brightness does.

3. Conclusion

In summary, we found EV Aqr to be variable with a strong periodic component. The period of variation is 123.6 days ± 2.1 days. The amplitude of variation changes with time between about 0.4 and 1.0 magnitude. We found no conclusive indication of a longer secondary period. Such a period could potentially exist, but may be longer than the span of our data. We found that the star sometimes exhibits shorter transient periodic behavior. The star varies by about 0.1 in (*B–V*), but does not do so periodically.

4. Acknowledgements

We would like to thank T. Kato, M. Morel, G. Poyner, P. Schmeer, L. Shaw, and B. Sumner for private communications about this star, and the Ontario Work-Study Program for support. This publication makes use of data products from the Two Micron All Sky Survey, which is a joint project of the University of Massachusetts and the Infrared Processing and Analysis Center/California Institute of Technology, funded by the National Aeronautics and Space Administration and the National Science Foundation.

References

Downes, R., Webbink, R. F., and Shara, M. M. 1997, *Publ. Astron. Soc. Pacific*, **109**, 345.

Henden, A. A. 2011, http://www.aavso.org/sites/default/files/arne_projects/p024.evaqr.txt.

Lenz, P., and Breger, M. 2005, *Commun. Asteroseismology*, **146**, 53.

Nicholls, C. P., Wood, P. R., Cioni, M.-R. L., and Soszynski, I. 2009, *Mon. Not. Roy. Astron. Soc.*, **399**, 2063.

Percy, J. R., and Mohammed, F. 2004, *J. Amer. Assoc. Var. Star Obs.*, **32**, 9.

Skrutskie, M. F., *et al.* 2006, Astron. J., **131**, 1163.

Tsesevich, V. P., and Kazanasmas, M. S. 1971, *Atlas of Finding Charts of Variable Stars*, "Nauka," Moscow.

Table 1. Summary of measured amplitudes of variation of EV Aqr.

Observation Period (JD)	*Amplitude (d)*
2451800–2453000	0.99
2453100–2454100	0.51
2454200–2455200	0.45

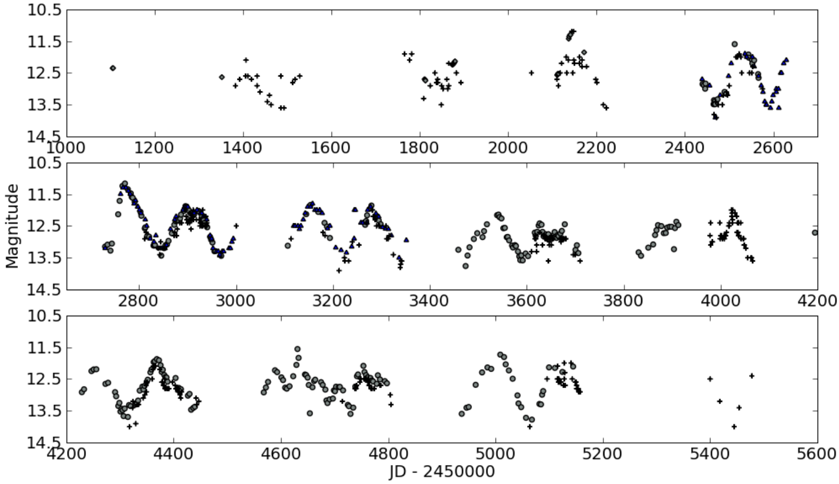

Figure 1. EV Aqr light curves: ASAS *V*-band data (open circles); AAVSO *V*-band data (triangles); Henden data (diamonds); AAVSO Visual data (plus-signs).

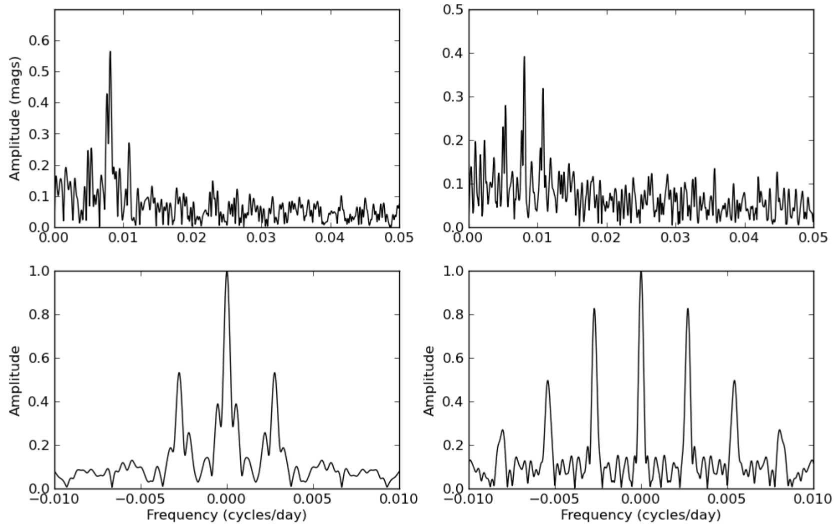

Figure 2. EV Aqr Fourier transforms: (top) and spectral windows (bottom) of *V*-band data (left) and Visual data (right).

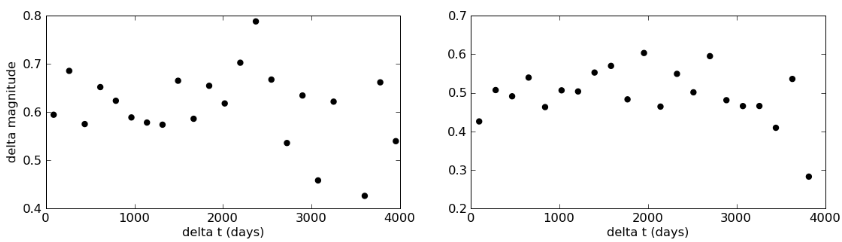

Figure 3. Self-correlation diagrams of EV Aqr *V*-band data (left) and Visual data (right).

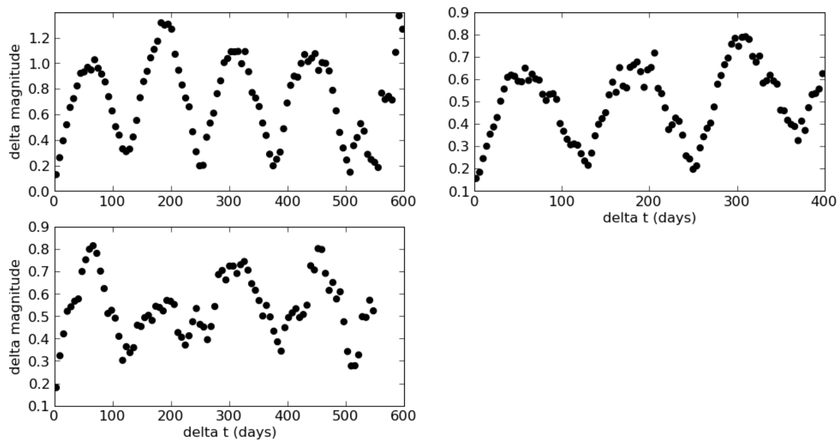

Figure 4. Self-correlation diagrams of EV Aqr *V*-band data: JD 2451800–2453000 (top left); JD 2453100–2454100 (top right); and JD 2454200–2455200 (bottom left).

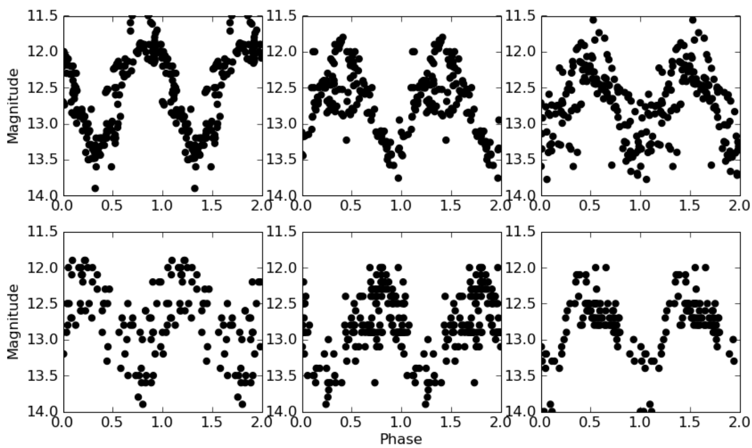

Figure 5. EV Aqr phase diagrams. Top row: *V*–band data, JD 2451800–2453000 (left), JD 2453100–2454100 (center), JD 2454200–2455200 (right). Bottom row: Visual data, JD 2451350–2452600 (left), JD 2452800–2454100 (center), JD 2454300–2455500 (right).

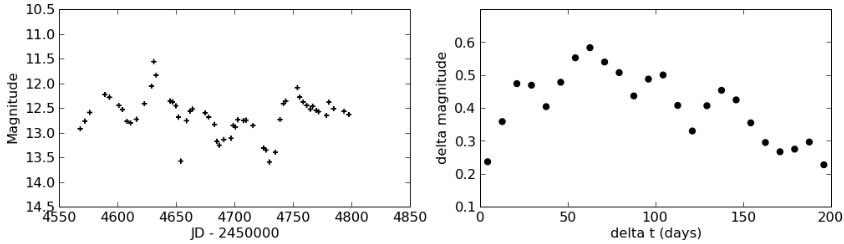

Figure 6. EV Aqr light curve of *V*-band data, JD 2454550–2454800 (left), and self-correlation diagram of the same observation season (right).

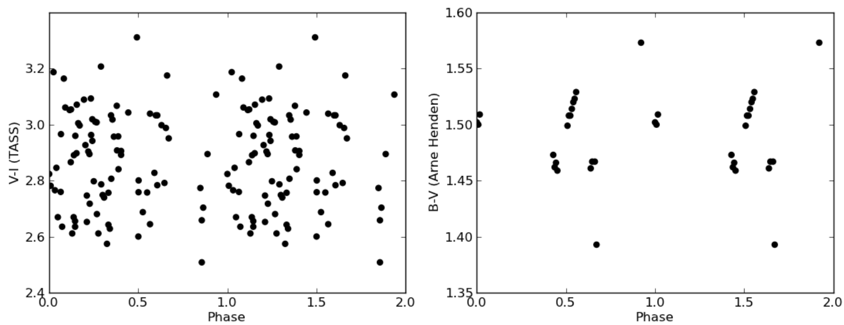

Figure 7. EV Aqr phase diagrams of *B–V* color indices from Henden data (left) and *V–I* color indices from TASS (right).

Light Curve of the Eccentric Eclipsing Binary GSC 3152-1202

Robert K. Buchheim
18 Altimira, Coto de Caza, CA 92679; rbuchheim@earthlink.net

Received February 25, 2011; accepted June 8, 2011

Abstract A complete light curve of this eccentric (~2.094d) eclipsing binary system has been determined, in *B*, *V*, and *R* bands. The primary and secondary minima are slightly different in depth, and the color index does not change during either primary or secondary eclipse. Newly-determined times of minimum confirm the previously-suspected rapid change in the orbital phase of the secondary minimum, implying significant apsidal motion.

1. Background

The star GSC 3152-1202 (J2000 coordinates: R.A. $20^h 27^m 17.3^s$, Dec. +37° 56' 26") is identified as an eccentric-orbit eclipsing binary in the catalogue of Bulut and Demircan (2007) on the basis of observations reported by Otero *et al.* (2006).

Kozyreva *et al.* (2009) reported *V*-band differential photometry light curves of the primary and secondary eclipses and times of both primary and secondary minima. They concluded that: the two stars must be nearly identical in terms of temperature and size; as inferred from the displacement of the secondary eclipse from the 0.5 phase, the orbit is eccentric; and their $T_{min,II}$ timings provide evidence for rapid change in the orbital phase of the secondary eclipse in the intervening decade between their observations and Otero's.

Broadband SuperWASP photometry (Pollaco *et al.* 2006) captured eclipses of this system, but no analysis of their times of minimum light has been reported.

Shortly before the preparation of this paper, Bloomer *et al.* (2011) published several recent times of minimum (including one that was also observed for this study).

Considering the rapid apsidal motion and the lack of absolute photometry, it seemed worthwhile to record the complete light curve in three bands (*B*, *V*, and *R*), and to make additional measurements of the times of minima to support future modeling of this system. To that end, nineteen nights during July–September 2010 were devoted to photometry of this target at the author's Altimira Observatory.

2. Observations

All observations were made at Altimira Observatory, Coto de Caza, California, using a 28-cm (=11-in) Schmidt-Cassegrain telescope operating at *f*/6.3, an SBIG ST-8XE CCD imager (non-anti-blooming), and photometric *B*-, *V*-, and *R*-band filters from Custom Scientific. The image scale is 1.1 arcsec/pixel, and typical seeing was between 2 to 3 arcsec. For each observing session, the filter wheel was cycled to provide an imaging sequence of R-R-V-V-B-B for four to eight hours per night. Exposure durations were one minute in *R*-band, two minutes in *V*-band, and five minutes in *B*- band. These provided typical signal-to-noise ratio (SNR) on the target of about 125:1 in *V*- and *R*- bands, and 50:1 in *B*-band. Comparison stars were all somewhat brighter than the target, hence presented higher SNR.

All images were examined for problems such as poor tracking, poor focus, cosmic ray hits, or aircraft trails affecting the stars of interest, and problematic images were not used in the photometric analysis. Also, any images exposed at high air mass ($X \geq 2$) were removed from the analysis. Many nights were "non-photometric," but the overall consistency of the results demonstrates that modest light pollution and high (or variable) extinction did not adversely affect the resulting differential photometry. The target field, identifying the comparison stars used, is shown in Figure 1.

Comparison star colors and standard magnitudes were assessed in two ways: 1) On two clear and stable nights at Altimira Observatory, the target field-of-view, one or two Landolt fields, and the AAVSO field of M-27 (at essentially the same air mass as the target) were imaged. Using the known transforms for Altimira Observatory, the standard magnitudes of the comparison stars were determined. 2) The "Big Mak" telescope at Tzec Maun Observatory, New Mexico Skies, near Mayhill, New Mexico, was used to image the target field and two Landolt fields, to calibrate the comparison stars. The resulting comparison star properties are given in Table 1.

Differential photometry (using the ensemble of comparison stars) was done with the software package MPO CANOPUS/PHOTORED using a circular measuring aperture of 13 pixels diameter (≈ 14 arc-sec), and sky annulus surrounding the measuring aperture. The stability of the comparison stars was checked by intercomparing them throughout the observing season. Comparison stars 1, 2, 3, and 5 showed no evidence of variability throughout the duration of this project.

Instrumental-band photometry ("var-comp") was translated into standard *B*-, *V*-, and *R*-band magnitudes by use of the calibrated comparison star magnitudes and colors, and the known transformation coefficients of the Altimira Observatory equipment (previously determined by reference to Landolt standard star fields).

3. Times of Minimum

In the course of this observing campaign, three primary minima and one secondary minimum were recorded. The times of minimum based on the method of Kwee and vanWoerden (1956) are given in Table 2.

Light curve data for this star were extracted from the recently-released SuperWASP database (Butters *et al.* 2010) for three nights that contain eclipses (two primary and one secondary eclipse). From these data, the times of minimum light were determined using the Kwee-van Woerden method, and are given in Table 3.

4. O–C evidence

Otero *et al.* (2006) reported $P_{Otero} = 2.09372$ d, HJD_{0min} I = 2451478.596 (UT date = 1999-10-27), and indicated that the orbital phase of the secondary minimum was $\varphi_{sec} \approx 0.489$; however, they also noted that their reported HJD_0 might refer to the secondary minimum. Based on Kozyreva's data and the data presented here, it appears that Otero's $HJD_{0min\ I}$ was, indeed, the primary minimum. From these data a reference time was establishedfor secondary minima as $HJD_{0min\ II} = HJD_{0min\ I} + 0.489\ P_{Otero} = 2451479.6198$.

Kozyreva *et al.* (2009) reported one primary and one secondary eclipse, whose times of minimum are given in Table 4; they observed that $\varphi_{sec} \approx 0.5475$, based on their recommended period P = 2.093731.

To display the changing orbit, all of these times of minima were compared to an ephemeris based on the Otero times of minimum and the period determined by Kozyreva.

The resulting O–C curve is shown in Figure 2. It confirms Kozyreva's key result, that the phase of secondary minimum is changing quite rapidly. Kozyreva *et al.* explain this by rapid apsidal motion in the system. Times of minimum that were taken within a couple of months of the times determined in this study were recently reported by Bloomer *et al.* (2011), and are also included in Figure 2.

5. Light curve

Using the calibrated colors and magnitudes of the comparison stars and the known photometric transforms of Altimira Observatory, the ensemble differential photometry was transformed to standard *B*, *V*, and *R* magnitudes, and phased to the orbital period. The resulting light curves are shown in Figure 3. Note that the eclipse depths are essentially the same in all bands. The primary eclipse depth is 0.6 magnitude, and the secondary eclipse depth is ~ 0.5 magnitude in all bands (±0.05).

To determine the color index vs. phase, these light curves were binned into bins of 0.02 phase (e.g. 0.00 to 0.02, 0.02 to 0.04, and so on), and the brightness averaged in each bin. From this, the averaged [*B–V*] and [*V–R*] colors were determined for each phase bin. The results are shown in Figure 4. There is no sensible change in color during the eclipses: the colors are constant at [*B–V*] = 1.36 ± 0.06 and [*V–R*] = 0.83 ± 0.02.

(These are colors on the standard Johnson-Cousins system, but "as measured"—no correction has been made for interstellar reddening. Considering the star's position in the heart of the Cygnus Milky Way, it seems reasonable to suspect that it may be subject to significant interstellar extinction and reddening, which will have to be taken into account in any modeling of the system).

6. Conclusions

GSC 3152:1202 is an eclipsing binary composed of two stars of nearly-equal temperature and nearly-equal radii in an eccentric orbit. The times of secondary minimum display a large rate of change (i.e., changing orbital phase, relative to the primary minimum). This might make it an interesting test system to validate models of stellar parameters and orbital apsidal motion.

7. Acknowledgements

I am pleased to acknowledge the assistance of the Tzec Maun Foundation Observatory, which provided telescope time for calibration of the comparison stars.

This work made use of the following on-line databases: VizieR (http://vizier.u-strasbg.fr/viz-bin/VizieR) (Ochsenbein *et al.* 2000); TASS (The Amateur Sky Survey) http://sallman.tass-survey.org/servlet/markiv/template/Welcome.vm (Droege *et al.* 2006); Super WASP http://www.wasp.le.ac.uk/public/, the WASP consortium which comprises the University of Cambridge, Keele University, University of Leicester, The Open University, The Queen's University Belfast, St. Andrews University and the Isaac Newton Group. Funding for WASP comes from the consortium universities and from the UK's Science and Technology Facilities Council.

References

Bloomer, R. H., Della-Rose, D. J., Todt, A., Zimmerman, J. D., and Hitefield, S. D. 2011, *Inf. Bull. Var. Stars*, No. 5962, 1.

Bulut, I., and Demircan, O. 2007, *Mon. Not. Roy. Astron. Soc.*, **378**, 179.

Butters, O. W., *et al.* 2010, *Astron. Astrophys.*, **520**, L10.

Droege, T. F., *et al.* 2006, *Publ. Astron. Soc. Pacific*, **118**, 1666.

Kozyreva, V. S., Kusakin, A. V., and Bagaev, L. A. 2009, *Inf. Bull. Var. Stars*, No. 5909, 1.

Kwee, K. K., and van Woerden, H. 1956, *Bull. Astron. Inst. Netherlands*, **12**, 327.

Ochsenbein, F., Bauer, P., and Marcout, J. 2000, *Astron. Astrophys., Suppl. Ser.*, **143**, 23.

Otero, S. A., Wils, P., Hoogeveen, G., and Dubovsky, P. A. 2006, *Inf. Bull. Var. Stars*, No. 5681, 1.

Pollacco, D. L. *et al.* 2006, *Publ. Astron. Soc. Pacific*, **118**, 1407.

Table 1. Comparison stars (photometry from Altimira Observatory).

Star	*B* ±0.05	*V* ±0.02	*R* ±0.01	*B–V* ±0.05	*V–R* ±0.02
comp 1 = GSC 3152:376	13.84	12.68	11.95	1.16	0.73
comp 2 = GSC 3152:1192	12.58	11.75	11.23	0.83	0.51
comp 3 = GSC 3152:1020	13.00	12.42	12.04	0.58	0.38
comp 5 = GSC 3152:474	12.41	11.96	11.63	0.45	0.33

Table 2. Times of minimum of GSC 3152:1202 measured at Altimira Observatory (this study).

	Primary Eclipse Times of minimum (HJD)				
UT date	*V band*	*B band*	*R band*	*average*	*±*
2010-07-14	2455391.78289	0.77598	0.78217	2455391.7803	0.005
2010-08-04	2455412.71940	0.71915	0.71829	2455412.7189	0.001
2010-08-27	2455435.75103	0.75345	0.75074	2455435.7517	0.002
	Secondary Eclipse Time of minimum (HJD)				
2010-09-16	2455455.74945	0.74868	0.74895	2455455.7490	0.001

Table 3. WASP times of minimum (star = 1SWASP J202717.24+375626.8).

UT Date	*HJD per WASP TMID*	*±*	*min*
2007-07-11	2454292.561	0.002	I
2007-08-21	2454334.437	0.002	I
2007-10-24	2454398.371	0.002	II

Table 4. Kozyreva times of minimum.

UT Date	*HJD Tmin*	*±*
2009-06-21	2455004.4386	0.0002
2009-08-22	2455066.3026	0.0003

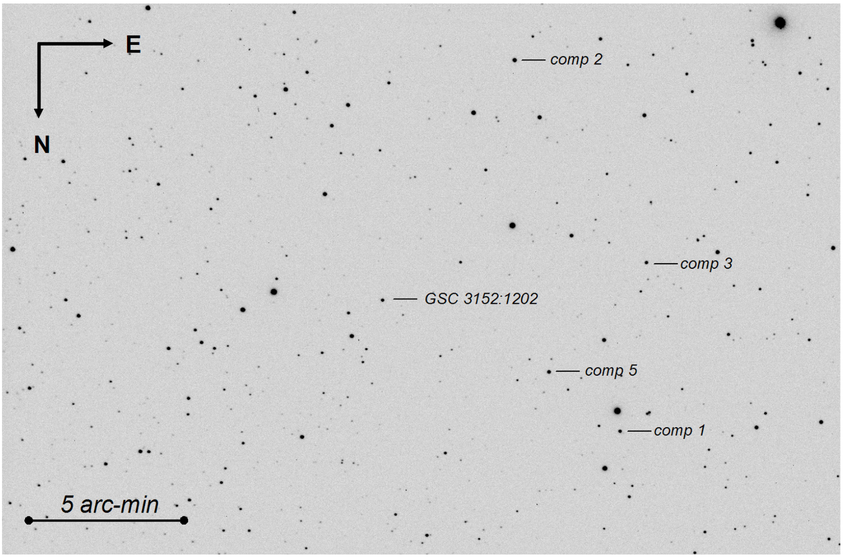

Figure 1. Field of view of GSC 3152:1202 showing comparison stars used.

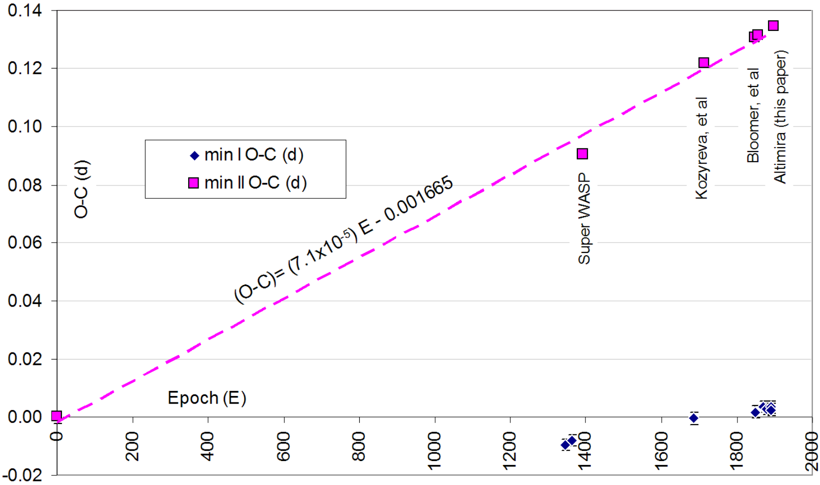

Figure 2. O–C diagram of GSC 3152:1202 showing significant rate of change of the times of secondary minimum. (Based on $HJD_{0min,I} = 2451478.596 + 2.093731E$ and $HJD_{min,II} = 2451479.6198 + 2.093731E$).

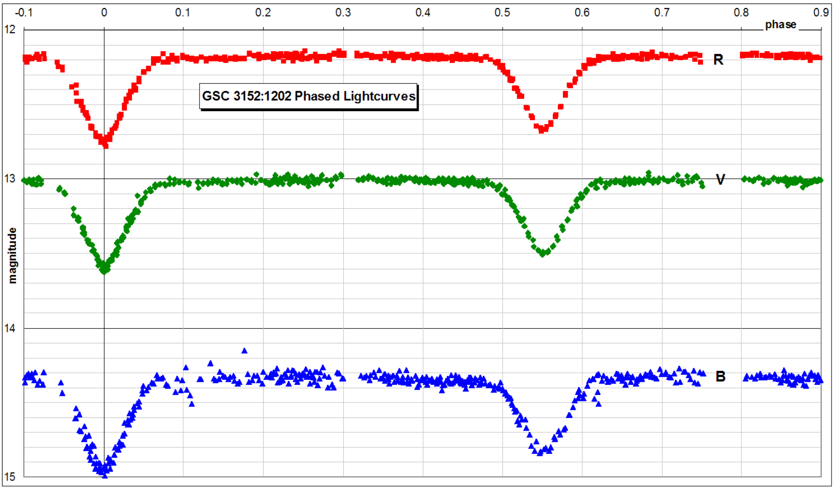

Figure 3. Light curve of GSC 3152:1202 in *B*-, *V*-, and *R*-bands.

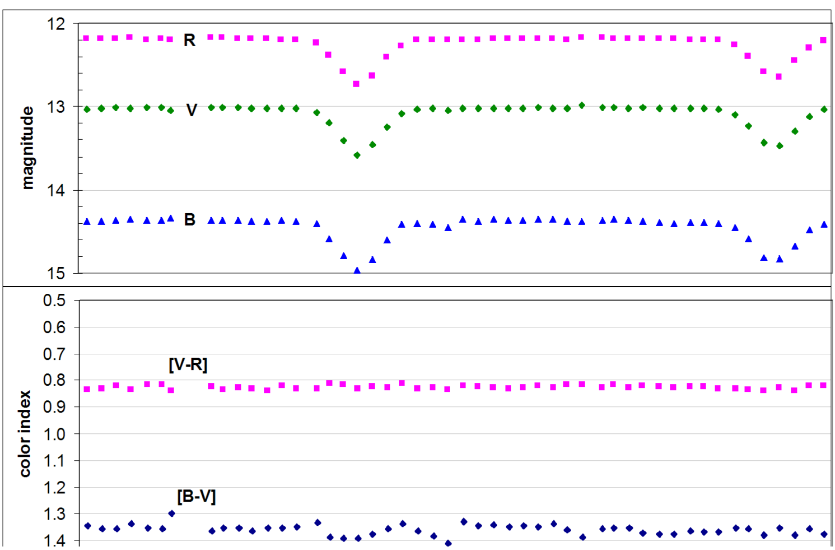

Figure 4. Color index as a function of phase, showing that there is no change in color during eclipses.

Recent Minima of 146 Eclipsing Binary Stars

Gerard Samolyk
P.O. Box 20677, Greenfield, WI 53220; gsamolyk@wi.rr.com

Received July 12, 2011; accepted July 12, 2011

Abstract This paper continues the publication of times of minima for eclipsing binary stars from observations reported to the AAVSO Eclipsing Binary Section. Times of minima from observations made from October 2010 thru March 2011, along with a few unpublished times of minima from older data, are presented.

1. Recent Observations

The accompanying list contains times of minima calculated from recent CCD observations made by participants in the AAVSO's eclipsing binary program; the data used to determine these times of minimum are in the AAVSO International Database. This list will be web-archived and made available through the AAVSO ftp site at ftp://ftp.aavso.org/public/datasets/gsamj392.txt. This list, along with eclipsing binary data from earlier AAVSO publications, is also included in the Lichtenknecker database administrated by the Bundesdeutsche Arbeitsgemeinschaft für Veränderliche Sterne e. V. (BAV) at: http://www.bav-astro.de/LkDB/index.php?lang=en. These observations were reduced by the observers or the writer using the method of Kwee and Van Worden (1956). The standard error is included when available. Column F in Table 1 indicates the filter used. A blank indicates no filter.

The linear elements in the *General Catalogue of Variable Stars* (GCVS, Kholopov *et al.* 1985) were used to compute the O–C values for most stars. For a few exceptions where the GCVS elements are missing or are in significant error, light elements from another source are used: CD Cam (Baldwin and Samolyk 2007), AC CMi (Samolyk 2008), CW Cas (Samolyk 1992a), MR Del (Kreiner 2004, 2011), Z Dra (Danielkiewicz-Krośniak and Kurpińska-Winiarska 1996), DF Hya (Samolyk 1992b), DK Hya (Samolyk 1990), EF Ori (Baldwin and Samolyk 2005), GU Ori (Samolyk 1985), VY UMi (Otero and Dubovsky 2004), and HT Vir (Kreiner 2011). O–C values listed in this paper can be directly compared with values published in recent numbers of the AAVSO *Observed Minima Timings of Eclupsing Binaries* series.

References

Baldwin, M. E., and Samolyk, G. 2005, *Observed Minima Timings of Eclipsing Binaries No. 10*, AAVSO, Cambridge, MA.
Baldwin, M. E., and Samolyk, G. 2007, *Observed Minima Timings of Eclipsing*

Binaries No. 12, AAVSO, Cambridge, MA.
Danielkiewicz-Krośniak, E., and Kurpińska-Winiarska, M., eds. 1996, *Rocznik Astron.* (SAC 68), **68**, 1.
Kreiner, J. M. 2004, *Acta Astron.*, **54**, 207 (http://www.as.up.krakow.pl/ephem/).
Kreiner, J. M. 2011, Lichtenknecker-Database of the BAV, http://www.bavdata-astro.de/~tl/cgi-bin/varstars_cgi
Kholopov, P. N., *et al.* 1985, *General Catalogue of Variable Stars*, 4th ed., Moscow.
Kwee, K. K., and Van Woerden, H. 1956, *Bull. Astron. Inst. Netherlands*, **12**, 327.
Otero, S. A., and Dubovsky, P. A. 2004, *Inf. Bull. Var. Stars*, No. 5557.
Samolyk, G. 1985, *J. Amer. Assoc. Var. Star Obs.*, **14**, 12.
Samolyk, G. 1990, *J. Amer. Assoc. Var. Star Obs.*, **19**, 5.
Samolyk, G. 1992a, *J. Amer. Assoc. Var. Star Obs.*, **21**, 34.
Samolyk, G. 1992b, *J. Amer. Assoc. Var. Star Obs.*, **21**, 111.
Samolyk, G. 2008, *J. Amer. Assoc. Var. Star Obs.,* **36**, 171.

Table 1. Recent times of minima of stars in the AAVSO eclipsing binary program.

Star	*HJD 2400000+*	*Cycle*	*O–C (day)*	*F*	*Observer*	*Standard Error (day)*
RT And	55516.6920	22856	–0.0100	V	R. Poklar	0.0001
TW And	55486.7378	3994	–0.0320	V	G. Samolyk	0.0001
WZ And	55578.5457	21140	0.0540	V	K. Menzies	0.0001
XZ And	54107.5655	22199	0.1597	V	G. Lubcke	0.0001
XZ And	54107.5656	22199	0.1598	I	G. Lubcke	0.0001
XZ And	55486.5740	23215	0.1737	V	G. Samolyk	0.0001
XZ And	55490.6459	23218	0.1738	V	K. Menzies	0.0001
AA And	50701.613:	22266	–0.073		S. Cook	
AA And	51436.593	23052	–0.081		S. Cook	
AA And	52471.7390	24159	–0.0916	V	S. Dvorak	0.0003
AB And	55466.6649	58323.5	–0.0262	V	N. Simmons	0.0003
AB And	55485.7484	58381	–0.0265	V	G. Samolyk	0.0002
AB And	55498.3605	58419	–0.0263	R	L. Corp	0.0002
AB And	55506.6572	58444	–0.0269	V	N. Simmons	0.0001
AB And	55527.5660	58507	–0.0273	V	K. Menzies	0.0002
AD And	54743.5596	15961.5	–0.0563	V	G. Lubcke	0.0002
AD And	54743.5599	15961.5	–0.0560	I	G. Lubcke	0.0005
AN And	50361.617	4431	–0.008		S. Cook	
BL And	50005.293	14675	–0.004		S. Cook	
BL And	52504.7146	18135	–0.0031	V	S. Dvorak	0.0004
BX And	55521.6166	31130	–0.0516	V	K. Menzies	0.0003
DS And	55472.6220	19129	0.0030	V	G. Samolyk	0.0002
EP And	52975.6594	25580	0.0663	V	S. Dvorak	0.0001

Table continued on following pages

Table 1. Recent times of minima of stars in the AAVSO eclipsing binary program, cont.

Star	HJD 2400000+	Cycle	O–C (day)	F	Observer	Standard Error (day)
EP And	53374.5089	26567	0.0616	V	S. Dvorak	0.0002
GZ And	50749.627	–5739	–0.002		S. Cook	
GZ And	53000.502	1640.5	0.001	V	S. Dvorak	0.002
GZ And	55614.3426	10210	–0.0010		C. F. Rivero	0.0004
RX Ari	55500.7173	16610	0.0597	V	R. Poklar	0.0002
SS Ari	55477.7559	40517	–0.2818	V	G. Samolyk	0.0001
SS Ari	55498.6653	40568.5	–0.2811	V	R. Poklar	0.0002
RY Aur	55486.8022	6310	0.0220	V	G. Samolyk	0.0001
SX Aur	55543.6794	12711	0.0145	V	R. Poklar	0.0001
SX Aur	55612.6544	12768	0.0149	V	G. Samolyk	0.0003
TT Aur	55478.8692	25689	–0.0166	V	K. Menzies	0.0001
TT Aur	55541.5097	25736	–0.0147	R	L. Corp	0.0003
WW Aur	55607.5887	8975	0.0019	V	G. Samolyk	0.0001
AP Aur	55584.6630	23080	1.3215	V	R. Poklar	0.0002
AP Aur	55647.5811	23190.5	1.3305	V	K. Menzies	0.0004
AR Aur	55639.6022	4169	–0.1245	V	G. Samolyk	0.0005
CL Aur	55477.9579	18090	0.1421	V	G. Samolyk	0.0006
CL Aur	55527.7325	18130	0.1421	V	K. Menzies	0.0004
CL Aur	55532.7114	18134	0.1436	V	R. Poklar	0.0001
EM Aur	55540.6776	13474	–1.1094	V	R. Poklar	0.0006
EM Aur	55540.6802	13474	–1.1068	V	K. Menzies	0.0005
EP Aur	55527.6501	49438	0.0146	V	K. Menzies	0.0002
EP Aur	55639.3476	49627	0.0116	V	C. F. Rivero	0.0001
HP Aur	55596.5852	9024.5	0.0600	V	G. Samolyk	0.0003
HU Aur	52279.6238	18162	–0.0238	V	S. Dvorak	0.0002
HU Aur	52372.5540	18228	–0.0223	V	S. Dvorak	0.0001
IM Aur	55541.6150	12047	–0.1064	R	L. Corp	0.0010
TU Boo	55629.6569	69578.5	–0.1362	V	K. Menzies	0.0004
TU Boo	55647.8175	69634.5	–0.1357	V	K. Menzies	0.0002
TZ Boo	55611.7557	53771.5	0.0674	V	G. Samolyk	0.0002
TZ Boo	55648.7537	53896	0.0687	V	K. Menzies	0.0003
UW Boo	55639.7611	13173	–0.0073	V	G. Samolyk	0.0001
AD Boo	55605.7757	13700	0.0285	V	K. Menzies	0.0004
AR Boo	55597.7114	45441	0.0416	R	L. Corp	0.0001
CK Boo	50554.656	21562	0.034		S. Cook	
CK Boo	53087.8032	28694.5	0.0728	V	S. Dvorak	0.0003
ET Boo	54623.8123	–556	–0.0007	R	R. Buchheim	0.0005
ET Boo	54623.8126	–556	–0.0005	V	R. Buchheim	0.0005

Table continued on following pages

Table 1. Recent times of minima of stars in the AAVSO eclipsing binary program, cont.

Star	HJD 2400000+	Cycle	O–C (day)	F	Observer	Standard Error (day)
ET Boo	54624.7791	–554.5	–0.0016	V	R. Buchheim	0.0005
ET Boo	54624.7803	–554.5	–0.0003	R	R. Buchheim	0.0005
SV Cam	55533.6751	21817	0.0528	V	R. Poklar	0.0001
AL Cam	55589.6607	21966	–0.0327	V	R. Poklar	0.0001
AS Cam	50188.635	2910	–0.005		S. Cook	
AS Cam	50562.597:	3019	–0.019		S. Cook	
AS Cam	50833.640	3098	–0.023		S. Cook	
AW Cam	50180.603	14834	–0.007		S. Cook	
AW Cam	50858.619	15713	–0.005		S. Cook	
AW Cam	51924.623	17095	–0.003		S. Cook	
CD Cam	55544.7090	3640.5	–0.0022	V	R. Poklar	0.0006
NR Cam	55616.3686	15736	0.0052		C. F. Rivero	0.0003
NR Cam	55638.3754	15822	0.0059	V	C. F. Rivero	0.0002
AD Cnc	52403.600	32578.5	–0.0178	V	S. Dvorak	0.010
AD Cnc	52645.9121	33435.5	–0.0123	V	S. Dvorak	0.0006
AD Cnc	53326.8873	35844	–0.0122	V	S. Dvorak	0.0003
SX CMa	55639.6093	16958	0.0357	V	G. Samolyk	0.0002
TU CMa	55588.6974	25369	–0.0098	V	R. Poklar	0.0002
TU CMa	55631.5533	25407	–0.0105	V	G. Samolyk	0.0004
UU CMa	55586.7133	5072	–0.1066	V	R. Poklar	0.0002
XZ CMi	54167.6029	20254	–0.0064	I	G. Lubcke	0.0004
XZ CMi	54167.6029	20254	–0.0064	V	G. Lubcke	0.0005
XZ CMi	55585.6890	22704	–0.0036	V	R. Poklar	0.0001
XZ CMi	55611.7354	22749	–0.0036	V	G. Samolyk	0.0002
YY CMi	55583.7056	25192	0.0143	V	R. Poklar	0.0003
AC CMi	55577.7013	4150	0.0016	V	R. Poklar	0.0002
AK CMi	55579.6905	22050	–0.0214	V	R. Poklar	0.0001
AK CMi	55641.3732	22159	–0.0215	V	C. F. Rivero	0.0001
AM CMi	55621.6882	29805	0.1965	V	R. Poklar	0.0005
TV Cas	52938.5642	4599	–0.0164	R	G. Lubcke	0.0001
TV Cas	54040.6301	5207	–0.0086	V	G. Lubcke	0.0001
TV Cas	54736.6526	5591	–0.0228	I	G. Lubcke	0.0001
TV Cas	54736.6526	5591	–0.0228	V	G. Lubcke	0.0001
TV Cas	55510.6300	6018	–0.0237	I	G. Lubcke	0.0001
TV Cas	55510.6303	6018	–0.0234	V	G. Lubcke	0.0006
TV Cas	55539.6310	6034	–0.0243	I	G. Lubcke	0.0003
TV Cas	55539.6319	6034	–0.0234	B	G. Lubcke	0.0003
TV Cas	55539.6329	6034	–0.0224	V	G. Lubcke	0.0003

Table continued on following pages

Table 1. Recent times of minima of stars in the AAVSO eclipsing binary program, cont.

Star	*HJD 2400000+*	*Cycle*	*O–C (day)*	*F*	*Observer*	*Standard Error (day)*
AB Cas	55527.6444	9374	0.1067	V	R. Poklar	0.0001
CW Cas	55492.6714	43468.5	–0.0577	V	K. Menzies	0.0003
CW Cas	55503.6704	43503	–0.0595	V	R. Poklar	0.0003
DN Cas	50842.660	4091	–0.028		S. Cook	
DN Cas	51466.618:	4361	–0.028		S. Cook	
DO Cas	50427.589	24101	–0.006		S. Cook	
DO Cas	50848.658	24716	–0.007		S. Cook	
DO Cas	54096.7199	29460	–0.0007	V	V. Petriew	0.0001
GT Cas	55478.6633	9411	0.1929	V	K. Menzies	0.0006
IR Cas	55519.6688	19327	0.0081	V	R. Poklar	0.0001
IT Cas	55485.6401	6858	0.0627	V	G. Samolyk	0.0003
OR Cas	55517.6889	9077	–0.0243	V	R. Poklar	0.0002
V364 Cas	55539.6582	13743	–0.0233	V	R. Poklar	0.0002
V380 Cas	55479.6565	21981	–0.0663	V	G. Samolyk	0.0002
SU Cep	55478.5844	32342	0.0050	V	G. Samolyk	0.0001
SU Cep	55486.6964	32351	0.0044	V	N. Simmons	0.0002
SU Cep	55523.6550	32392	0.0056	V	R. Poklar	0.0001
WZ Cep	55531.6427	65855.5	–0.1008	V	R. Poklar	0.0003
TT Cet	55486.8004	47208	–0.0641	V	G. Samolyk	0.0001
TT Cet	55508.6689	47253	–0.0636	V	R. Poklar	0.0001
TW Cet	55486.7429	41386.5	–0.0263	V	G. Samolyk	0.0001
TW Cet	55513.6749	41471.5	–0.0267	V	R. Poklar	0.0002
TX Cet	55514.6843	16781	0.0098	V	R. Poklar	0.0002
RW Com	55572.8347	65518	–0.0103	V	K. Menzies	0.0002
RW Com	55594.6706	65610	–0.0102	R	L. Corp	0.0001
RW Com	55596.8072	65619	–0.0097	V	K. Menzies	0.0002
RW Com	55628.6115	65753	–0.0098	V	K. Menzies	0.0001
RW Com	55637.3927	65790	–0.0104	V	C. F. Rivero	0.0001
RW Com	55642.3773	65811	–0.0100	V	C. F. Rivero	0.0002
RW Com	55646.4119	65828	–0.0103	V	C. F. Rivero	0.0003
RZ Com	55645.5991	61470.5	0.0438	V	G. Samolyk	0.0001
SS Com	55622.7055	74176.5	0.7371	V	K. Menzies	0.0003
SS Com	55640.6625	74220	0.7377	V	K. Menzies	0.0003
CC Com	55560.9109	72625	–0.0132	V	K. Menzies	0.0001
YY CrB	53823.7658	3515	0.0017	V	V. Petriew	0.0001
YY CrB	53835.8107	3547	–0.0031	V	V. Petriew	0.0008
YY CrB	53875.7299	3653	0.0013	V	V. Petriew	0.0002
AE Cyg	55485.7040	11246	–0.0040	V	C. Hesseltine	0.0003

Table continued on following pages

Table 1. Recent times of minima of stars in the AAVSO eclipsing binary program, cont.

Star	HJD 2400000+	Cycle	O–C (day)	F	Observer	Standard Error (day)
CG Cyg	55044.6620	24748	0.0624	V	H. Gerner	0.0001
MY Cyg	55479.6219	5401	–0.0017	V	G. Samolyk	0.0005
V346 Cyg	55479.6802	7215	0.1506	V	G. Samolyk	0.0002
V387 Cyg	55478.5986	42918	0.0213	V	G. Samolyk	0.0001
V387 Cyg	55487.5663	42932	0.0207	V	K. Menzies	0.0002
V704 Cyg	55485.7342	30745	0.0307	V	N. Simmons	0.0004
V836 Cyg	50977.9323	9373	0.0094	V	J. Roe	0.0003
V836 Cyg	50981.8506	9379	0.0073	V	J. Roe	0.0005
V836 Cyg	55477.3420	16259	0.0227	R	L. Corp	0.0006
YY Del	55485.6209	15794	0.0107	V	G. Samolyk	0.0001
FZ Del	55507.5453	30877	–0.0392	V	N. Simmons	0.0001
MR Del	54684.8884	4187.5	0.0012	V	R. Buchheim	0.0003
MR Del	54684.8886	4187.5	0.0014	B	R. Buchheim	0.0002
MR Del	54688.8002	4195	0.0003	B	R. Buchheim	0.0001
MR Del	54688.8002	4195	0.0003	V	R. Buchheim	0.0002
Z Dra	55570.7244	4218.5	–0.0191	B	G. Lubcke	0.0006
Z Dra	55570.7247	4218.5	–0.0188	V	G. Lubcke	0.0006
Z Dra	55625.6971	4259	–0.0225	V	R. Poklar	0.0001
Z Dra	55648.7737	4276	–0.0224	B	G. Lubcke	0.0001
Z Dra	55648.7737	4276	–0.0224	V	G. Lubcke	0.0001
Z Dra	55648.7737	4276	–0.0224	I	G. Lubcke	0.0001
S Equ	55485.6055	3751	0.0625	V	G. Samolyk	0.0001
TZ Eri	55478.7646	5013	0.2963	V	G. Samolyk	0.0002
YY Eri	55585.5665	43558.5	0.1396	V	G. Samolyk	0.0001
YY Eri	55600.3566	43604.5	0.1409	R	L. Corp	0.0002
SX Gem	55559.6336	26724	–0.0573	V	K. Menzies	0.0004
SX Gem	55574.6674	26735	–0.0592	V	R. Poklar	0.0002
SX Gem	55585.6037	26743	–0.0579	V	K. Menzies	0.0003
SX Gem	55611.5745	26762	–0.0578	V	N. Simmons	0.0003
WW Gem	55602.6179	23928	0.0193	V	G. Samolyk	0.0002
AL Gem	55521.7569	20985	0.0718	V	K. Menzies	0.0006
UX Her	55648.8303	10315	0.0857	V	K. Menzies	0.0002
LV Her	54647.7333	4427.5	–0.0132	V	R. Buchheim	0.0001
WY Hya	55634.7080	21038.5	0.0297	V	R. Poklar	0.0002
AV Hya	55646.6844	27763	–0.0979	V	R. Poklar	0.0002
DF Hya	55600.7008	38756	–0.0118	V	R. Poklar	0.0002
DF Hya	55611.7749	38789.5	–0.0129	V	G. Samolyk	0.0001
DF Hya	55614.4203	38797.5	–0.0124		C. F. Rivero	0.0002

Table continued on following pages

Table 1. Recent times of minima of stars in the AAVSO eclipsing binary program, cont.

Star	HJD 2400000+	Cycle	O–C (day)	F	Observer	Standard Error (day)
DF Hya	55631.6114	38849.5	–0.0127	V	G. Samolyk	0.0001
DK Hya	55639.6525	24517	0.0047	V	G. Samolyk	0.0002
VX Lac	55486.6520	9519	0.0757	V	G. Samolyk	0.0001
CO Lac	55486.5801	18125	–0.0036	V	G. Samolyk	0.0001
DG Lac	55486.6725	4975	–0.2211	V	C. Hesseltine	0.0002
UZ Leo	55625.5767	25605.5	–0.0912	R	L. Corp	0.0003
VZ Leo	55560.7093	22384	–0.0626	V	K. Menzies	0.0005
VZ Leo	55561.7948	22385	–0.0670	V	K. Menzies	0.0003
VZ Leo	55608.6646	22428	–0.0632	V	R. Poklar	0.0003
WZ Leo	55650.6549	17424	–2.4968	V	G. Samolyk	0.0002
RY Lyn	55651.6262	8895	–0.0351	V	G. Samolyk	0.0001
RU Mon	55606.6494	3867.5	–0.5621	V	G. Samolyk	0.0002
XZ Mon	55596.4164	28317	0.0212	R	L. Corp	0.0001
BB Mon	55591.6552	39457	–0.0042	V	R. Poklar	0.0002
BM Mon	55597.3744	22605	0.0489	R	L. Corp	0.0001
V456 Mon	55597.4760	14349	–0.1337	R	L. Corp	0.0001
V508 Oph	55646.6092	30639	–0.0199	V	C. F. Rivero	0.0002
EF Ori	55631.5972	2026	0.0048	V	G. Samolyk	0.0004
EQ Ori	55572.7029	13822	–0.0400	V	R. Poklar	0.0001
ER Ori	55548.7048	32882	0.0937	V	N. Simmons	0.0001
ER Ori	55589.5589	32978.5	0.0899	V	K. Menzies	0.0002
ER Ori	55611.5805	33030.5	0.0947	V	G. Samolyk	0.0001
ET Ori	55612.6918	30421	–0.0031	V	G. Samolyk	0.0002
FH Ori	55581.7207	13798	–0.3720	V	R. Poklar	0.0006
FT Ori	55528.7170	4501	0.0158	V	K. Menzies	0.0002
FT Ori	55569.6724	4514	0.0158	V	R. Poklar	0.0001
FZ Ori	55602.6160	28946.5	–0.0544	V	G. Samolyk	0.0001
FZ Ori	55631.6152	29019	–0.0542	V	G. Samolyk	0.0001
GU Ori	55566.6698	26550.5	–0.0491	V	R. Poklar	0.0002
GU Ori	55631.6244	26688.5	–0.0485	V	G. Samolyk	0.0002
U Peg	55502.6431	50672.5	–0.1376	V	R. Poklar	0.0002
U Peg	55511.6382	50696.5	–0.1373	V	N. Simmons	0.0002
U Peg	55541.4310	50776	–0.1396	R	L. Corp	0.0004
UX Peg	55491.6642	9754	–0.0090	V	G. Samolyk	0.0002
BG Peg	55479.6635	5095	–1.9629	V	C. Hesseltine	0.0003
Z Per	55472.8072	3211	–0.2383	V	G. Samolyk	0.0001
RT Per	55504.7051	26052	0.0697	V	R. Poklar	0.0001
ST Per	54102.6182	4405	0.2826	I	G. Lubcke	0.0003

Table continued on following pages

Table 1. Recent times of minima of stars in the AAVSO eclipsing binary program, cont.

Star	HJD 2400000+	Cycle	O–C (day)	F	Observer	Standard Error (day)
ST Per	54102.6185	4405	0.2829	V	G. Lubcke	0.0004
XZ Per	55501.6927	10415	–0.0541	V	R. Poklar	0.0002
IU Per	55506.6581	11546	0.0103	V	R. Poklar	0.0003
IU Per	55585.5061	11638	0.0120	V	K. Menzies	0.0002
IU Per	55602.6466	11658	0.0120	V	G. Samolyk	0.0001
KW Per	55528.5748	14093	0.0120	V	K. Menzies	0.0001
PS Per	55594.4557	44244	0.0644		C. F. Rivero	0.0003
PS Per	55598.3207	44249.5	0.0674		C. F. Rivero	0.0006
β Per	55602.6367	3474	0.1081	V	G. Samolyk	0.0002
UZ Pup	55607.6758	13831.5	–0.0069	V	R. Poklar	0.0002
AV Pup	55612.6958	43920	0.1603	V	G. Samolyk	0.0002
AV Pup	55622.7003	43938	0.1507	V	R. Poklar	0.0002
CK Sge	54664.8100	3597	–0.0385	R	R. Buchheim	0.0007
CK Sge	54681.8534	3604	–0.0395	R	R. Buchheim	0.0007
RW Tau	55521.6360	3553	–0.2409	V	R. Poklar	0.0001
RZ Tau	55525.7002	42940	0.0616	V	K. Menzies	0.0002
RZ Tau	55525.7002	42940	0.0616	V	R. Poklar	0.0001
RZ Tau	55545.6529	42988	0.0619	V	N. Simmons	0.0001
WY Tau	55477.7672	26092	0.0570	V	K. Menzies	0.0001
WY Tau	55570.5974	26226	0.0576	V	N. Simmons	0.0002
AM Tau	55595.6262	5060	–0.0564	V	G. Samolyk	0.0001
AQ Tau	55490.8540	21248	0.5518	V	K. Menzies	0.0003
AQ Tau	55607.5783	21344	0.5493	V	G. Samolyk	0.0003
CT Tau	55540.7910	15201	–0.0554	V	K. Menzies	0.0002
EQ Tau	55485.7443	44741.5	–0.0237	V	G. Samolyk	0.0002
EQ Tau	55511.6870	44817.5	–0.0235	V	R. Poklar	0.0002
EQ Tau	55539.6771	44899.5	–0.0240	V	N. Simmons	0.0001
TY UMa	55611.8276	45352	0.2965	V	G. Samolyk	0.0001
TY UMa	55639.6603	45430.5	0.2979	V	R. Poklar	0.0004
UX UMa	55612.7210	92438	0.0008	V	G. Samolyk	0.0001
VV UMa	53813.6399	11636	–0.0503	R	G. Lubcke	0.0001
VV UMa	54165.5750	12148	–0.0537	I	G. Lubcke	0.0003
VV UMa	54165.5785	12148	–0.0502	V	G. Lubcke	0.0001
VV UMa	54554.6355	12714	–0.0503	V	G. Lubcke	0.0005
VV UMa	54554.6370	12714	–0.0488	I	G. Lubcke	0.0023
VV UMa	55285.6625	13777.5	–0.0520	I	G. Lubcke	0.0026
VV UMa	55285.6645	13777.5	–0.0500	V	G. Lubcke	0.0015
VV UMa	55295.6327	13792	–0.0488	I	G. Lubcke	0.0002

Table continued on following page

Table 1. Recent times of minima of stars in the AAVSO eclipsing binary program, cont.

Star	*HJD 2400000+*	*Cycle*	*O–C (day)*	*F*	*Observer*	*Standard Error (day)*
VV UMa	55295.6329	13792	–0.0486	V	G. Lubcke	0.0001
VV UMa	55305.5993	13806.5	–0.0492	V	G. Lubcke	0.0006
VV UMa	55305.5997	13806.5	–0.0488	I	G. Lubcke	0.0002
VV UMa	55594.6425	14227	–0.0493	V	R. Poklar	0.0004
VV UMa	55605.6392	14243	–0.0506	V	K. Menzies	0.0003
ZZ UMa	55598.6593	8545	–0.0014	V	R. Poklar	0.0004
AF UMa	55592.5874	5477	0.5587	V	G. Samolyk	0.0008
AW UMa	55631.4286	24996.5	–0.0826	R	L. Corp	0.0006
VY UMi	55639.5253	13413	0.0221	V	C. F. Rivero	0.0018
AH Vir	55645.4516	24123.5	0.2338	R	L. Corp	0.0003
AZ Vir	55593.6159	33223.5	–0.0229	R	L. Corp	0.0001
AZ Vir	55631.5554	33332	–0.0220	R	L. Corp	0.0006
HT Vir	55631.5847	7681	–0.0023	R	L. Corp	0.0001
NY Vir	55595.5366	53181.5	–0.0065	R	L. Corp	0.0002
NY Vir	55595.5869	53182	–0.0067	R	L. Corp	0.0001

The Ross Variable Stars Revisited. I.

Wayne Osborn
O. Frank Mills
Yerkes Observatory, 373 W. Geneva Street, Williams Bay, WI 53191; email correspondence should be sent to Wayne.Osborn@cmich.edu

Received May 2, 2011; revised May 6, 2011; accepted May 6, 2011

Abstract Better magnitudes and epochs have been determined for 189 of the 379 confirmed and suspected variable stars discovered by Ross from 1925 to 1931. Accurate positions have been determined for those objects for which unambiguous identifications had been lacking.

1. Introduction

Frank E. Ross of Yerkes Observatory published ten lists of suspected new variable stars between 1925 and 1931 (Ross 1925, 1926a, 1926b, 1927a, 1927b, 1928a, 1928b, 1929, 1930, and 1931). These objects were detected in connection with a search for stars of large proper motion conducted by comparing (blinking) plates taken by Edward E. Barnard from 1904 to 1915 with second epoch plates of similar exposure that Ross took in the period 1924–1930. The ten lists contain 379 objects. Most of the Ross variables have now been confirmed and accurate positions determined. Nevertheless, a number of these objects have yet to be certainly identified and it is still not known if these are indeed variables.

Many of the Ross stars were cases where an object was visible at one epoch but not seen at the other. The plates were taken with the Bruce photographic telescope, which actually consisted of three telescopes on the same mounting: 10-inch and 6-inch refractors for photographs and a guide telescope (Barnard 1905). Both Barnard and Ross obtained simultaneous exposures with the two photographic instruments, and this enabled Ross to confirm that that an object visible at only one epoch was not a plate defect. However, Ross realized that some of his suspects visible at just a single epoch could be minor planets (Ross 1926b). First Bedient (2003) and then Marsden (2007) were able to identify fifteen such cases using modern orbital elements for known minor planets. Their work left about forty of the Ross variables still unconfirmed or awaiting identification.

While engaged in another project using Yerkes Observatory plates, we discovered Ross had marked his variable discoveries on the plates he utilized. Shortly thereafter, we came across a box containing Ross's original note cards for this work. The box contained two sets of cards. The first set has a card for each object giving the plates that were compared that led to the suspected variability, the star number marked on the plate, the two magnitude estimates, and a finding chart; the chart often also identifies one or more comparison stars that Ross used to determine his magnitudes. For many of the earlier discoveries the back of the card contains notes showing the star was subsequently examined on other plates or observed visually with the Yerkes 40-inch refractor. The second card set contains the summarized information that Ross later published: assigned variable number, 1875 coordinates, adopted magnitudes, and dates.

2. The project

A number of the unconfirmed Ross variables lie in crowded fields in the Milky Way, and Ross's coordinates are not sufficiently accurate to unambiguously identify the correct object. Our discovery of Ross's finding charts resolved this problem, and we decided to re-examine the plates to obtain reliable identifications.

We elected to examine all the Ross variables, not just those needing confirmation. This was done because in most cases these observations are earlier than any of those archived in the variable star databases (such as that of the AAVSO) and the expanded time range of observations may prove useful. Also, Ross's published magnitudes are known to be systematically 1–2 magnitudes too bright for photographic ones (Marsden 2007), and modern sky survey data permitted us to determine magnitudes approximately on the B system. At the same time, we obtained better epochs for the observations. Ross published only the local dates of the plates. His observing log, however, gives the local astronomical start and end times of his exposures. Barnard's observing log lacks the times of his exposures, but we found he recorded his start and end times on the plates themselves and these were recorded as we re-examined the plates.

3. Procedure

As a project evolves, a researcher gains experience and the later work generally is carried out in a better and more systematic fashion. Our first steps on this project quickly revealed that Ross's early notes were less detailed and contained more errors than those made later. We therefore began our work with his higher-numbered variables, only returning to the initial ones once we ourselves had gained experience with Ross's methods (such as his notation codes). As a consequence, while this paper presents results for the stars in six of Ross's ten lists, they are lists 1, 2, and 7–10. The results from work on lists 3–6 will be published in a subsequent paper.

Our procedure was to use ALADIN (Bonnarel *et al.* 2000; available at http://aladin.u-strasbg.fr/aladin.gml) to produce a sky survey print (when possible a POSS I blue one) of the region of the Ross star. The same plate pair used by Ross was examined and, using his finding chart, the correct star and its variability were confirmed. The epochs of the two plates were then noted and several convenient comparison stars adopted and used to eye-estimate the variable's brightness on the two plates. The comparison stars' approximate B magnitudes were later obtained by averaging the values from the *USNO B1.0* (Monet *et al.* 2003) and *GSC 2.3* (Bucciarelli *et al.* 2008) catalogs and these were used to derive the B magnitude of the variable. Finally, the star's position was checked for known variables and other identifications (such as IRAS sources).

4. Results

Our results are given in Table 1 for the stars in Ross's first and second lists and in Table 2 for the stars in his lists 7–10. The tables present the Ross number and corresponding variable star name if a named variable, the Julian Dates (actually JD – 2400000.0) and B magnitudes for the two compared plates, and (if needed) another identification. As recommended by Eastman *et al.* (2010), the epochs have not been converted to heliocentric ones. Following each table are notes for many of the stars; these give such information as errors detected in Ross's papers and comments on the identification.

Our magnitudes are, of course, not strictly B ones but are much closer to the B system than Ross's published values. He apparently used visual magnitudes for his determinations although his plates had blue-sensitive emulsions. We estimate our magnitudes are accurate to ±0.2. The epochs have been determined from the dates and times of mid-exposure, assuming that the recorded times were Central Standard Time (or occasionally Pacific Time for those plates taken when the telescope was temporarily moved to Mt. Wilson). As a check, we compared our derived values of UT with those derived by Marsden (2007) from the best fits of Ross's positions to the orbits for those objects found to be minor planets; our agreement with Marsden was excellent, confirming our time determinations.

Our results can be used to derive some general facts about Ross's data. The published coordinates for the stars, precessed from 1875 to J2000 and neglecting (the usually unknown) proper motion, compared to modern precise ones show that his positions are typically within 25 arcsec of the true location. There are a few cases of large arc-minute errors. The difference between Ross's published magnitudes and our B ones varies with location on the plate and from field to field, but on average the published values are 1.8 magnitudes brighter.

As mentioned in the introduction, Ross's note cards contain comments for a number of the earlier variable discoveries, including the results from visual observations by him or his colleagues with the Yerkes 40-inch refractor. While no doubt mainly of historical interest, this material is presented in Appendix A (Table A) so it will not be lost.

This paper gives our results for 189 of the 379 Ross variables. Of these, 151 are named variables, seventeen are suspected variables listed in the NSV catalog (Kholopov *et al.* 1982, Kazarovets *et al.* 1998), ten are suspects not in the NSV, eight were observations of minor planets, two are the result of erroneous brightness variations due to plate flaws, and one is probably an erroneous star identification produced by a Ross copying error.

5. Acknowledgements

This research made use of the SIMBAD database, operated at CDS, Strasbourg, France, and the Digitized Sky Surveys (DSS) produced at the Space Telescope Science Institute under U.S. Government grant NAG W-2166. The DSS images are from photographic data obtained using the Oschin Schmidt Telescope on Palomar Mountain and the UK Schmidt Telescope through funding provided by The National Geographic Society, the National Science Foundation, the Sloan Foundation, the Samuel Oschin Foundation, the Eastman Kodak Corporation, and the UK Science and Engineering Research Council.

References

Barnard, E. E. 1905, *Astrophys. J.*, **21**, 35.
Bedient, J. R. 2003, *Inf. Bull. Var. Stars*, No. 5478.
Bonnarel, F., *et al.* 2000, *Astron. Astrophys., Suppl. Ser.*, **143**, 33.
Brown, S. J., Mills, O. F., Osborn, W., and Hoette, V. 2010, *J. Amer. Assoc. Var. Star Obs.*, **38**, 176.
Bucciarelli, B., *et al.* 2008, in *A Giant Step: from Milli- to Micro-arcsecond Astrometry*, Proc. IAU Symp., 248, 316.
Eastman, J., Siverd, R., and Gaudi, B. S. 2010, *Publ. Astron. Soc. Pacific*, **122**, 935.
Kazarovets, E. V., Samus, N. N., and Durlevich, O. V. 1998, *Inf. Bull. Var. Stars*, No. 4655.
Kholopov, P. N. *et al.* 1982, *New Catalogue of Suspected Variable Stars,* Moscow.
Marsden, B. G. 2007, *Perem. Zvezdy*, **27**, 3.
Monet, D. G., *et al.* 2003, *Astron. J.*, **125**, 984.
Ross, F. E. 1925, *Astron. J.*, **36**, 99 (first list).
Ross, F. E. 1926a, *Astron. J.*, **36**, 122 (second list).
Ross, F. E. 1926b, *Astron. J.*, **36**, 167 (third list).
Ross, F. E. 1927a, *Astron. J.*, **37**, 91 (fourth list).
Ross, F. E. 1927b, *Astron. J.*, **37**, 155 (fifth list).
Ross, F. E. 1928a, *Astron. J.*, **38**, 99 (sixth list).
Ross, F. E. 1928b, *Astron. J.*, **38**, 144 (seventh list).
Ross, F. E. 1929, *Astron. J.*, **39**, 140 (eighth list).
Ross, F. E. 1930, *Astron. J.*., **40**, 34 (ninth list).
Ross, F. E. 1931, *Astron. J.*, **41**, 88 (tenth list).

Table 1. Identifications and improved data for Ross Variables 1–104.

Ross	*Note (*)*	*Variable*	*First JD 2400000.0+*	*B*	*Second JD 2400000.0+*	*B*	*Other identification*
1		BB And	18298.576	<16.9	24090.577	13.9	
2		FI Per	16740.830	13.3	24144.554	15.2	
3		AQ Per	16786.669	<15.7	24165.556	14.3	
4	*	NSV 1436	16786.669	12.8	24165.556	16.4	
5	*	NSV 1488	16740.830	<16.5	24144.554	15.0	
6	*		17236.581	13.8	24195.565	13.8	GSC1 0714-00599 (plate flaw)
7		V962 Ori	17236.581	15.1	24195.565	13.8	
8		CL Ori	17236.581	13.7	24195.565	15.3	
9		FQ Ori	17236.581	<15.5	24195.565	12.1	
10	*		16903.727	11.3	24195.673	11.2	BD-10 2106 (plate flaw)
11	*	NSV 2913			24198.628	13.3	Minor planet (449) *Hamburga*
12		ZZ Gem	16767.799	14.8	24198.628	13.4	
13		CD Gem	16767.799	<15.8	24198.628	13.0	
14		AY Aur	16936.663	12.1	24199.550	<16.0	
15		DT Ori	16900.705	<16.2	24224.595	13.0	
16	*	CM Ori	16900.705	13.0	24224.595	14.0	
17		V1796 Ori	16900.705	<16.3	24224.595	14.8	
18		RX Ser	18122.720	15.0	24320.766	<16.0	
19		RY Ser	19158.816	14.4	24320.766	15.4	
20		SV Ser	18122.720	<15.9	24320.766	13.3	
21		V405 Ser	19158.816	14.3	24320.766	<15.7	
22		SX Ser	19158.816	<15.0	24320.766	13.4	
23		CU Ser	19158.816	<15.7	24320.766	14.7	
24		V406 Ser	18122.720	14.9	24320.766	<15.5	
25	*	NSV 9194	18122.720	14.6	24320.766	<16.3	2MASS 17353909-1442210
26		V407 Ser	18122.720	14.2	24320.766	<14.4	
27		AD Ser	18122.720	13.9	24320.766	16.1	
28		VX Ser	18122.720	16.0	24320.766	13.2	
29	*	NSV 9437	19158.816	15.0	24320.766	<15.3	2MASS 17400077-1454108
30		V408 Ser	18122.720	15.4	24320.766	<15.3	
31		BG Oph	18122.720	<14.0	24320.766	12.6	
32		V836 Oph	18122.720	15.5	24320.766	<15.9	
33		AE Ser	18122.720	13.5	24320.766	<16.2	

Table continued on following pages

Table 1. Identifications and improved data for Ross Variables 1–104, cont.

Ross	*Note (*)*	*Variable*	*First JD 2400000.0+*	*B*	*Second JD 2400000.0+*	*B*	*Other identification*
34		LU Ser	18122.720	<15.8	24320.766	14.7	
35		FK Sgr	18122.720	13.4	24320.766	<14.8	
36	*	NSV 9668	19158.816	14.7	24320.766	<16.5	
37		FV Ser	18122.720	<15.8	24320.766	12.7	
38	*	NSV 4748			24240.588	12.3	Minor planet (24) *Themis*
39	*	NSV 4796			24240.644	12.3	Minor planet (39) *Laetitia*
40	*	NSV 4849	17666.577	13.5			Minor planet (162) *Laurentia*
41		V2643 Oph	17060.755	14.7	24342.679	<15.0	
42		BH Oph	16644.711	14.0	24384.637	12.5	
43		AZ Oph	17037.920	<16.0	24354.684	14.5	
44		V2090 Oph	18476.751	15.4	24354.684	15.0	
45		AV Her	16644.711	<14.4	24384.637	12.4	
46		V2204 Oph	16644.711	13.7	24384.637	<15.9	
47		BI Oph	16644.711	11.9	24384.637	14.2	
48		AG Ser	17037.920	14.0	24354.684	<16.8	
49		DS Her	16644.711	<13.0	24384.637	13.2	
50		BK Oph	17037.920	15.6	24354.684	12.4	
51	*	V648 Oph	17037.920	<15.6	24354.684	14.0	
52		V652 Oph	17037.920	12.4	24354.684	<16.4	
53		AX Lyr	17470.601	<16.0	24329.667	13.8	
54		SV Lyr	17470.601	13.4	24329.667	16.8	
55		FN Sgr	16654.831	14.0	24384.601	11.0	
56		FQ Sgr	18117.785	14.4	24414.569	12.8	
57	*	BP Lyr	17470.601	13.1	24329.667	14.8	
58		V2113 Sgr	18117.785	12.6	24414.569	<14.7	
59		V2130 Sgr	18117.785	14.3	24414.569	<15.9	
60		AI Lyr	16621.803	<15.0	24381.656	13.7	
61		DF Sgr	18117.785	14.2	24414.569	15.8	
62		V925 Sgr	18117.785	<16.2	24414.569	13.4	
63	*		18117.785	12.8	24414.569	15.6	Probably TT Sgr
64	*	V2141 Sgr	18117.785	<15.4	24414.569	13.9	
65		EN Sgr	18117.785	13.9	24414.569	15.4	
66	*		18117.785	14.6	24414.569	15.6	2MASS 19240756-1957360

Table continued on following pages

Table 1. Identifications and improved data for Ross Variables 1–104, cont.

Ross	*Note (*)*	*Variable*	*First JD 2400000.0+*	*B*	*Second JD 2400000.0+*	*B*	*Other identification*
67	*		18117.785	14.0	24414.569	14.7	2MASS 19254760-2131216
68		ET Sgr	18117.785	12.8	24414.569	14.3	
69	*	V926 Sgr	18117.785	14.1	24414.569	15.2	
70		V1316 Sgr	18117.785	<15.0	24414.569	12.3	
71		EX Sgr	18117.785	14.3	24414.569	12.5	
72	*		18117.785	13.5	24414.569	14.5	2MASS 19363760-1436197
73		EZ Sgr	18117.785	15.0	24414.569	13.5	
74	*	V731 Sgr	18117.785	<14.6	24414.569	13.2	
75	*	YZ Vul	18066.781	12.1	24381.656	15.3	
76	*		16706.838	13.9	24407.657	15.1	2MASS 19550819+4620450
77	*	NSV 12634	16706.838	13.3	24407.657	15.9	
78		NSV 12676	16706.838	13.7	24407.657	15.0	
79	*	NSV 12682	16706.838	15.3	24407.657	<16.4	
80		V452 Cyg	17058.944	<16.3	24381.660	13.9	
81		AU Vul	17755.657	13.2	24433.557	11.8	
82	*	V346 Cyg	17755.657	11.6	24433.557	13.2	
83		AV Vul	17755.657	12.1	24433.557	11.1	
84		V837 Aql	17800.655	15.2:	24414.638	12.3	
85		RZ Cap	17800.655	14.0	24414.638	15.3	
86		FF Cyg	17058.944	<15.4	24382.660	11.9	
87		V517 Cyg	16706.838	12.9	24407.657	14.5	
88		VY Aqr	17800.655	10.2	24414.638	<14.3	
89	*	NSV 13752	16651.818	11.8			Minor planet (115) *Thyra*
90		PY Cep	16738.792	15.4	24463.560	<16.2	
91		YY Cep	16738.792	<15.9	24463.560	13.7	
92		RZ Cep	16738.792	12.1	24463.560	14.0	
93		BH Lac	17795.595	12.8	24410.599	11.7	
94		BX Cep	16682.819	13.8	24385.674	<14.4	
95		OQ Cep	16681.805	14.3	24450.593	15.7	
96		V397 Cas	16681.805	15.9	24450.593	14.2	
97		AO And	18535.729	14.6	24475.599	13.4	
98		AI And	18535.729	16.2	24475.599	13.7	

Table continued on following pages

Table 1. Identifications and improved data for Ross Variables 1–104, cont.

Ross	*Note (*)*	*Variable*	*First JD 2400000.0+*	*B*	*Second JD 2400000.0+*	*B*	*Other identification*
99		AK And	18535.729	12.6	24475.599	<15.1	
100	*	AL And	18535.729	13.3	24475.599	<16.8	
101		V339 And	18535.729	14.3	24475.599	<16.9	
102		EY And	18535.729	<15.9	24475.599	14.9	
103	*		18535.729	14.4	24475.599	15.6	2MASS 23491886+4751319
104		AM And	18535.729	15.0	24475.599	11.9	

Notes

R4: Ross's note card has his 1925 estimated magnitude as 14, not 15 as published. Our more complete study of this star has been published elsewhere (Brown et al. 2010).

R5: Marsden (2007) showed this suspected variable was not a minor planet observation.

R6: Ross (1927b) said the suspected variability was due to a plate defect. We confirmed the apparent variation as due to the 1906 plate having a defect that gave an anomalously bright value. Magnitude given here for that epoch is from the 6-inch plate.

R10: Ross (1926a) said this listing was an error. His note card has "B-132 [Barnard plate 132] shows this star = 10 m (same as R-28); a defect in B-148 (desensitized area) accounts for its non-appearance there." and we confirmed this. First magnitude is from 6-inch plate.

R11: Marsden (2007) showed object seen in 1925 was a minor planet.

R16: Ross's published magnitudes are reversed from what was correctly noted on his card.

R25: Marsden (2007) showed this suspected variable was not a minor planet observation.

R29: Marsden (2007) showed this suspected variable was not a minor planet observation.

R36: Marsden (2007) showed this suspected variable was not a minor planet observation.

R38: Bedient (2003) and Marsden (2007) showed object seen in 1925 was a minor planet.

R39: Bedient (2003) and Marsden (2007) showed object seen in 1925 was a minor planet.

R40: Marsden (2007) showed object seen in 1907 was a minor planet.

R51: Date of first plate is 1905 July 10, not July 2 as published by Ross.

R57: Ross published that star was not visible on 1925 plate, but card has "not certainly visible" and we see star faintly on plate.

R63: Ross's published magnitudes disagree with those of the star he marked on his finding chart, which we do not find variable. Ross's magnitudes are consistent with this being TT Sgr, and we suggest he miscopied his notes for the star he labeled 17 on the plate (TT Sgr) as being for the star marked 19.

R64: Ross's published magnitudes for the two plates are reversed.

R66: Not listed in NSV catalog.

Table continued on following page

Table 1. Identifications and improved data for Ross Variables 1–104, cont.

R67: Not listed in NSV catalog.

R69: Simbad identifies this as V926 Sgr, but R69 is not that star but 2MASS 19272423-1852224. Star identified in Simbad as V926 is faint on our plates but does seem to vary slightly.

R72: Not listed in NSV catalog.

R74: Simbad identifies this as V931 Sgr, but R74 is not that star but likely 2MASS 19382061-1405267.

R75: Date of first plate is 1908 June 4, not June 24 as published by Ross.

R76: Not listed in NSV catalog.

R77: Marsden (2007) showed this suspected variable was not a minor planet observation.

R79: Marsden (2007) showed this suspected variable was not a minor planet observation. Probably 2MASS 20000260+4600323.

R82: Ross's published right ascension has a 15' error but his finding chart and our rexamination of the plates confirms this identification.

R89: Bedient (2003) and Marsden (2007) showed object seen in 1904 was a minor planet.

R100: Ross's card has nv (not visible) for 1925 plate, so published magnitude should have been <15.

R103: Not listed in NSV catalog.

Table 2. Identifications and improved data for Ross Variables 295–379.

Ross	*Note (*)*	*Variable*	*First JD 2400000.0+*	*B*	*Second JD 2400000.0+*	*B*	*Other identification*
295	*		19277.792	14.9	25233.567	15.5	2MASS 01563501+4123466
296		AH And	19277.792	12.1	25233.567	<16.0	
297		CG Her	17732.690	<15.7	25172.554	14.1	
298	*	AO Lyr	17732.690	12.5	25172.554	15.0	
299		AZ Her	17732.690	15.9	25172.554	12.7	
300	*		17732.690	14.9	25172.554	13.8	2MASS 18224071+2931163
301	*	NSV 10876	17732.690	<15.4	25172.554	14.7	2MASS 18280925+2724041
302		AP Lyr	17732.690	13.0	25172.554	14.7	
303	*		17732.690	16.7	25172.554	15.0	2MASS 18323706+2709256
304	*	V643 Her	17732.690	15.2	25172.554	14.1	
305		AB Lyr	17708.749	14.7	25169.565	12.7	

Table continued on following pages

Table 2. Identifications and improved data for Ross Variables 295–379, cont.

Ross	*Note (*)*	*Variable*	*First JD 2400000.0+*	*B*	*Second JD 2400000.0+*	*B*	*Other identification*
306	*	BU Lyr	17708.749	12.9	25169.565	13.3	
307	*	FP Aql	18119.758	12.2	25173.558	14.1	
308		V1213 Aql	18119.758	14.7	25173.558	<15.6	
309		V816 Aql	18119.758	14.7	25173.558	<15.7	
310	*	NSV 11971	18119.758	14.8	25173.558	<16.3	2MASS 19233640-0215347
311		FT Aql	18119.758	<15.9	25173.558	13.5	
312		ZZ Aql	18119.758	15.1	25173.558	13.4	
313		FW Aql	18119.758	<15.3	25173.558	14.1	
314		V820 Aql	18119.758	<16.0	25173.558	14.1	
315		V924 Aql	18119.758	15.8:	25173.558	14.1	
316		FS Cyg	17708.749	13.0	25173.558	<14.5	
317	*		18119.758	14.7	25173.558	14.7	GSC2.3 S9YZ000896
318		V601 Aql	18119.758	15.3	25173.558	13.3	
319		CE Aql	18119.758	15.2	25173.558	<17.0	
320		V1698 Aql	18119.758	14.4	25173.558	13.5	
321		V1715 Aql	18119.758	<15.2	25173.558	13.0	
322		V543 Aql	18119.758	<14.5	25173.558	12.8	
323	*	NSV 12985	20750.615	13.5	25171.585	<15.1	
324	*	NSV 13021	20750.615	14.4	25171.585	<16.4	
325		V363 Cyg	19217.797	<15.3	25173.558	14.3	
326	*	NSV 13047	19217.797	<17.0	25173.558	15.3	
327		V365 Cyg	19217.797	16.4	25173.558	14.2	
328	*	SY Cap	20750.615	14.3	25171.585	16.0	
329	*	NSV 13179			25171.585	14.2	Minor planet (24) *Themis*
330		V518 Cyg	19217.797	15.0	25173.558	15.6	
331	*	NSV 13449	18502.663	<16.4	25178.551	15.7	
332		V376 Cyg	18502.663	<16.3	25178.551	14.1	
333		V377 Cyg	18502.663	14.6	25178.551	15.8	
334		CT Cyg	18502.663	16.0	25178.551	14.1	
335		AK Vul	18502.663	18:	25178.551	14.2	
336	*	NSV 13592	18502.663	14.9	25178.551	14.8	USNO B1.0 1190-0542073
337		V472 Cyg	18502.663	<16.3	25178.551	13.9	
338		V363 Cyg	18502.663	<16.2	25178.551	13.9	
339		V598 Cyg	18502.663	15.1	25178.551	<15.3	

Table continued on following pages

Table 2. Identifications and improved data for Ross Variables 295–379, cont.

Ross	*Note (*)*	*Variable*	*First JD 2400000.0+*	*B*	*Second JD 2400000.0+*	*B*	*Other identification*
340		GS Cyg	18502.663	<14.6	25178.551	12.3	
341		WW Aqr	20724.500	<15.7	25179.801	12.0	
342		DN Peg	20724.500	12.3	25179.801	11.3	
343	*	DM Aqr	20775.613	<14.7	25210.531	13.0	
344	*	NSV 14721			25210.531	13.3	Minor planet (59) *Elpis*
345		TU Psc	20688.844	14.5	25255.531	13.5	
346		AR And	17872.525	<14.8	24933.544	12.6	
347		NSV 998	20120.566	15.4	25257.601	13.3	
348	*	V719 Tau	17496.782	13.4	24933.601	<14.2	
349	*	NSV 1797	17496.782	13.1	24933.601	<15.0	
350		X Lep	17856.879	11.7	24931.569	16.3	
351		ST Lep	17856.879	13.9	24931.569	13.2	
352	*	NSV 1982			24933.601	12.4	Minor planet (451) *Patientia*
353		AQ Lep	20128.666	<15.0	25286.604	13.8	
354		SY Lep	20128.666	<15.1	25286.604	13.0	
355		VV Hya	20463.893	<15.0	24934.672	13.9	
356		CL Lib	18448.690	14.3	25001.797	15.6	
357		XX Ser	16606.688	12.5	25433.663	11.7	
358		CW Her	16697.684	13.5	25388.674	12.1	
359	*	V854 Oph	19160.820	15.4	25443.676	12.8	
360		V856 Oph	19160.820	14.1	25443.676	<15.9	
361		V850 Oph	19160.820	12.7	25443.676	14.7	
362		V1482 Oph	16972.857	13.7	25437.670	16.2	
363		V2600 Oph	16972.857	13.4	25437.670	12.1	
364	*	V862 Oph	16972.857	13.0	25437.670	<15.4	
365		V1898 Oph	19160.820	<15.0	25443.676	14.3	
366	*	V2554 Oph	16972.857	14.2	25437.670	13.6	
367		OU Aql	17783.615	13.2	25490.658	15.1	
368	*		16986.692	12.9	24993.701	13.3	2MASS 13101752-2508253
369		V436 Hya	16986.692	13.7	24993.701	<15.7	
370		CF Vir	17349.703	13.3	24998.688	15.8	IRAS 14130-0538
371	*	V867 Sco	18096.723	14.3:	24999.795	12.8	
372		M4 V28	18096.723	14.4	24999.795	13.3	
373		FT Ser	16693.638	14.5	24999.869	13.8	
374	*	CU Ser	16693.638	14.1	24999.869	<16.5	

Table continued on following pages

Table 2. Identifications and improved data for Ross Variables 295–379, cont.

Ross	Note (*)	Variable	First JD 2400000.0+	B	Second JD 2400000.0+	B	Other identification
375	*	BD Ser	16693.638	13.9	24999.869	16.0	
376		CY Ser	16693.638	15.6	24999.869	13.4	
377		MV Her	18446.767	13.3	26128.747	<15.6	
378		V471 Her	18446.767	15.7	26128.747	14.3	
379		LU Her	18446.767	13.4	26128.747	15.1	

Notes

R295: Not listed in NSV catalog. Star has different brightnesses on the two 10-inch plates, but the second plate set does not go deep enough to confirm variability.

R298: Ross marked the star just to the east of AO Lyr on his chart but our examination of his plates confirms AO Lyr as the variable he detected.

R300: Not listed in NSV catalog. X-ray source ROTSE1 J182240.62+293115.0.

R301: Marsden (2007) showed this suspected variable was not a minor planet observation.

R303: Not listed in NSV catalog.

R304: Ross did not identify the variable on his finding chart, but V643 Her is in the center of his charted field and confirmed as the variable on re-examination of plate pair.

R306: Date of first plate is 1907 May 12, not March 12 as published by Ross.

R307: Ross did not identify the variable on his finding chart, but FP Aql is in the center of his charted field and confirmed as the variable on re-examination of plate pair.

R310: Marsden (2007) showed this suspected variable was not a minor planet observation.

R317: Not listed in NSV catalog and perhaps not variable. Star appears fainter on 1927 10-inch plate than on the 1908 plate but at about the same brightness on the two 6-inch plates; examination of other plates suggests a small variation.

R323: Marsden (2007) showed this suspected variable was not a minor planet observation.

R324: Marsden (2007) showed this suspected variable was not a minor planet observation.

R326: Marsden (2007) showed this suspected variable was not a minor planet observation.

R328: 1927 plate was exposed for 20 minutes on October 16 and then for 71 minutes more on October 17 with images superimposed; JD refers to October 17.

R329: Marsden (2007) showed object seen in 1927 was a minor planet.

Table continued on following page

Table 2. Identifications and improved data for Ross Variables 295–379, cont.

R331: Marsden (2007) showed this suspected variable was not a minor planet observation; object seen by Ross is at about R.A. 20^h 59^m 39^s Dec. +29° 29.7' (J2000) but there is no obvious counterpart on POSS images.

R336: Only a small variation but confirmed on 6-inch plates.

R343: Date of first plate is 1915 October 4, not October 11 as published by Ross.

R344: Marsden (2007) showed object seen in 1927 was a minor planet.

R348: Variable seen by Ross is not the star identified in Simbad as V719 Tau; approximate J2000 coordinates are R.A. 04^h 48^m 46^s Dec. +25° 13.8' (J2000), but no obvious counterpart on POSS images; position is close to radio source NVSS J044852+251452; possibly a minor planet.

R349: Marsden (2007) showed this suspected variable was not a minor planet observation; approximate J2000 position is R.A. 05^h 00^m 30^s Dec. +26° 40.3'; no obvious counterpart on POSS images.

R352: Bedient (2003) and Marsden (2007) showed object seen in 1927 was a minor planet.

R359: Ross's note card indicates the 1928 magnitude should have been published as 11, not 10.

R364: POSS images show two stars 14" apart where variable was seen; both stars are IR sources; Simbad has the southern star identified as the variable, but Ross's chart seems to indicate the northern star.

R366: Ross's published declination has a 2.5' error but his finding chart and our re-examination of the plates confirm this identification.

R368: Not listed in NSV catalog. There are two nearby stars at Ross's indicated position but 2MASS 13101752-2508253 was confirmed as the variable.

R371: Our magnitude estimates are uncertain.

R374: This is Ross 23 rediscovered on a second plate pair.

R375: Ross's published coordinates have arc-minute errors but his finding chart and our re- examination of the plates confirm this identification.

Appendix

Many of Ross's cards for his earlier discoveries contain notes showing that additional work on these objects was carried out. The cards for his second list of objects reveal that one suspected variable was later identified as the minor planet (41) *Daphne*. Ross then realized that some of his suspects visible at just a single epoch would be minor planets, and a number of cards have a notation such as "variable or asteroid." Other notes give the results from examining the stars visually with the Yerkes 40-inch refractor.

The following table gives this supplementary material. Ross's comments are reproduced verbatim (omitting the common indication that the object might be an asteroid). A "v" refers to the variable while letters (a, b, c) refer to comparison stars that are indicated on Ross's finding charts. For those cases where a visual magnitude estimate was made, we follow the reproduced comments with the approximate Julian Date of the observation and V magnitude, derived by using modern magnitude values for the comparison stars.

Table A. Ross's notes and derived V magnitude estimates.

Ross	*Comments on Ross's note cards reproduced verbatim*	*JD 2400000.0+*	*m(V)*
1	1925 Aug 31: v reddish; v = b = c	24394.6	11.7
2	1925 Dec 7: 40"; v = a + .2 = 13±; Reddish	24492.6	11.9
3	1925 Dec 7: 40"; v = a = 13±; reddish	24492.6	13.2
4	1925 Dec 7: (40"); v = a – .2 (ftr) = 14±	24492.6	14.8
5	1925 Dec 7: (40"); v = a = abt 14m	24492.6	12.7
6	1925 Dec 17: 40"; v = a = 15m	24502.6	13.3
7	1925 Dec 17: 40"; v = a + .2 = 14m	24502.6	13.7
8	1925 Dec 17: 40"; v = 1/2(a + b) = 15m	24502.6	14.1
9	1925 Dec 17: 40"; v = a - .2 = 12½m = reddish	24502.6	11.4
11	1926 Jan 11: 40"; star a not vis v = b = 14m; repeat on better night	24527.6	13.4
12	1926 Jan 11: 40"; v very red = 9½ m; v = a + 0.4	24527.6	10.5
13	1926 Jan 11: 40"; v = a = 14m, conditions v.p.	24527.6	13.5
14	1926 Jan 11: 40"; v not vis, but conditions v.p.; limit being about m=14	24527.6	<13.3
15	1925 Dec 17: 40"; v = 15m = c	24502.6	14.9
16	1925 Dec 17: 40"; v = a ~~Discard this as variation not confirmed. ea night it appears as bright as a and a & b do not appear to differ much in magnitude.~~ Keep on program	24502.6	11.7
17	1925 Dec 17: 40"; v not visible	24502.6	<13.5:
18	40" for a very clear night; get 8 x 10 plate at α = 17 56 δ = –22.6; rich field, stars of all magn		

Table continued on following page

Table A. Ross's notes and derived V magnitude estimates, cont.

Ross	*Comments on Ross's note cards reproduced verbatim*	*JD 2400000.0+*	*m(V)*
20	1925 June 29: v = a + .2 = b + .2	24331.6	13.4
23	1925 June 29: v = a = b = c	24331.6	13.6
26	1925 July 20: v ≡ a + .2 ≡ b – .3	24352.6	13.8:
27	1925 July 20: v ≡ a	24352.6	13.9
28	1925 June 29: Slightly reddish; v = a + .1; v < b	24331.6	11.5
29	1925 July 20: v ≡ a – .2	24352.6	14.0
37	1925 June 29: v and b are both reddish; v ≡ a ≡ b + .2	24331.6	11.2
38	1926 Apr 16: 40"; Var. n.s.; condition v. poor		
39	1926 Apr 16: 40"; Var n.s.—condition v. poor; Strongly suspect this is an <u>asteroid</u>		
40	1926 Apr 16: 40"; v. not vis—condition v. poor; ? an asteroid at s.p.		
43	1925 Aug 27: v = a + 0.2; v = 14m±	24390.6	12.4
44	1925 Aug 27: v = a:; v = 15m	24930.6	13.8
47	Appears to be an unusual v. Seems from 3 plates of constant magn (= 11) until 1925 July 22. In one month it had fallen <u>one</u> magn. Follow closely.		
48	1925 Aug 27: v not vis in 40"; sky very transparent		
50	1925 Aug 27: v slightly reddish; v = a = 13m.	24390.6	11.1
51	1925 Aug 27: v = a – 0.1 = 15m	24390.6	13.9
52	1925 Aug 27: v is not vis in 40"; sky very transp.		
53	1925 Aug 31: v = b – .2 (v fainter)	24394.6	14.9
54	1925 Aug 31: v = a (est 14½)	24394.6	13.2
55	1925 Aug 31: v = c + .2 (+ means brighter)	24394.6	11.3
57	1925 Aug 31: 40"; v = a - .3 fainter; = b + .2 brighter	24394.6	14.3
77	1925 Sept 24: (40"); not seen. <u>a</u> was just visible	24418.6	<15.9
78	1925 Sept 24: v = <u>b</u> or <u>c</u> + .2 (brighter)	24418.6	11.7
79	1925 Sept 24: 40"; v = a = 15½m	24418.6	14.9
80	1925 Aug 31: (40"); v = reddish; = a + .2 (brighter)	24394.6	11.4
86	1925 Aug 31: (40"); v = <u>very</u> red; = a + .2 (v brighter)	24394.6	10.5
87	1925 Sept 24: (40"); v = a = 14±m	24418.6	14.3
88	<u>Shapley</u> says this is a <u>nova</u>		
90	1925 Dec 7: (40"); Not visible in 40"; Not on Barnard plate No 304, of 1905 Sept 2; Hence this is probably an asteroid		
98	1925 Dec 7: 40"; v = c	24492.6	12.5
99	1925 Dec 7: (40"); v = barely visible = 16±m; Shapley finds this is a l.p. variable; see his letter	24492.6	12.5

A Search for Eclipsing Binary Light Curve Variations Among MACHO Project Light Curves of 3,256 Fundamental-Mode RR Lyrae Variables in the Galactic Bulge

Michael W. Richmond
Physics Department, Rochester Institute of Technology, 84 Lomb Memorial Drive, Rochester, NY 14623; mwrsps@rit.edu

Received April 5, 2011; revised April 29, 2011; accepted May 27, 2011

Abstract The MACHO Project collected photometry of many RR Lyrae stars from its observations of the Milky Way's bulge. We examined the light curves of 3,256 stars identified as RRab Lyr variables by Kunder *et al.* (2008), subtracting an empirical model of the pulsation light curve and searching for periodic variation in the residuals. There are no systems which show the brief dips in light characteristic of detached eclipsing binary systems. We discuss the results for objects which show the largest residual periodic modulation, most of which are probably due to aliases of the fundamental period.

1. Introduction

Measuring the distances to objects is one of the most fundamental tasks in astronomy, yet it is also one of the most difficult. Among the many indirect methods astronomers have devised for dealing with this problem is the technique of "standard candles": identifying a class of sources which have the same luminosity and are easy to recognize. RR Lyrae stars fit into this category: they vary in brightness by a considerable amount (amplitudes of order half a magnitude) in a short time (periods of order half a day). Moreover, their light curves exhibit a characteristic shape: a rapid rise in brightness followed by a leisurely fall (Preston 1964; Jameson 1986; Smith 1995).

Although RR Lyr stars have become important tools for the investigation of galactic structure, they are not as well understood as one would wish for such fundamental calibrators. For example, we cannot compare rigorously our models of stellar structure and their predictions for pulsation to observations, because we do not know precisely the mass of any RR Lyr star. The reason is simple: despite a few false alarms (Soszyński *et al.* 2003; Prsa *et al.* 2008), and one case—TU UMa—of what may be a very wide binary containing an RR Lyr (Wade *et al.* 1999), we have found no RR Lyr stars in eclipsing binary systems which can be studied via photometric and spectroscopic methods. The discovery of even a few RR Lyr in eclipsing binary systems would provide a very valuable check to our understanding of these stars and improve our use of them as distance indicators. On the other hand, if comprehensive searches reveal that RR Lyr stars occur in binary systems at rates far below that of other, similar, stars, such as the pulsating W Vir variables which *have* been seen in eclipsing binary systems (Soszyński *et al.* 2008), we may deduce some features of the evolutionary sequence which leads to RR Lyr stars.

2. Analysis of the MACHO photometry

We begin with the collection of data described in Kunder *et al.* (2008), which includes measurements of 3,256 stars in the Galactic Bulge made during the course of the MACHO project (Alcock *et al.* 1997; Alcock *et al.* 1999). The data are available freely from the MACHO collaboration (http://wwwmacho.anu.edu.au/), but we could not find the detailed description of their analysis promised by the reference "Cook *et al.* (2007, in preparation)." We therefore do not know the particular procedures used to identify these stars as RR0 (= RRab) Lyr variables, nor to determine their fundamental periods. All we have are the results of that analysis: photometry of several thousand RR0 Lyr stars in the B_M (blue) and R_M (red) passbands of the MACHO project.

Each star in this dataset is listed with its Right Ascension and Declination and a MACHO identifier of the form *NNN.xxxxx.sssss*, in which *NNN* identifies the field, *xxxxx* the tile, and *sssss* the star within that tile. We will use this MACHO identifier as a label for particular stars throughout this paper. The data for each star consists of a fundamental period, a mean *V*-band magnitude, and a series of measurements: the Julian Date, red magnitude and estimated uncertainty, blue magnitude and estimated uncertainty. The mean *V*-band magnitudes fall largely in the range $16 < m_V < 19$, but the red and blue magnitudes listed for each measurement are on an instrumental system and lie between –5 and –8. Figure 1 shows a histogram of the number of epochs of measurements of each star, which is typically several hundred.

For the benefit of readers who may decide to use this database for their own work, let us mention that some caution is required. Some measurements ought to be discarded, for example, those marked with magnitude values of –99 or magnitude uncertainties of 9.999. We found that others are so noisy that they provide no significant information. Both the "crowding" and "FWHM" attributes associated with each measurement can be used to identify data of low significance. After examining the pattern of outliers in several test cases, we decided to discard any measurements in which the "FWHM" values for both the red and blue images were larger than 6.5 pixels.

This catalogue includes measurements made over a span of seven austral winters, starting in April 1993 and ending in October 1999, but most fields were not observed during all seven seasons. Let us choose a single star as an example, and follow it through our analysis. Star 101.21167.00060 is one of the brighter stars in the catalogue, with a mean *V*-band magnitude of 16.34. A graph of its photometry, Figure 2, reveals that its field was not part of the regular observing sequence during the second season.

The goal of this work is to seek evidence of eclipses in the light curves of RR Lyr stars. It would be easier to find such evidence if the large variations in light due to the RR Lyr pulsations are removed. Therefore, we created a model for the regular RR Lyr light curve of each star and subtracted it from the measurements, leaving the residuals for further consideration. Our method to create the model for each star was simple: we phased the data with the period given in the MACHO catalogue, divided the data into twenty bins of equal size in phase, and computed the median magnitude within each bin. We assigned this median magnitude to the phase in the middle of its bin. Finally, we interpolated linearly between these median values to determine the magnitude at any phase. Figure 3 shows the resulting models—one for the red magnitudes, one for the blue magnitudes—for star 101.21167.00060.

Note that this simple approach has an obvious drawback: it does not match the actual light curve well in places where there is sharp change, such as phase 0.7 in Figure 3. However, it does provide a reasonable model for stars with relatively few measurements, and it handles noisy data very well.

After creating separate models for the red and blue measurements of each star, we subtracted the model from the data, leaving a set of residual magnitudes. We show an example of these residuals, phased with the RR Lyr period, in Figure 4.

3. Identifying eclipsing binary candidates

Having subtracted model RR Lyr light curves from the measurements of each star in the red and blue passbands, our next task was to search for patterns in the residuals which might indicate eclipses. There are many approaches to this problem, in general, but given the nature of our data—very inhomogeneous sampling with large gaps and often high noise levels—and the uncertain nature of our expected signal—which could range from sharp, narrow dips in light to smooth, continuous variation—we chose the "string length" method (Dworetsky 1983; Bhatti *et al.* 2010).

Our implementation of this technique follows closely the description given in Bhatti *et al.* (2010). We generated string lengths for periods between 0.10 and 100 days, using steps equally spaced in frequency of size 0.0001 cycle per day. For each possible period, we computed a string length separately for the red and blue measurements, then added the two lengths to form an overall figure of merit for that period. We set thresholds for significance following the suggestions of Dworetsky (1983) and ignored periods which exceeded these thresholds. We saved the periods which yielded the ten shortest string lengths for further consideration. In addition, we computed the string length for a period of 9,999 days; since this was much longer than the actual span of observations, it yielded a "phased" light curve which was simply in chronological order. Stars with very long periods of variation would show a short string length for this artificial period.

The next step was to examine the results for each star visually. We created a graphical representation of the star's light phased with the best three periods, as shown in Figure 5. In addition to the measurements, the graph displayed the candidate periods, both in days and as a fraction of the star's RR Lyr period. A relatively quick view of this graph was sufficient to decide if any of the candidate periods yields any significant signal, and if the candidate periods are simply multiples or fractions of the RR Lyr period. The author examined graphs for all 3,256 stars in the catalogue and noted those which deserved further consideration.

Stars which did show promising signs were subjected to additional tests. First, light curves were generated for all ten of the best candidate periods, in order to see which candidate period looked most significant to the eye. Second, we sometimes tried new periods, generating graphs and string lengths manually, in order to yield a phased light curve with two maxima. For example, if the best period P created a light curve with five maxima, we checked the period $0.4P$. When the results looked good, we replaced the best automatically generated candidate period with the manually chosen period.

The final step was to improve the value of the best candidate period, and to derive an estimate for the uncertainty in that period. We set a small range around the best candidate period, extending 0.05 day in both directions, and divided the range into 10,000 pieces. After computing string lengths for each piece, we identified the range of periods which led to a local minimum in string length (see Figure 6). Following the precepts of Belserene (1983) and Fernie (1989), we fit a parabola to this local minimum and used the parameters of the fitted curve to estimate both the period and the uncertainty in the period.

Based on a visual scan of the phased light curves of the residuals for the best three candidate periods, we selected 25 of the 3,256 stars in the Kunder *et al.* (2008) catalogue for further analysis. After additional checks, we found that eleven stars show clear, periodic patterns in their residuals. We list these eleven stars, which we shall call "candidates," in Table 1. Values in the column labelled "main period" are taken from the catalogue of Kunder *et al.* (2008), while those in the column labelled "residual period" were determined by this paper. Phased light curves of each candidate are shown in Figures 7 to 17.

4. Discussion

None of these candidates shows the sharp, narrow dips of a detached system. We suggest two reasons to explain the absence of such stars: first, stars with dips of large amplitude may have been excluded from the catalogue of Kunder *et al.* (2008), if that catalogue was constructed to contain only stars with light curve shapes of an isolated RRab variable. Correspondence with the first author of Kunder *et al.* (2008) suggests that this was not the case, but we cannot dismiss it as a possibility. Second, stars with dips of small amplitude may have escaped our analysis due to the relatively low signal-to-noise ratio of the individual measurements. The dataset of Kunder *et al.* (2008) includes an estimated uncertainty with each magnitude measurement. We computed the mean value of the uncertainties for each star; the median over 3,565 stars of all those mean uncertainties is 0.023 magnitude in the red band and 0.028 magnitude in the blue band. A system of shallow eclipses, with an amplitude of only two or three times the typical uncertainty and involving only a small fraction of the measurements, would not be found by our methods. The smallest amplitude among our eleven candidates is 0.07 magnitude peak-to-peak, and that variation involves all the measurements in the light curve, not just a few.

All the candidates have gently undulating light curves, rather than the sharp dips of a detached eclipsing system. What might cause this sort of periodic variation? Among the possibilities are artifacts from the subtraction of the model light curve; aliases of the RR Lyr frequency; an additional frequency of oscillation in the RR Lyr star; Blazhko variations in the RR Lyr star; blended light from another variable star(s); or the orbital motion of the RR Lyr star around a close companion. Let us examine these possibilities.

Our method for subtracting the main RR Lyr light curve from each star's measurements was based on a simple model made of linear segments. If the model failed to reproduce some features properly, the subtraction would leave a signal with the same period as the RR Lyr pulsation. Our eleven candidates include three stars for which the residual period is within three percent of the main RR Lyr period; we mark these in Table 1 with an "A" in the "Notes" column. It is possible that these candidates may be due to a low-amplitude version of the Blazhko effect, of which we say more below.

The majority of the measurements described in Kunder *et al.* (2008) were collected on a nightly basis; that is, each star was observed once per night, and often at roughly the same time. We therefore expect to see aliases of the true frequency ω_0 in the measurements with frequencies

$$\omega_{\text{alias}} = | \, \omega_0 \pm N \, \omega_{\text{sample}} \, | \tag{1}$$

where $\omega_{\text{sample}} = 1$ day^{-1} and N is some small integer. We computed the alias frequencies for all candidates using $N = 1$ and 2, and compared them to the frequencies of the residual variations. We found two cases in which the residual frequencies were within one percent of the main RR Lyr frequency (marked "B" in Table 1, two more cases within two percent (marked "C") and one more case within three percent (marked "D").

Some RR Lyr stars are known to oscillate at two frequencies; these double-mode stars always have a ratio of periods $P_1 \, / \, P_0 \simeq 0.746$ (Nemec 1985; Szczygiel and Fabrycky 2007). None of our candidates have periods in their residuals which yield this ratio with the periods listed in Kunder *et al.* (2008). The lack of such double-mode pulsators may not be unexpected, since they appear to be very rare in the central regions of our Milky Way; Mizerski (2003) found only three such stars among a sample of 1942 RRab and 771 RRc stars observed near the center of the Milky Way in the OGLE-II database (Udalski *et al.* 1997). Their absence may also be a reflection of the selection criteria used by Kunder *et al.* (2008) to create the catalogue of RR Lyr stars.

Some RR Lyr stars exhibit slow changes in the shape and amplitude of their light curves, with periods of tens to hundreds of days; this is known as the Blazhko effect. Mizerski (2003) finds roughly twenty-five percent of all RRab stars in a sample near the galactic center show the Blazhko effect. Could it be responsible for any of our candidates? MACHO 124.22289.00461, with a residual period of just over 17 days, is the only candidate for which this seems a possibility. Unfortunately, since the main RR Lyr period is almost exactly half a day, the measurements made during each observing season cover only a small range in phase; thus, we cannot see if the shape of the light curve changes over this 17-day interval. The three stars marked with an "A" in Table 1 have residual periods which could be produced by Blazhko-like periods of 15 to 50 days beating against the main RR Lyr period; however, we examined the phased light curves of these stars over each season and see no strong evidence of Blazhko variations.

The MACHO study area in the galactic bulge was, by design, chosen to have a very high stellar density. If the density is high enough, we may expect that blends of unrelated foreground or background variable stars may cause periodic signals in the residuals of RR Lyr light curves. Let us perform a very quick quantitative check on this idea. We examined one of the fields in this area, number 102, counting all the stars in the MACHO database (not just the variable ones) as a function of apparent V-band magnitude. Since the typical FWHM in these measurements is 3.5", a rough estimate of the area of the seeing disk is about ten square arcseconds. We find that, on average, there are 1.8 stars with $V \leq 20.1$ in each seeing disk, and about 0.5 star with $V \leq 18.1$. The RR Lyr stars in the catalogue of Kunder (2008) range roughly $16 \leq V \leq 19$, so indeed a significant fraction of all the RR Lyr stars in the catalogue must be contaminated by light from nearby stars at a level of 0.1 magnitude. It may in fact be surprising that we find so few objects with periodic variations in their residuals; however, since we do not know the details of the process by which RR Lyr stars were selected from the MACHO database, we cannot comment further.

Could any of the candidates be due to the effects of a binary companion of the RR Lyr star? If two stars orbit each other with a separation which is only slightly larger than their combined radii, their shapes may grow distorted enough that they produce a gently undulating light curve, even in the absence of eclipses. An RR Lyr star of mass 0.7 $M_{\odot}$ with a companion of equal mass in a circular orbit of period 2 days would have a separation of about 7 $R_{\odot}$. The radius of a typical RR Lyr star varies from about 4 $R_{\odot}$ to 6 $R_{\odot}$ (Sodor *et al.* 2009), leaving little room for a companion. If an RR Lyr star did orbit a more compact companion with a period in this range, it would surely be greatly distorted, and so liable to vary in brightness as it moved in its orbit. Whether an RR Lyr star would have stable pulsations in such a close orbit is beyond the scope of this paper. Note that in this situation, the period listed in Table 1 would be *half* of the orbital period.

5. Conclusion

We conclude that our search through a sample of 3,256 RRab Lyr stars failed to find any detached eclipsing binary systems, and very likely failed to find eclipsing systems of any sort with amplitudes of ≥ 0.07 magnitude. The implied disjunction between stars pulsing in the fundamental RRab Lyr mode and stars in binary systems may provide clues to the evolution of RRab Lyr stars. Our simple technique for removing the ordinary variation of light in order to seek some signal in the residuals would be well suited to the more sinusoidal variations of RRc Lyr stars, many of which can be found in the catalogues of Soszyński *et al.* (2009) and Soszyński *et al.* (2003).

6. Acknowledgements

This paper utilizes public domain data obtained by the MACHO Project, jointly funded by the U.S. Department of Energy through the University of California, Lawrence Livermore National Laboratory under contract No. W-7405-Eng-48, by the National Science Foundation through the Center for Particle Astrophysics of the University of California under cooperative agreement AST-8809616, and by the Mount Stromlo and Siding Spring Observatory, part of the Australian National University. The author thanks Doug Welch for reviewing an early version of this paper and providing many suggestions which improved it.

References

Alcock, C., *et al.* 1997, *Astrophys. J.*, **486**, 697.
Alcock, C., *et al.* 1999, *Publ. Astron. Soc. Pacific*, **111**, 1539.
Belserene, E. P. 1983, in *Microcomputers in Astronomy*, R. M. Genet, A. M. Genet, eds., Fairborn Observatory, Fairborn, Ohio, 229.
Bhatti, W. A., Richmond, M. W., Ford, A. C., and Petro, L. D. 2010, *Astrophys. J., Suppl. Ser.*, **186**, 233.
Dworetsky, M. M. 1983, *Mon. Not. Roy. Astron. Soc.*, **203**, 917.
Fernie, J. D. 1989, *Publ. Astron. Soc. Pacific*, **101**, 225.
Jameson, R. F. 1986, *Vistas Astron.*, **29**, 17.
Kunder, A., Popowski, P., Cook, K. H., and Chaboyer, B. 2008, *Astron. J.*, **135**, 631.

Mizerski, T. 2003, *Acta Astron.*, **53**, 307.
Nemec, J. M. 1985, *Astron. J.*, **90**, 240.
Preston, G. W. 1964, *Ann. Rev. Astron. Astrophys.*, **2**, 23.
Prsa, A., Guinan, E. F., Devinney, E. J., and Engle, S. G. 2008, *Astron. Astrophys.*, **489**, 1209.
Smith, H. A. 1995, *RR Lyrae Stars*, Cambridge Univ. Press, New York.
Sodor, A., Jurcsik, J., and Szeidl, B. 2009, *Mon. Not. Roy. Astron. Soc.*, **394**, 261.
Soszyński, I., *et al.* 2003, *Acta Astron.*, **53**, 93.
Soszyński, I., *et al.* 2008, *Acta Astron.*, **58**, 293.
Soszyński, I., *et al.* 2009, *Acta Astron.*, **59**, 1.
Szczygiel, D. M., and Fabrycky, D. C. 2007, *Mon. Not. Roy. Astron. Soc.*, **377**, 1263.
Udalski, A., Kubiak, M., and Szymanski, M. 1997, *Acta Astron.*, **47**, 319.
Wade, R. A., Donley, J., Fried, R., White, R. E., and Saha, A. 1999, *Astron. J.*, **118**, 2442.

Table 1. Candidate stars with periodic residuals.

MACHO identification	*R.A. (J2000) h m s*	*Dec. (J2000) ° ′ ″*	*V*[1]	*Main Period*	*Residual Period (d)*	*Amplitude*[2]	*Notes*[3]
101.21042.00862	18 05 18.60	–27 16 14.5	17.55	0.413096	0.402423 ± 0.000005	0.13	A
102.22598.00556	18 08 54.96	–27 31 49.4	17.36	0.444434	0.448350 ± 0.000005	0.13	A
115.22566.00425	18 09 09.00	–29 40 30.4	16.83	0.530609	1.15473 ± 0.00004	0.08	D
121.21518.00593	18 06 25.92	–30 12 03.2	17.44	0.452635	0.83703 ± 0.00003	0.07	C
124.22289.00461	18 08 15.72	–30 50 30.5	17.72	0.498851	17.076 ± 0.002	0.12	
125.23719.00262	18 11 45.96	–30 50 13.2	16.47	0.684945	0.403118 ± 0.000005	0.10	B
147.31018.00579	18 28 43.68	–29 31 55.6	18.45	0.528649	0.46484 ± 0.00001	0.22	
159.25743.00689	18 16 18.12	–25 52 22.4	17.56	0.459778	0.86010 ± 0.00003	0.15	B
163.27167.00172	18 19 39.36	–26 15 58.0	16.98	0.428079	0.71677 ± 0.00003	0.16	
307.35371.00305	18 14 57.12	–24 04 48.7	17.62	0.611346	0.59703 ± 0.00001	0.07	A
311.38064.00227	18 19 33.60	–23 46 16.0	16.86	0.528800	1.13961 ± 0.00005	0.17	C

[1] Mean magnitude, from Table 3 of Kunder et al. (2008). [2] Magnitude of residual variation, peak–to–peak in blue band. [3] A = residual period within 3% of main period; B = residual period within 1% of 1–day alias; C = within 2% ; D = within 3%.

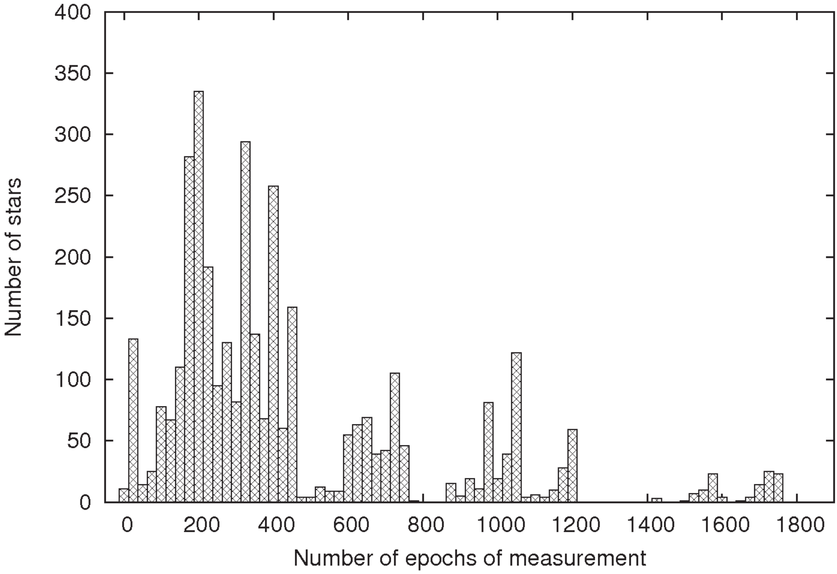

Figure 1. Number of epochs of measurements for stars in the MACHO Bulge RR0 Lyr catalogue.

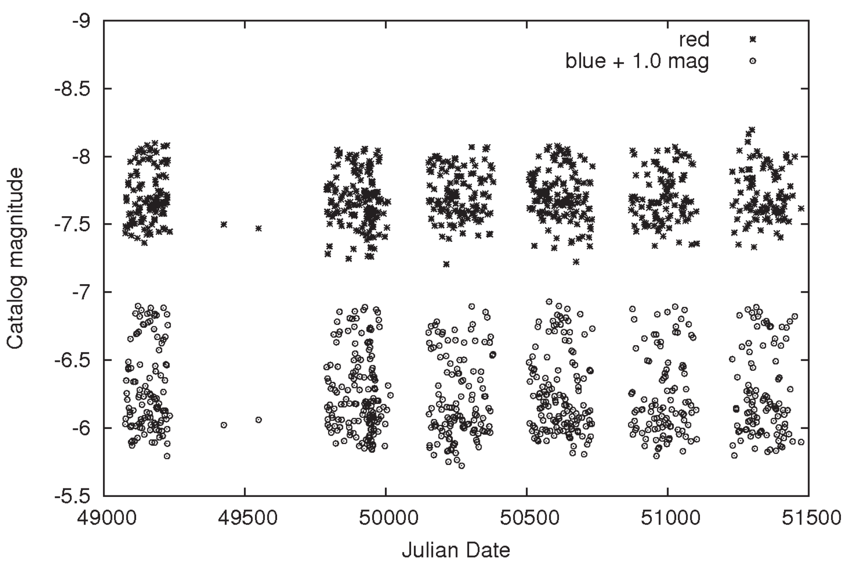

Figure 2. Photometry of one bright star. From raw measurements in the MACHO RR0 Lyr catalogue: star 101.21167.00060.

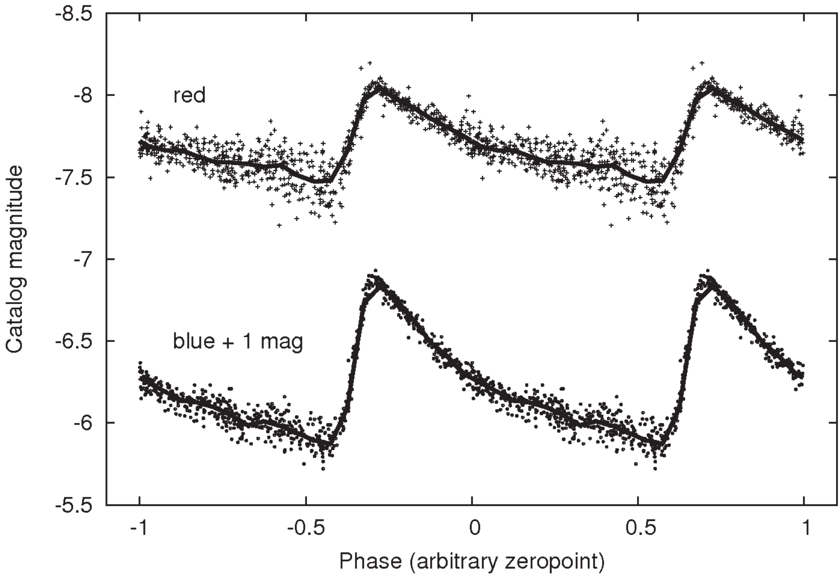

Figure 3. The model light curves for one bright star. Light curve of star 101.21167.00060, phased with catalogue RR Lyr period.

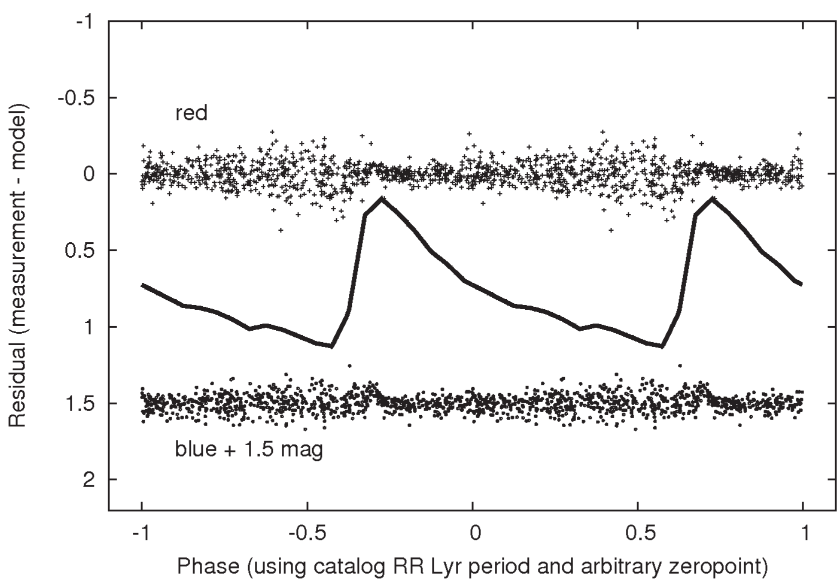

Figure 4. Residuals from the model light curves for one bright star; the blue model curve is shown, offset from the measurements for clarity. Residuals from fit to light curve of star 101.21167.00060.

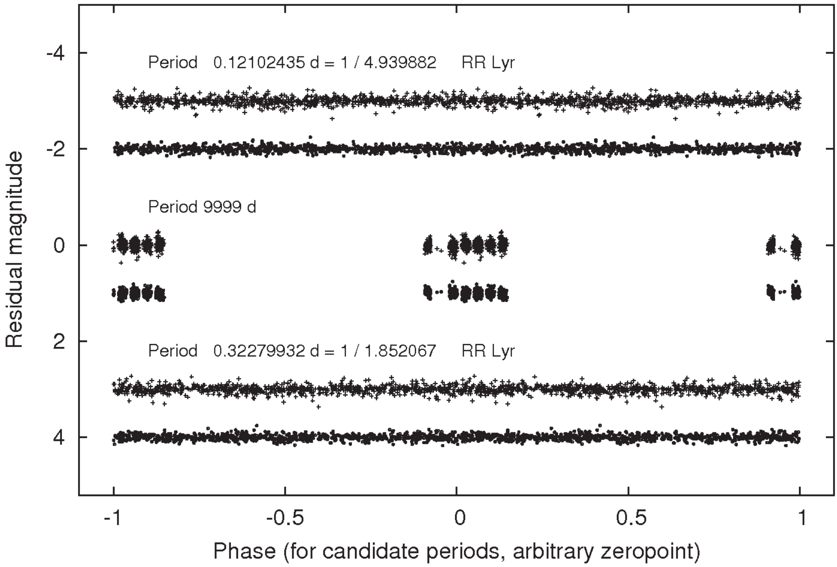

Figure 5. Light curves for the residuals of a bright star, phased with the best three candidate periods. Top three candidate periods for star 101.21167.00060.

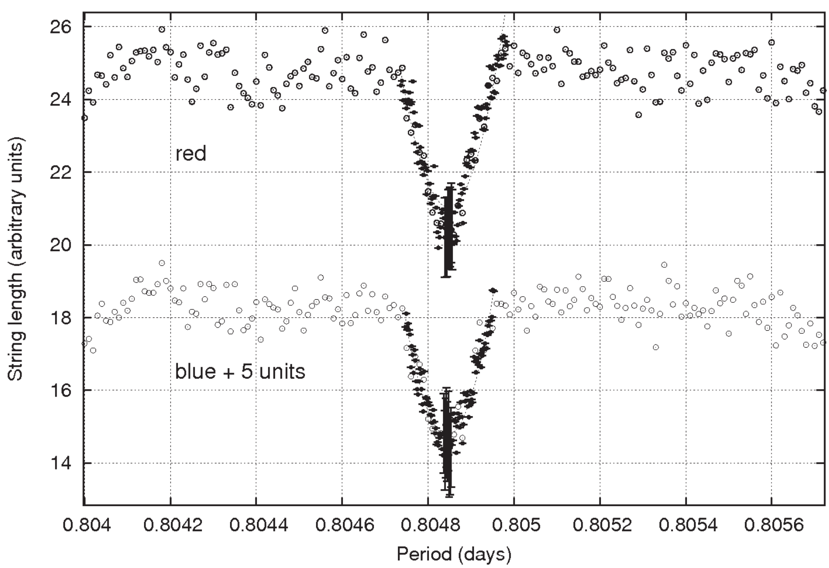

Figure 6. Determining the uncertainty in the best candidate period; the symbols with vertical error bars span the uncertainty in period. Results of finetune period search on MACHO 101.21042.00862.

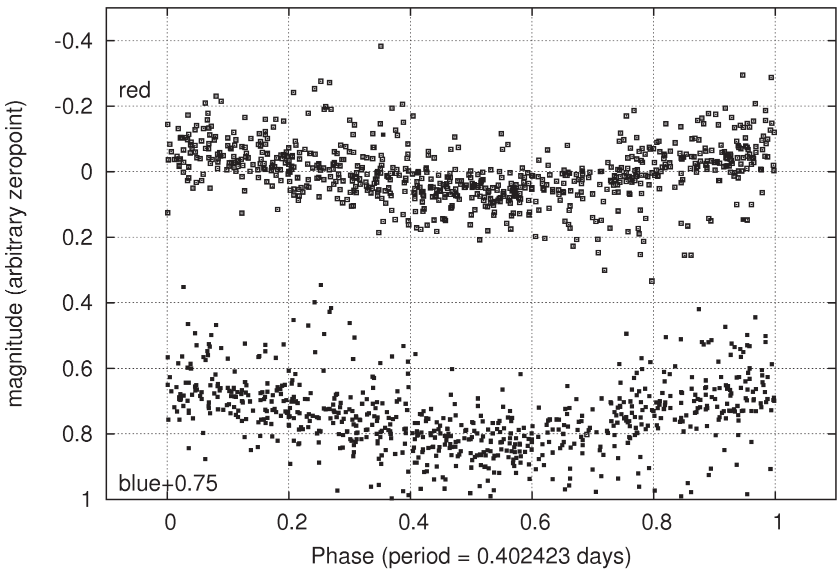

Figure 7. Phased light curve of residuals of star 101.21042.00862.

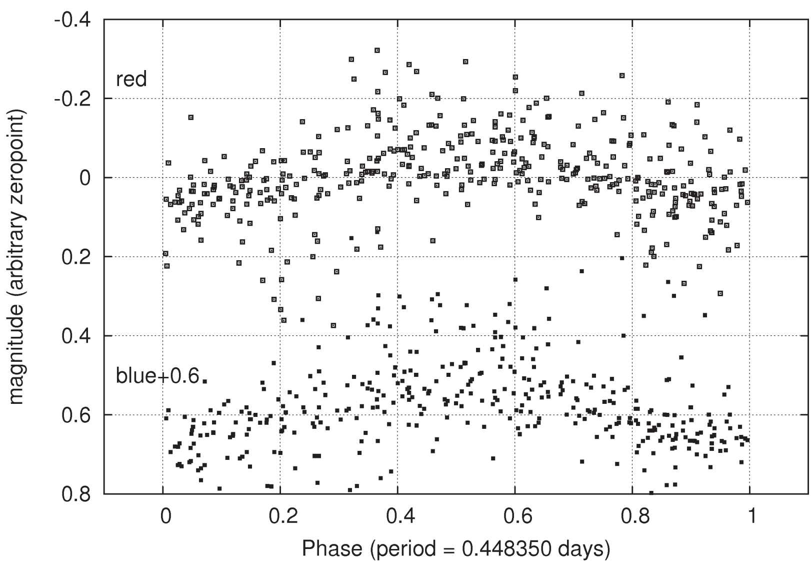

Figure 8. Phased light curve of residuals of star 102.22598.00556.

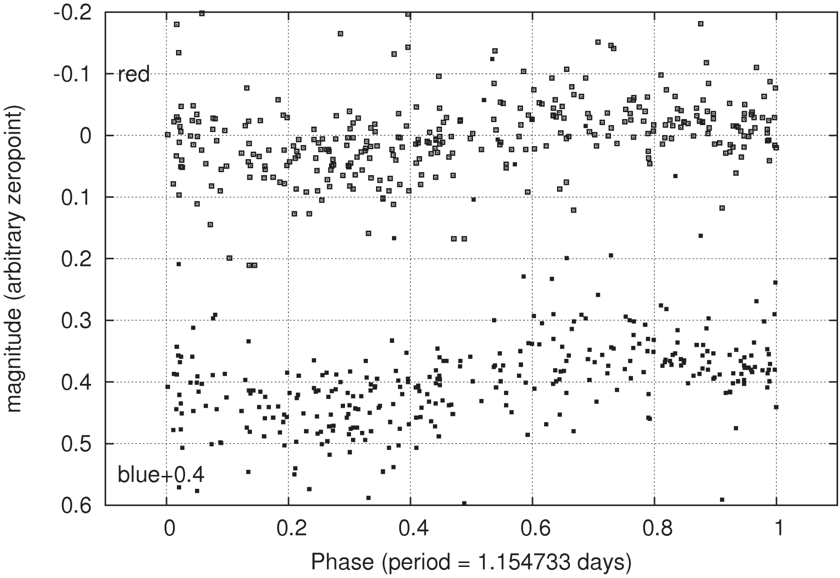

Figure 9. Phased light curve of residuals of star 101.22566.00425.

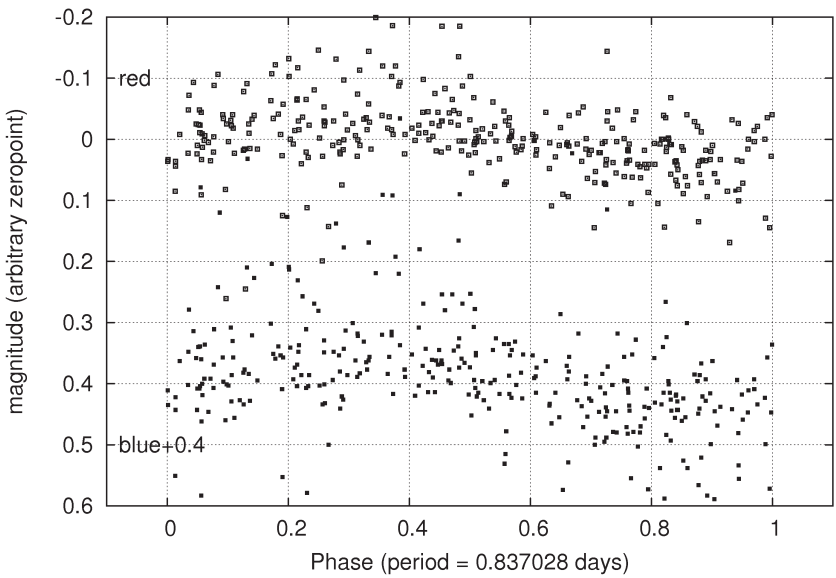

Figure 10. Phased light curve of residuals of star 121.21518.00593.

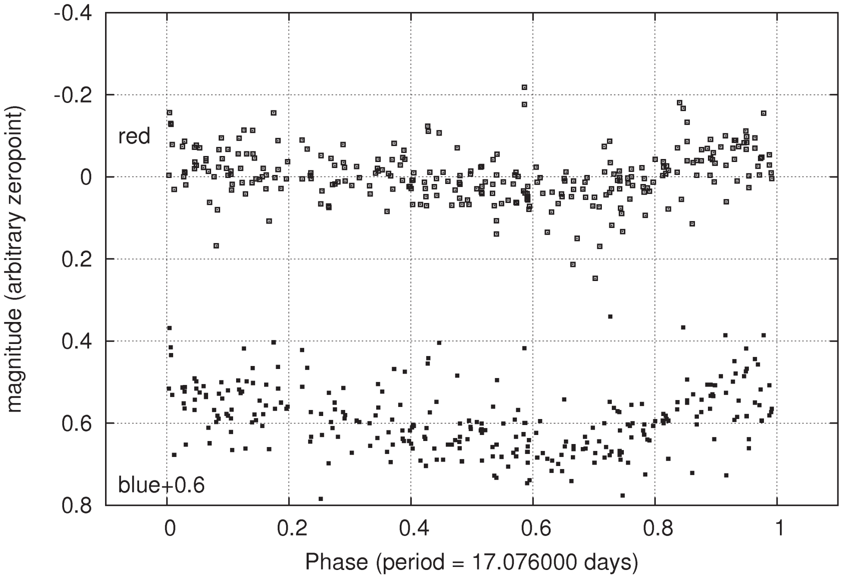

Figure 11. Phased light curve of residuals of star 124.22289.00461.

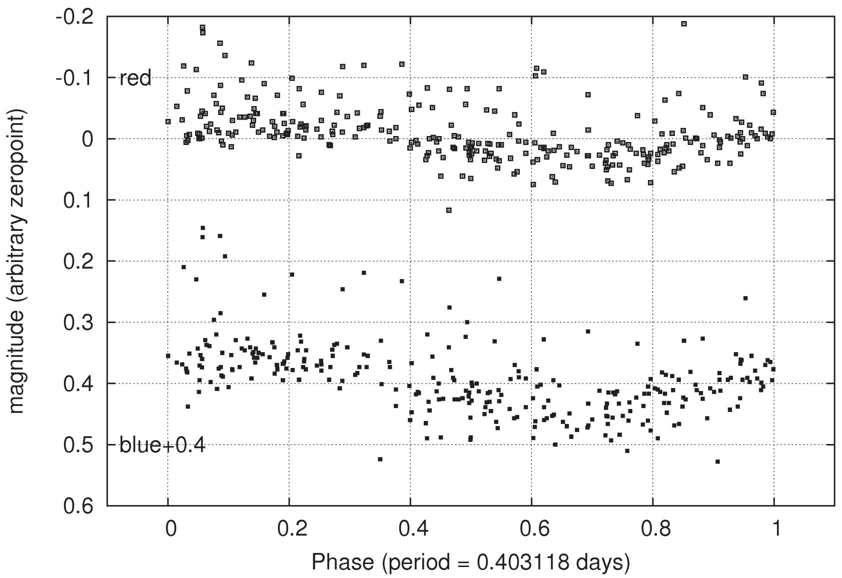

Figure 12. Phased light curve of residuals of star 125.23719.00262.

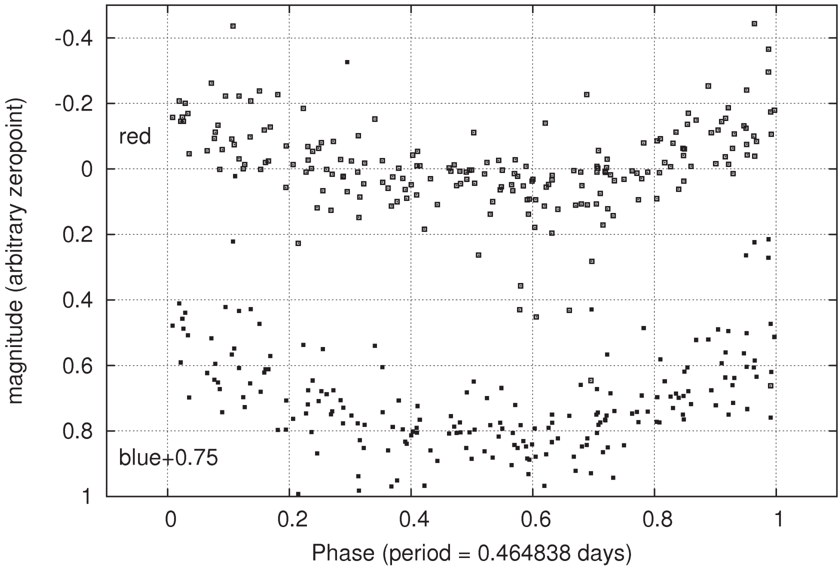

Figure 13. Phased light curve of residuals of star 147.31018.00579.

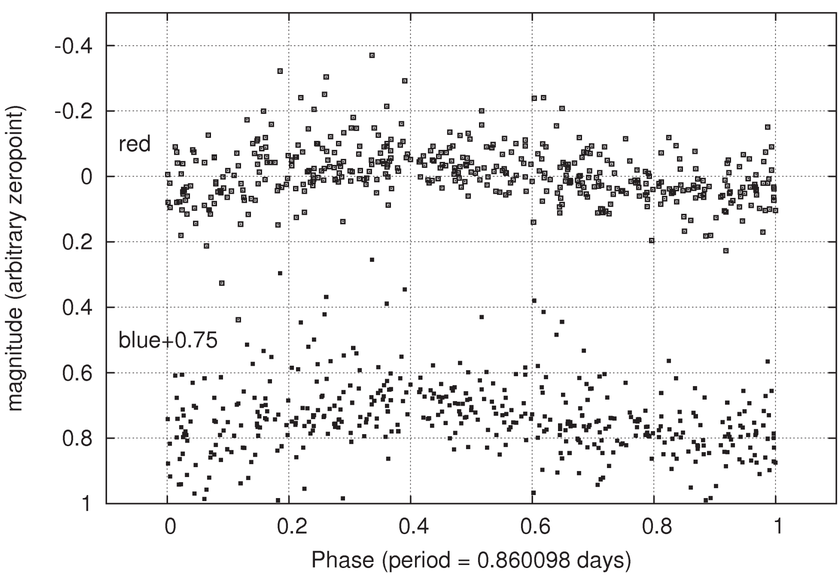

Figure 14. Phased light curve of residuals of star 159.25743.00689.

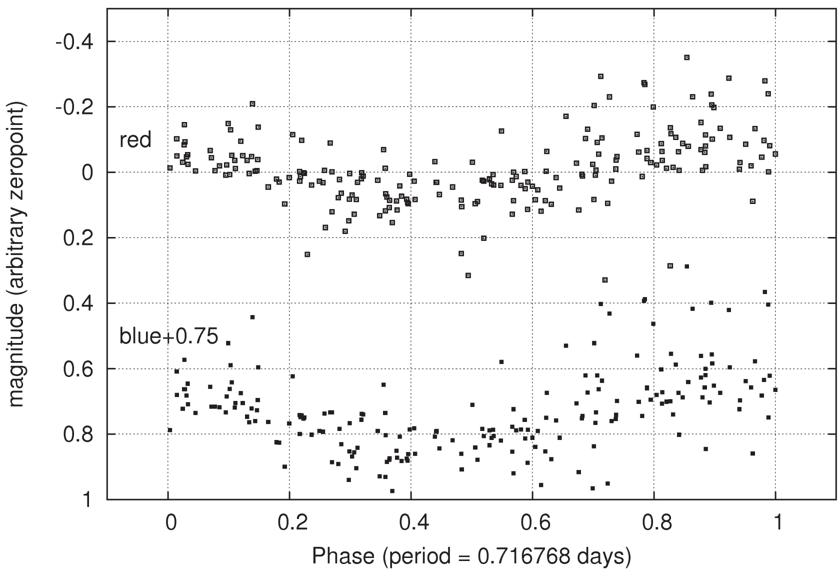

Figure 15. Phased light curve of residuals of star 163.27167.00172.

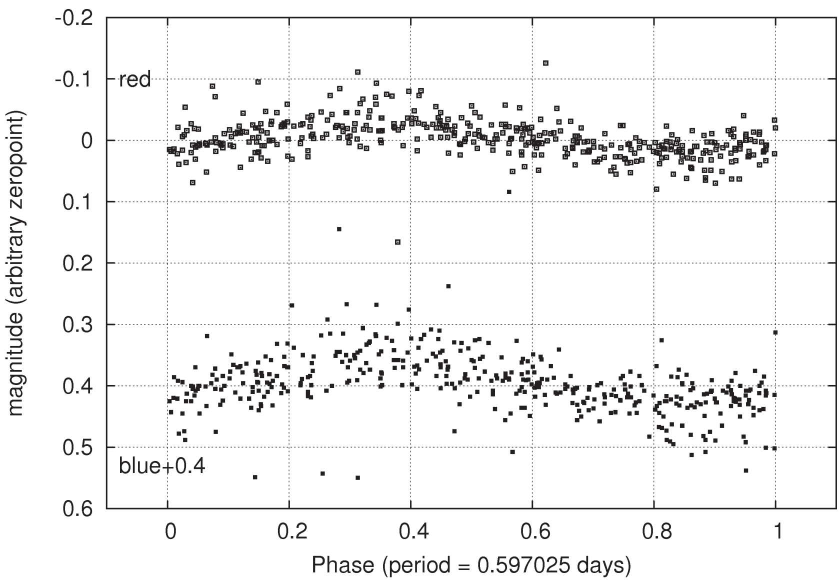

Figure 16. Phased light curve of residuals of star 307.35371.00305.

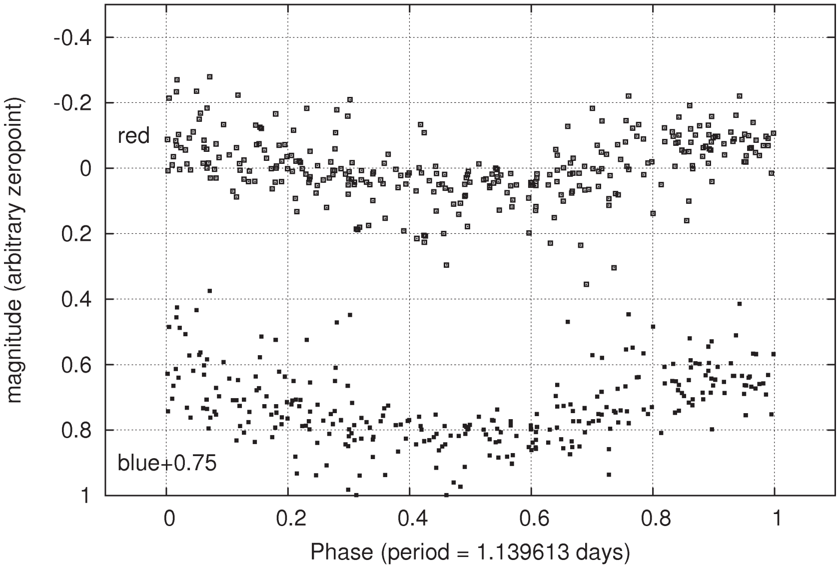

Figure 17. Phased light curve of residuals of star 307.35371.00305.

Deep Infrared ZAMS Fits to Benchmark Open Clusters Hosting δ Scuti Stars

Daniel J. Majaess
David G. Turner
David J. Lane
Saint Mary's University, Department of Astronomy and Physics, Halifax, Nova Scotia, B3H 3C3, Canada; dmajaess@ap.smu.ca

and

The Abbey Ridge Observatory, Stillwater Lake, Nova Scotia, Canada

Tom Krajci
Astrokolkhoz Telescope Facility, P.O. Box 1351, Cloudcroft, NM 88317

Received December 14, 2010; revised February 23, 2011; accepted February 23, 2011

Abstract This research aims to secure precise distances for cluster δ Scuti stars in order to investigate their properties via a *VI* Wesenheit framework. Deep JHK_s color-color and zero-age main sequence (ZAMS) relations derived from ≃ 700 unreddened stars featuring 2MASS photometry and precise Hipparcos parallaxes ($d \lesssim 25$ pc) are applied to establish distances to several benchmark open clusters that host δ Scuti stars: Hyades, Pleiades, Praesepe, α Persei, and M67 (d = 47 ± 2, 138 ± 6, 183 ± 8, 171 ± 8, 815 ± 40 pc). That analysis provided constraints on the δ Sct sample's absolute Wesenheit magnitudes ($W_{VI,0}$), evolutionary status, and pulsation modes (order, n). The reliability of JHK_s established cluster parameters is demonstrated via a comparison with van Leeuwen (2009a) revised Hipparcos results. Distances for seven of nine nearby ($d \leq 250$ pc) clusters agree, and the discrepant cases (Pleiades and Blanco 1) are unrelated to (insignificant) $T_e - (J–K_s)$ variations with cluster age or iron abundance. JHK_s photometry is tabulated for $\simeq 3 \times 10^3$ probable cluster members on the basis of proper motions (NOMAD). The deep JHK_s photometry extends into the low mass regime (≃ 0.4 $M_\odot$) and ensures precise (≤ 5%) ZAMS fits. Pulsation modes inferred for the cluster δ Scuti stars from *VI* Wesenheit and independent analyses are comparable (± n), and the methods are consistent in identifying higher order pulsators. Most small-amplitude cluster δ Scuti stars lie on *VI* Wesenheit loci characterizing n ≥ 1 pulsators. A distance established to NGC 1817 from δ Scuti stars ($d \simeq 1.7$ kpc) via a universal *VI* Wesenheit template agrees with estimates in the literature, assuming the variables delineate the n ≥ 1 boundary. Small statistics in tandem with other factors presently encumber the use of mmag δ Scuti stars as viable distance indicators to intermediate-age open clusters, yet a *VI* Wesenheit approach is a pertinent means for studying δ Scuti stars in harmony with other methods.

1. Introduction

δ Sct variables are unique among standard candles of the classical instability strip for permitting the determination of distances to population I and II environments from a single *VI* Wesenheit calibration. SX Phe and other metal-poor population II δ Scuti stars lie toward the short-period extension of the Wesenheit ridge characterizing population I δ Scuti stars (Figure 3 in Majaess *et al.* 2010; see also Petersen and Høg 1998). That presents an opportunity to bridge and strengthen the distance scales tied to globular clusters, open clusters, nearby galaxies, and the Galactic center where such variables are observed (McNamara *et al.* 2000, 2007; Poleski *et al.* 2010; Majaess *et al.* 2010). To that end the present research examines δ Sct calibrators associated with benchmark open clusters via a *VI* Wesenheit framework, an analysis which relies on the establishment of precise cluster distances and multiband photometry ($VIJHK_s$).

In this study, infrared color-color and zero-age main sequence (ZAMS) relations are constructed from unreddened stars in close proximity to the Sun with precise Hipparcos parallaxes (section 2). The relations are subsequently employed to establish parameters for five benchmark open clusters which host δ Scuti stars, namely the Hyades, Pleiades, Praesepe, α Persei, and M67 (section 2). Cluster membership provides constraints on the absolute Wesenheit magnitudes ($W_{VI,0}$), evolutionary status, and pulsation modes (order, n) for the δ Scuti stars (section 3). An independent determination of the cluster parameters is pursued since the objects form the foundation of the open cluster scale and yet their distances are uncertain. Most notably the Hipparcos distance to stars in the Pleiades is $d = 120.2 \pm 1.9$ pc (van Leeuwen 2009a), whereas HST observations imply $d = 134.6 \pm 3.1$ pc (Soderblom *et al.* 2005). Likewise, four Hipparcos-based distances cited in the literature for α Persei disagree (Table 1). In section 3, a Wesenheit analysis (*VI*) is shown to be a viable means for investigating δ Scuti stars. Lastly, the distance to NGC 1817 is evaluated via a universal Wesenheit template using new *VI* photometry acquired from the Abbey Ridge Observatory (ARO, Lane 2007; Turner *et al.* 2009) for the cluster's numerous δ Scuti stars (section 3.4).

2. JHK_s intrinsic relations

Intrinsic color-color and ZAMS relations are derived from *JHKs* photometry for A, F, G, K, and M-type stars that feature precise parallaxes ($d \lesssim 25$ pc). The infrared photometry and parallaxes are provided via the 2MASS and Hipparcos surveys (Perryman *et al.* 1997; Cutri *et al.* 2003; Skrutskie *et al.* 2006). 2MASS photometry may be saturated for nearby stars, yet reliable data are available for fainter stars of late spectral type. The photometric uncertainties thus increase for brighter early-type stars (Figure 1), which are already undersampled owing to the nature of the initial mass function. Spurious data deviating from the evident intrinsic functions were excluded.

M_J / $(J–H)_0$ and M_J / $(J–K_s)_0$ color-magnitude diagrams for the calibration are presented in Figure 1 (red dots). The latter passband combination exhibits smaller uncertainties. $(J–H)_0$ / $(H–K_s)_0$ and $(J–K_s)_0$ / $(H–K_s)_0$ color-color diagrams are likewise shown in Figure 1 (red dots). Infrared relations offer advantages over those founded on *UBV* photometry owing to the mitigated impact of chemical composition (section 2.1, Figure 3), differential reddening, and total extinction.

Color-magnitude and color-color diagrams were assembled for the target clusters by obtaining 2MASS photometry for members on the basis of proper motions (Figures 1 and 2). The Naval Observatory Merged Astrometric Dataset (NOMAD, Zacharias *et al.* 2004) features proper motion data for the fields inspected. JHK_s photometry for $\sim 3 \times 10^3$ probable clusters members were tabulated, and the list includes several previously unidentified members. That sample shall be made available online via the Centre de Données astronomiques de Strasbourg. Photometry for the brighter stars may be saturated, as noted earlier, while lower mass members are catalogued despite being near the faint-limit of the 2MASS survey. High-precision multi-epoch JHK_s data for M67 are available from Nikolaev *et al.* (2000, see also Sarajedini *et al.* 2009).

Reddenings for the target clusters were secured by shifting the intrinsic color-color relations to the observed data (Figure 1). JHK_s extinction laws were adopted from Bonatto *et al.* (2008) and references therein. The distance to a cluster follows by matching the ZAMS to the observed data for the reddening established by the intrinsic color-color relations. Precise results were obtained because the trends for late-type stars in JHK_s color-magnitude and color-color diagrams provide excellent anchor points for fitting ZAMS and intrinsic relations (Figures 1 and 2). $J–K_s$ and $J–H$ were observed to remain nearly constant and become bluer with increasing magnitude ($M_J \gtrsim 6$) for low mass main-sequence stars beginning near spectral type M (Figures 1 and 2, see also Sarajedini *et al.* 2009 and references therein), and a sizable separation exists between main-sequence and evolved M-type stars in the JHK_s color-color diagram (see also Straižys and Laugalys 2009). Turner (2011) developed intrinsic JHK_s functions to describe early-type stars ($\lesssim$ K0) via an alternate approach.

Distances obtained for the benchmark clusters examined are summarized in Table 1.

2.1. Age and metallicity dependencies

The JHK_s distances agree with van Leeuwen (2009a) Hipparcos results for seven of nine star clusters within 250 pc (Table 1). The distance determined here to the Pleiades favors the HST estimate rather than that established by Hipparcos (Table 1. The HST and Hipparcos Pleiades surveys lack overlap, and the former exhibits comparatively smaller statistics). Soderblom *et al.* (2005) (and others) argue that the Hipparcos distance to the Pleiades is erroneous. Conversely, the reliability of the ZAMS distance to the Pleiades has been questioned owing to the possible neglect of color-T_e variations with stellar age and chemical composition. The matter is now investigated.

An age-luminosity effect has been proposed as a possible source for the disagreement between the ZAMS and Hipparcos distance to the Pleiades. That hypothesis is not supported by the infrared distances established here. The Hyades, Praesepe, and α Persei clusters bracket the discrepant cases of the Pleiades and Blanco 1 in age (Table 1). JHK_s and van Leeuwen (2009a) Hipparcos distances to the former clusters are in broad agreement (Table 1). The comparatively nearby ($d \leq 250$ pc) open clusters IC 2602, NGC 2451, IC 2391, and Coma Berenices were investigated to bolster the case, but proved more difficult to assess. The Hipparcos distance to the Pleiades implies that the cluster's ZAMS is a sizable $\simeq$ 0.4 magnitude below the faintest calibration stars (Figure 1), where the photometric uncertainties are minimized, M_J / $(J–K_s)_0$). The Hipparcos zero-point for the Pleiades is inconsistent with a M_J / $(J–K_s)_0$ ZAMS calibration (Figure 1) which features stars of differing age, chemical composition, and peculiarities.

The clusters in Table 1 exhibiting discrepant distances are not correlated with iron abundance. That supports Alonso *et al.* (1996) and Percival *et al.* (2005) assertion that $J–K_s$ is relatively insensitive to metallicity over the baseline examined. Percival *et al.* (2005) suggested that $J–K_s$ may exhibit a marginal dependence on metallicity, but cautioned that the errors are sizable and the correlation coefficient is consistent with zero. The impact of a marginal T_e – [Fe / H] – $(J–K_s)$ dependence appears insignificant since stars belonging to the clusters examined display near solar iron abundances (Mermilliod *et al.* 1997; van Leeuwen 1999, their Table 1.) 270 calibration stars (Figure 1) featured in Soubiran *et al.* (2010) PASTEL catalogue of stellar atmospheric parameters exhibit a peak distribution near [Fe / H] $\simeq$ –0.05, which is analogous to or inappreciably less than members of the Pleiades ([Fe / H] = –0.039 ± 0.014, +0.03 ± 0.05, +0.06 ± 0.01, Taylor 2008; Soderblom *et al.* 2009; Paunzen *et al.* 2010). Colors for calibrating stars (Figure 1) in PASTEL were plotted as a function of effective temperature and metallicity (Figure 2, optical photometry from Mermilliod 1991). $B–V$ and $U–B$ color indices appear sensitive to iron abundance whereby metal-rich stars are hotter at a given color (Figure 2), as noted previously (Turner 1979, and references therein). Conversely, $J–K_s$ appears comparatively insensitive to iron abundance over the restricted baseline examined (Figure 2). Yet the results should be interpreted cautiously and in tandem with the other evidence presented given the semi-empirical nature of that analysis (T_e and [Fe / H] are model dependent).

The clusters exhibit a similar ZAMS morphology in the infrared (M_J / $(J–K_s)_0$, Figures 1 and 2). The Hyades, Praesepe, Pleiades, and M67 ZAMS (unevolved members) are nearly indistinguishable (Figure 2). Stauffer *et al.* (2003) likewise noted that the Praesepe and Pleiades cluster share a ZAMS (M_v / $(V–I)_0$) that is essentially coincident throughout. By contrast, the apparent sensitivity of optical photometry to metallicity may explain (in part) certain anomalies which distinguish individual clusters in optical color-magnitude and color-color diagrams

(Figure 3, see also Turner 1979; Mermilliod *et al.* 1997; Stauffer *et al.* 2003; van Leeuwen 2009a). Compounded uncertainties prevent a direct assessment of the infrared color-color function's universality ($(J–K_s)_0$ / $(H–K_s)_0$). Minimizing the uncertainties associated with the JHK_s photometry and extending the restricted temperature baseline are desirable. Fainter JHK_s observations could be acquired from l'Observatoire Mont-Mégantique or the forthcoming *VVV* survey (Artigau *et al.* 2009, 2010; Minniti *et al.* 2010), whereas brighter stars could be observed as part of the AAVSO's IR photoelectric photometry program (Henden 2002; Templeton 2009).

In sum, neither variations in iron abundance or stellar age readily explain the discrepancies between the JHK_s ZAMS and Hipparcos distances (Table 1). It is emphasized that the problematic cases (the Pleiades and Blanco 1) constitute the minority (Table 1). Note that the four published Hipparcos distances to Blanco 1 exhibit a sizable 20% spread (Table 1, see also α Persei). Further research is needed, and the reader should likewise consider the interpretations of Mermilliod *et al.* (1997), Robichon *et al.* (1999b), Soderblom *et al.* (2005), and van Leeuwen (2009a, 2009b).

3. Cluster δ Scuti stars

3.1. *VI* photometry

The cluster δ Scuti stars examined are summarized in Table 4, along with references for their *VI* photometry. Certain sources feature *I*-band photometry not standardized to the Cousins system (e.g., Mendoza 1967). Additional observations for the δ Scuti stars were obtained via the AAVSO's Bright Star Monitor (BSM, http://www.aavso.org/aavsonet) and the Naval Observatory's Flagstaff Station (NOFS) (Table 2). The BSM features an SBIG ST8XME CCD (fov: 127' × 84') mounted upon a 6-cm wide-field telescope located at the Astrokolkhoz telescope facility near Cloudcroft, New Mexico. The AAVSO observations are tied to Landolt (1983, 1992) photometric standards according to precepts outlined in Henden and Kaitchuck (1990) (see also Henden and Munari 2008).

VI photometry is used since LMC and Galactic δ Scuti stars follow *VI* Wesenheit relations which vary as a function of the pulsation order *n* (Figure 4, Poleski *et al.* 2010; Majaess *et al.* 2010), thereby enabling constraints on that parameter for target δ Scuti stars at common or known distances (see section 3.3). Furthermore, the author has advocated that RR Lyrae variables and Cepheids—which partly form the basis for the calibration used in section 3.2—obey *VI* Wesenheit and period-color relations which are comparatively insensitive to metallicity (Majaess *et al.* 2008, 2009a, 2009b; Majaess 2009, 2010a, 2010b; see also Bono and Marconi 1999; Udalski *et al.* 2001; Bono 2003; Pietrzyński *et al.* 2004; Bono *et al.* 2008). For example, Majaess (2010b) reaffirmed that the slope of the *VI* Wesenheit function for Milky Way Classical Cepheids (Benedict *et al.* 2007; Turner 2010a) characterizes classical Cepheids in the LMC, NGC 6822, SMC, and IC 1613 (see Figure 2 in Majaess 2010b). Classical Cepheids in the aforementioned galaxies exhibit precise ground-based photometry, span a sizable abundance baseline, and adhere to a common *VI* Wesenheit slope to within the uncertainties ($\alpha = -3.34 \pm 0.08(2\sigma)$, Δ [Fe / H] $\simeq 1$). More importantly, Majaess (2010b) noted that a negligible distance offset exists between OGLE classical Cepheids and RR Lyrae variables in the LMC, SMC, and IC 1613 as established via a *VI* Wesenheit function, thereby precluding a dependence on metallicity. Admittedly, the impact of a reputed metallicity effect is actively debated in the literature (Smith 2004; Romaniello *et al.* 2008; Catelan 2009, and references therein. By contrast there appears to be a consensus that relations which rely on *BV* photometry are sensitive to variations in chemical abundance (Majaess *et al.* 2008, 2009b and references therein). The results are consistent (in part) with the findings of section 2.1, however, a direct comparison is not valid.

3.2. Wesenheit magnitudes

A Wesenheit diagram segregates variables into their distinct classes (Figure 4). Wesenheit magnitudes for the cluster δ Scuti stars were computed as follows:

$$W_{VI,0} = \langle V \rangle - R_{VI} (\langle V \rangle - \langle I \rangle) - \mu_0 \quad (1)$$

μ_0 is the distance modulus from Table 1 and $R_{VI} = 2.55$ is the canonical extinction law, although there are concerns with adopting a color-independent extinction law. *VI* Wesenheit magnitudes are reddening-free and comparatively insensitive to chemical composition and the width of the instability strip. The Wesenheit function is defined and discussed in the following references: Madore (1982), Opolski (1983, 1988), Madore and Freedman (1991, 2009), Kovács and Jurcsik (1997), Kovács and Walker (2001), Di Criscienzo *et al.* (2004, 2007), and Turner (2010a).

Cluster δ Scuti stars in Tables 3 and 4 are plotted on a universal *VI* Wesenheit template (Figure 4, see also Majaess *et al.* 2010). Thirty variables with distances measured by geometric means formed the calibration (Majaess *et al.* 2010, their Table 1). The sample consisted of eight SX Phe and δ Sct variables (HIP, van Leeuwen 2007), four RR Lyrae variables (HIP and HST, Benedict *et al.* 2002b; van Leeuwen 2007), two Type II Cepheids (HIP, van Leeuwen 2007), and ten classical Cepheids (HST, Benedict *et al.* 2002a, 2007). That sample was supplemented by six Type II Cepheids detected by Macri *et al.* (2006) in their comprehensive survey of the galaxy M106 (Majaess *et al.* 2009b), which features a precise geometric-based distance estimate (VLBA, Herrnstein *et al.* 1999). Type II Cepheids within the inner region of M106 were not incorporated into the calibration because of the likelihood of photometric contamination via crowding and blending (Majaess *et al.* 2009b, 2010; Majaess 2010b, see also Stanek and Udalski 1999; Mochejska *et al.* 2001; Macri *et al.* 2006; Vilardell *et al.* 2007; Smith *et al.* 2007). The stars employed were observed in the outer regions of M106 where the stellar density and surface brightness are diminished by comparison. Admittedly, it is perhaps ironic that stars 7.2 Mpc distant may be enlisted as calibrators owing to an absence of precise parallaxes for nearby objects. Additional observations of new variables in M106 are forthcoming (Macri and Riess 2009).

LMC variables catalogued by OGLE, including the latest sample of δ Scuti stars (Poleski *et al.* 2010), were added to the Wesenheit template (Figure 4, OGLE data: Udalski *et al.* 1999; Soszyński *et al.* 2002, 2003, 2008a, 2008b, 2009; see also Udalski 2009). The LMC data were calibrated with a distance established via the geometric-anchored universal Wesenheit template ($\mu_0 = 18.43 \pm 0.03$ ($\sigma\bar{x}$), Majaess *et al.* 2010). That distance agrees with a mean derived from 300+ results tabulated for the LMC at the NASA/IPAC Extragalactic Database (NED) (Madore and Steer 2007; Steer and Madore 2010 (http://nedwww.ipac.caltech.edu/level5/NED1D/intro.html, http://nedwww.ipac.caltech.edu/Library/Distances/) see also Figure 2 in Freedman and Madore 2010). Adding Turner (2010a) list of classical Cepheids in Galactic clusters to the universal *VI* Wesenheit calibration yields the same LMC distance with reduced uncertainties.

The universal Wesenheit template (Figure 4) unifies variables of the instability strip to mitigate uncertainties tied to establishing a distance scale based on Cepheids, RR Lyr, or δ Sct variables individually. Anchoring the distance scale via the universal Wesenheit template (Figure 4) mobilizes the statistical weight of the entire variable star demographic to ensure a precise distance determination. Moreover, the universal Wesenheit template may be calibrated directly via parallax and apparent magnitudes, mitigating the propagation of uncertainties tied to extinction corrections. F. Benedict and coauthors are presently acquiring HST parallaxes for additional population II variables which shall bolster the template (Feast 2008). Further calibration could likewise ensue via variables in clusters with distances secured by dynamical means or eclipsing binaries (Cluster AgeS Experiment, Pietrukowicz and Kaluzny 2004; Guinan and Engle 2006; Kaluzny *et al.* 2007), and variables in the Galactic bulge that are tied to a precise geometric-based distance (Kubiak and Udalski 2003; Eisenhauer *et al.* 2005; Reid *et al.* 2009, supported by observations from the upcoming *VVV* survey; Minniti *et al.* 2010).

Lastly, Majaess *et al.* (2010) plotted the universal Wesenheit template (Figure 4) as a function of the fundamentalized period to highlight the *first-order VI* period-magnitude continuity between RR Lyrae and Type II Cepheid variables (Matsunaga *et al.* 2006; Majaess 2009; see also Marconi and Di Criscienzo 2007 and references therein). The Wesenheit template presented here as Figure 4 is plotted as a function of the dominant period, so pulsation modes may be inferred directly from the diagram.

3.3. Pulsation mode

Wesenheit ridges in Figure 4 that define δ Scuti stars pulsating in the fundamental, first, second, and third overtone were constructed from data presented in Poleski *et al.* (2010, LMC) and Majaess *et al.* (2010, Galactic). LMC and Galactic δ Scuti stars pulsating in the overtone exhibit brighter *VI* Wesenheit magnitudes (W_{VI}) than their fundamental mode counterparts at a given period (Figure 4, or bottom panel of Figure 4 in Poleski *et al.* 2010). However, a clear separation was less evident in Garg *et al.* (2010) shorter-wavelength (*VR*) observations of LMC δ Scuti stars (their Figure 3), thereby motivating those authors to favor an alternate conclusion. The present research relies on *VI* observations of δ Scuti stars.

Estimates of the pulsation modes (order, *n*) for the cluster δ Scuti stars were inferred from the Wesenheit template (Figure 4) and are summarized in Table 4. Pulsation modes established from Wesenheit and seismological analyses for δ Scuti stars in the Pleiades, Praesepe, and M67 are comparable within the mutually expected (albeit large) uncertainties (± *n*) (Table 3). The methods identify high and low order pulsators in consistent fashion (e.g., HD23194 and HD73450, Table 3). Most small-amplitude cluster δ Scuti stars lie on Wesenheit loci characterizing n ≥ 1 pulsators (non-fundamental mode, Figure 4 and Table 4), and a sizable fraction are associated with $n = 1$ (Table4). The results are consistent with Poleski *et al.* (2010) findings and past predictions (Breger and Montgomery 2000; McNamara *et al.* 2007, and references therein).

A primary source of uncertainty associated with the analysis rests with the pulsation periods adopted. Periods for the cluster δ Scuti stars were taken from Rodríguez *et al.* (2000), the GCVS (Samus *et al.* 2009), and the AAVSO's VSX archive (Watson *et al.* 2010, http://www.aavso.org/vsx/). In several instances discrepant periods are cited and newer estimates were favored (SAO 38754, Li 2005). Efforts to extract the primary pulsation period (high SNR) for mmag δ Scuti stars in α Persei from ARO observations were unsuccessful, likely owing to increased humidity tied to summertime observations in Nova Scotia. That underscores the challenge such mmag pulsators present to low altitude observatories near sea-level. An additional source of uncertainty arises from a companion's influence on the observed Wesenheit magnitudes. The pulsation mode assigned to HD 28052, which is a spectroscopic binary and bright x-ray source, should therefore be interpreted cautiously (Table 3). A star's non-radial and multi-mode pulsation, and rotation/inclination along the line of sight likewise complicate a determination of *n* solely from the pulsation period and Wesenheit magnitude. Constraints established by Wesenheit analyses are admittedly limited by comparison to those inferred from uninterrupted space-based μmag time-series photometry (MOST, COROT, Kepler), yet the Wesenheit approach is a viable first-order tool that can be applied promptly to δ Scuti stars in any field and concurrently with other methods.

3.4. δ Sct distance to NGC 1817

A potential role for mmag δ Scuti stars as distance indicators for intermediate-age open clusters is now explored using the aforementioned framework.

Arentoft *et al.* (2005) observations of NGC 1817 indicated that the open cluster hosts a statistically desirable sample of eleven δ Scuti stars. Balaguer-Nuñez *et al.* (2004) proper motions implied that five of those stars are not cluster members (V1, V6, V8, V10, V12, see Arentoft *et al.* 2005). Yet Arentoft *et al.* (2005) concluded that eleven variables (V1–V12, excluding V10) exhibit positions in *V* vs. *B–V* and *b–y* color-magnitude diagrams consistent with δ Sct pulsation and cluster membership. A *preliminary V* vs. *V–I* color-magnitude diagram for NGC 1817 (Figure 5) confirms that most variables display positions consistent with membership (except V10). The *VI* data were obtained from the ARO and processed using ARAP (http://www.davelane.ca/aro/arap.html) (Lane 2007) and DAOPHOT (IRAF contains DAOPHOT, however a standalone newer edition can be obtained from Peter.Stetson@nrc-cnrc.gc.ca) (Stetson 1987). The ARO features an SBIG ST8XME CCD mounted upon a 35-cm telescope located near Stillwater Lake, Nova Scotia, Canada. The ARO is a remotely operated robotic observatory (Lane 2007). A description of the ARO observations for NGC 7062, including an analysis using VaST (Sokolovsky and Lebedev 2005), shall be provided in a subsequent study.

The *VI* Wesenheit diagram compiled for the δ Scuti stars (Figure 5) implies that V10, V11, and V12 either exhibit spurious data, are not *bona fide* δ Scuti stars, or are not cluster members. V10 is too faint, as corroborated by its position in the color-magnitude diagram (Figure 5). The variability detected in V11 is marred by low signal to noise and other complications (Arentoft *et al.* 2005). V12 is likewise too faint (W_{VI}) and features a period beyond that typically expected for δ Sct variables (Percy 2007). An advantage to applying the Wesenheit technique is that high and low-order pulsators may be identified. V1, V2, and V6 are likely pulsating at higher orders if the stars are members (Figure 5). V3, V4, V7, V8, and V9 are tightly clustered and may define the $n \geq 1$ boundary (Figure 5, see section 3.3). The resulting distance to NGC 1817 is $d \simeq 1.7$ kpc, assuming the aforementioned mode distribution. The δ Sct distance to NGC 1817 agrees with estimates established for the cluster by other means (Arentoft *et al.* 2005, see references therein). However, employing mmag δ Scuti stars as distance indicators for open clusters is complicated by the need for independently confirmed periods, and *a priori* knowledge of the pulsation modes or the adoption of a mode distribution ($n \geq 1$) given sizable statistics (see section 3.3). Establishing the distance to NGC 1817 or the Praesepe under the latter caveat may yield a pertinent result, yet the ensuing distance to α Persei would be in error owing to small statistics. α Persei certainly features more than three δ Scuti stars, however a detection bias emerges since nearby clusters exhibit large angular diameters which exceed the field of view of most CCDs. Continued research is needed.

4. Summary and future research

This research aimed to outline and evaluate a *VI* Wesenheit framework for investigating cluster δ Scuti stars, an analysis which relied on securing absolute Wesenheit magnitudes from precise open cluster distances. JHK_s ZAMS and color-color relations were derived from unreddened stars near the Sun with precise Hipparcos parallaxes and were applied to infer parameters for several benchmark star clusters which host δ Scuti stars (Figure 1, Table 1). That analysis yielded constraints on the absolute Wesenheit magnitudes ($W_{VI,0}$), evolutionary status, and pulsation modes (order, *n*) for the cluster δ Scuti stars (Figures 2 and 4, Tables 3 and 4). *VI* photometry for the variables were tabulated to facilitate further research (Table 4), and include new data acquired via the AAVSO's robotic telescopes (Table 2).

The JHK_s established cluster distances are bolstered by the relative insensitivity of $J–K_s$ photometry to variations in [Fe / H] and age over the baseline examined (section 2.1, Table 1, Figure 3). The deep JHK_s photometry extends into the low mass regime ($\simeq 0.4\ M_{\odot}$) and indicates that the clusters feature a common ZAMS in the infrared, and that $J–K_s$ remains constant with increasing magnitude ($M_J \gtrsim 6$) for low mass M-type dwarfs whereas *J–H* exhibits an inversion (section 2.1, Figures 1 and 2). The trends ensure precise (≤ 5%) JHK_s ZAMS fits by providing distinct anchor points in color-magnitude and color-color diagrams (Figures 1 and 2). JHK_s distances for seven of nine clusters within 250 pc agree with van Leeuwen (2009a) revised Hipparcos estimates (Table 1). However, the JHK_s distance to the Pleiades supports the HST estimate rather than that derived from Hipparcos data (Table 1). van Leeuwen (2009a, 2009b) argues in favor of the revised Hipparcos distances to open clusters and the reader is referred to that comprehensive study. Yet the distance scale can (presently) rely on a suite of clusters that are independent of the Pleiades. Models should be calibrated and evaluated using those nearby clusters where consensus exists regarding the distances (Table 1).

The general agreement between the JHK_s distances derived here and van Leeuwen (2009a) Hipparcos estimates is noteworthy (Table 1). The ~ 10–20% offset in distance for the discrepant cases (Pleiades and Blanco 1) is not atypical for studies of open clusters (Figure 2 in Paunzen and Netopil 2006; see also Dias *et al.* 2002; Mermilliod and Paunzen 2003). Several clusters feature distance estimates spanning nearly a factor of two, such as NGC 2453 (Majaess *et al.* 2007, their Table 4, ESO 096-SC04, Collinder 419, Shorlin 1, and Berkeley 44 (Turner 2011). The universal *VI* Wesenheit template could be applied to cluster δ Scuti stars so to isolate viable distance solutions, provided certain criteria are satisfied (section 3.4, e.g., sizable statistics). A Wesenheit analysis (*VI*) is a viable means for establishing pertinent constraints on a target population of δ Sct variables, particularly in tandem with other methods (Figures 2, 4, and 5, Tables 3 and 4).

5. Acknowledgements

DJM is grateful to the following individuals and consortia whose efforts and surveys were the foundation of this study: 2MASS (R. Cutri, M. Skrutskie, S. Nikolaev), OGLE (I. Soszyński, R. Poleski, M. Kubiak, A. Udalski), F. van Leeuwen, Z. Li, E. Michel, T. Arentoft, P. Stetson (DAOPHOT), B. Taylor, WebDA/GCPD (E. Paunzen, J. -C. Mermilliod), NOMAD (N. Zachrias), TASS (T. Droege, M. Sallman, M. Richmond), NED (I. Steer), PASTEL (C. Soubiran), Astrometry.net (Lang *et al.* 2010), Skiff (2010), CDS, AAVSO (M. Saladyga, A. Henden), arXiv, and NASA ADS. T. Krajci, J. Bedient, D. Welch, D. Starkey, A. Henden, and others kindly funded the AAVSO's Bright Star Monitor (BSM).

References

Alonso, A., Arribas, S., and Martinez-Roger, C. 1996, *Astron. Astrophys.*, **313**, 873.

Arentoft, T., Bouzid, M. Y., Sterken, C., Freyhammer, L. M., and Frandsen, S. 2005, *Publ. Astron. Soc. Pacific*, **117**, 601.

Artigau, É., Bouchard, S., Doyon, R., and Lafrenière, D. 2009, *Astrophys. J.*, **701**, 1534.

Artigau, É., Lamontagne, R., Doyon, R., and Malo, L. 2010, in *Observatory Operations: Strategies, Processes, and Systems III*, ed. D. R. Silva, A. B. Peck, B. T. Soifer, Proc. SPIE, 7737 (http://spiedigitallibrary.org/proceedings/resource/2/psisdg/7737/1/77371O_1?isAuthorized=no), Amer. Inst. Physics, New York.

Balaguer-Núñez, L., Jordi, C., Galadí-Enríquez, D., and Zhao, J. L. 2004, *Astron. Astrophys.*, **426**, 819.

Benedict, G. F., *et al.* 2002a, *Astron. J.*, **123**, 473.

Benedict, G. F., *et al.* 2002b, *Astron. J.*, **124**, 1695.

Benedict, G. F., *et al.* 2007, *Astron. J.*, **133**, 1810.

Bonatto, C., Bica, E., and Santos, J. F. C. 2008, *Mon. Not. Roy. Astron. Soc.*, **386**, 324.

Bono, G. 2003, in *Stellar Candles for the Extragalactic Distance Scale*, ed. D. Alloin and W. Gieren, Lecture Notes in Physics, 635, Springer, New York, 85.

Bono, G., Caputo, F., Fiorentino, G., Marconi, M., and Musella, I. 2008, *Astrophys. J.*, **684**, 102.

Bono, G., and Marconi, M. 1999, in *New Views of the Magellanic Clouds*, ed. Y. -H. Chu, N. Suntzeff, J. Hesser, and D. Bohlender, Astron. Soc. Pacific Conf. Ser., 190, Astron. Soc. Pacific, San Francisco, 527.

Breger, M., and Montgomery, M., eds. 2000, δ *Scuti and Related Stars*, Astron. Soc. Pacific Conf. Ser, 210, Astron. Soc. Pacific, San Francisco.

Catelan, M. 2009, *Astrophys. Space Sci.*, **320**, 261.

Cutri, R. M., *et al.* 2003, The IRSA 2MASS All-Sky Point Source Catalog, NASA/IPAC Infrared Science Archive (http://irsa.ipac.caltech.edu/applications/Gator/).

Dias, W. S., Alessi, B. S., Moitinho, A., and Lépine, J. R. D. 2002, *Astron. Astrophys.*, **389**, 871.

Di Criscienzo, M., Caputo, F., Marconi, M., and Cassisi, S. 2007, *Astron. Astrophys.*, **471**, 893.

Di Criscienzo, M., Marconi, M., and Caputo, F. 2004, *Astrophys. J.*, **612**, 1092.

Droege, T. F., Richmond, M. W., Sallman, M. P., and Creager, R. P. 2006, *Publ. Astron. Soc. Pacific*, **118**, 1666.

Eisenhauer, F., *et al.* 2005, *Astrophys. J.*, **628**, 246.

Feast, M. W. 2008, arXiv:0806.3019.

Fox Machado, L., Pérez Hernández, F., Suárez, J. C., Michel, E., and Lebreton, Y. 2006, *Astron. Astrophys.*, **446**, 611.

Freedman, W. L., and Madore, B. F. 2010, arXiv:1004.1856.

Garg, A., *et al.* 2010, *Astron. J.*, **140**, 328.

Guinan, E. F., and Engle, S. G. 2006, *Astrophys. Space Sci.*, 304, 5.

Henden, A. A. 2002, *J. Amer. Assoc. Var. Star Obs.*, **31**, 11.

Henden, A. A., and Kaitchuck, R. H. 1990, *Astronomical Photometry*, Willmann-Bell, Richmond.

Henden, A. A., and Munari, U. 2008, *Inf. Bull. Var. Stars*, No. 5822, 1.

Henden, A. A., and Sallman, M. P. 2007, in *The Future of Photometric, Spectrophotometric and Polarimetric Standardization*, ed. C. Sterken, Astron. Soc. Pacific Conf. Ser., 364, Astron. Soc. Pacific, San Francisco, 139.

Herrnstein, J. R., *et al.* 1999, *Nature*, **400**, 539.

Joner, M. D., Taylor, B. J., Laney, C. D., and van Wyk, F. 2006, *Astron. J.*, **132**, 111.

Kaluzny, J., Thompson, I. B., Rucinski, S. M., Pych, W., Stachowski, G., Krzeminski, W., and Burley, G. S. 2007, *Astron. J.*, **134**, 541.

Kovács, G., and Jurcsik, J. 1997, *Astron. Astrophys.*, **322**, 218.

Kovács, G., and Walker, A. R. 2001, *Astron. Astrophys.*, **371**, 579.

Kubiak, M., and Udalski, A. 2003, *Acta Astron.*, **53**, 117.

Landolt, A. U. 1983, *Astron. J.*, **88**, 439.

Landolt, A. U. 1992, *Astron. J.*, **104**, 340.

Lane, D. J. 2007, presentation made at the 96th Spring Meeting of the AAVSO, (http://www.aavso.org/aavso/meetings/spring07present/Lane.ppt; see also http://www.davelane.ca/aro/).

Lang, D., Hogg, D. W., Mierle, K., Blanton, M., and Roweis, S. 2010, *Astron. J.*, **139**, 1782.

Li, Z. P. 2005, *Astron. J.*, **130**, 1890.

Li, Z. P., and Michel, E. 1999, *Astron. Astrophys.*, **344**, L41.

Macri, L. M., and Riess, A. G. 2009, in *Stellar Pulsation: Challenges for Theory and Observation*, AIP Conf. Ser., 1170, American Institute of Physics, New York, 23.

Macri, L. M., Stanek, K. Z., Bersier, D., Greenhill, L. J., and Reid, M. J. 2006, *Astrophys. J.*, **652**, 1133.

Madore, B. F. 1982, *Astrophys. J.*, **253**, 57.

Madore, B. F., and Freedman, W. L. 1991, *Publ. Astron. Soc. Pacific*, **103**, 933.

Madore, B. F., and Freedman, W. L. 2009, *Astrophys. J.*, **696**, 1498.

Madore, B. F., and Steer, I. 2007, NASA/IPAC Extragalactic Database Master List of Galaxy Distances (http://nedwww.ipac.caltech.edu/level5/NED1D/intro.html).

Majaess, D. J. 2009, arXiv:0912.2928.
Majaess, D. J. 2010a, *Acta Astron.*, **60**, 55.
Majaess, D. J. 2010b, *Acta Astron.*, **60**, 121.
Majaess, D. J., Turner, D. G., and Lane, D. J. 2007, *Publ. Astron. Soc. Pacific*, **119**, 1349.
Majaess, D. J., Turner, D. G., and Lane, D. J. 2008, *Mon. Not. Roy. Astron. Soc.*, **390**, 1539.
Majaess, D. J., Turner, D. G., and Lane, D. J. 2009a, *Mon. Not. Roy. Astron. Soc.*, **398**, 263.
Majaess, D., Turner, D., and Lane, D. 2009b, *Acta Astron.*, **59**, 403.
Majaess, D. J., Turner, D. G., Lane, D. J., Henden, A., and Krajci, T. 2010, arXiv:1007.2300.
Marconi, M., and Di Criscienzo, M. 2007, *Astron. Astrophys.*, **467**, 223.
Matsunaga, N., *et al.* 2006, *Mon. Not. Roy. Astron. Soc.*, **370**, 1979.
McNamara, D. H., Clementini, G., and Marconi, M. 2007, *Astron. J.*, **133**, 2752.
McNamara, D. H., Madsen, J. B., Barnes, J., and Ericksen, B. F. 2000, *Publ. Astron. Soc. Pacific*, **112**, 202.
Mendoza, E. E. 1967, *Bol. Obs. Tonantzintla Tacubaya*, **4**, 149.
Mermilliod, J. -C. 1991, http://vizier.u-strasbg.fr/viz-bin/VizieR?-source=II/168.
Mermilliod, J. -C., and Paunzen, E. 2003, *Astron. Astrophys.*, **410**, 511.
Mermilliod, J. -C., Turon, C., Robichon, N., Arenou, F., and Lebreton, Y. 1997, in *Proceedings of the EAS Symposium "Hipparcos-Venice '97"*, ESA SP-402, ESA Publications Division, Noordwiijk, The Netherlands, 643.
Minniti, D., *et al.* 2010, *New Astron.*, **15**, 433.
Mochejska, B. J., Macri, L. M., Sasselov, D. D., and Stanek, K. Z. 2001, arXiv: astro-ph/0103440.
Nikolaev, S., Weinberg, M. D., Skrutskie, M. F., Cutri, R. M., Wheelock, S. L., Gizis, J. E., and Howard, E. M. 2000, *Astron. J.*, **120**, 3340.
Opolski, A. 1983, *Inf. Bull. Var. Stars*, No, 2425, 1.
Opolski, A. 1988, *Acta Astron.*, **38**, 375.
Paunzen, E., Heiter, U., Netopil, M., and Soubiran, C. 2010, *Astron. Astrophys.*, **517**, A32.
Paunzen, E., and Netopil, M. 2006, *Mon. Not. Roy. Astron. Soc.*, **371**, 1641.
Pena, J. H., *et al.* 1998, *Astron. Astrophys., Suppl. Ser.*, **129**, 9.
Percival, S. M., Salaris, M., and Groenewegen, M. A. T. 2005, *Astron. Astrophys.*, **429**, 887.
Percy, J. R. 2007, *Understanding Variable Stars*, Cambridge Univ. Press, Cambridge.
Perryman, M. A. C., European Space Agency Space Science Department, and the Hipparcos Science Team 1997, *The Hipparcos and Tycho Catalogues*, ESA SP-1200, ESA Publications Division, Noordwiijk, The Netherlands.
Petersen, J. O., and Høg, E. 1998, *Astron. Astrophys.*, **331**, 989.
Pietrukowicz, P., and Kaluzny, J. 2004, *Acta Astron.*, **54**, 19.

Pietrzyński, G., Gieren, W., Udalski, A., Bresolin, F., Kudritzki, R. -P., Soszyński, I., Szymański, M., and Kubiak, M. 2004, *Astron. J.*, **128**, 2815.

Poleski, R., *et al.* 2010, *Acta Astron.*, **60**, 1.

Reid, M. J., Menten, K. M., Zheng, X. W., Brunthaler, A., and Xu, Y. 2009, *Astrophys. J.*, **705**, 1548.

Robichon, N., Arenou, F., Lebreton, Y., Turon, C., and Mermilliod, J. C. 1999a, in *Harmonizing Cosmic Distance Scales in a Post-HIPPARCOS Era*, Astron. Soc. Pacific Conf. Ser., 167, Astron. Soc. Pacific, San Francisco, 72.

Robichon, N., Arenou, F., Mermilliod, J.-C., and Turon, C. 1999b, *Astron. Astrophys.*, **345**, 471.

Rodríguez, E., López-González, M. J., and López de Coca, P. 2000, *Astron. Astrophys., Suppl. Ser.*, **144**, 469.

Romaniello, M., *et al.* 2008, *Astron. Astrophys.*, **488**, 731.

Samus, N. N., *et al.* 2009, *General Catalogue of Variable Stars* (Samus+ 2007-2011), VizieR Online Data Catalog, 1, 2025 (http://vizier.cfa.harvard.edu/viz-bin/VizieR?-source=B/gcvs).

Sarajedini, A., Dotter, A., and Kirkpatrick, A. 2009, *Astrophys. J.*, **698**, 1872.

Skiff, B. 2010, *Catalogue of Stellar Spectral Classifications* (http://vizier.u-strasbg.fr/viz-bin/VizieR?-source=B/mk).

Skrutskie, M. F., *et al.* 2006, *Astron. J.*, **131**, 1163.

Smith, H. A. 2004, *RR Lyrae Stars*, Cambridge Univ. Press, Cambridge, 166.

Smith, M. C., Woźniak, P., Mao, S., and Sumi, T. 2007, *Mon. Not. Roy. Astron. Soc.*, **380**, 805.

Soderblom, D. R., Laskar, T., Valenti, J. A., Stauffer, J. R., and Rebull, L. M. 2009, *Astron. J.*, **138**, 1292.

Soderblom, D. R., Nelan, E., Benedict, G. F., McArthur, B., Ramirez, I., Spiesman, W., and Jones, B. F. 2005, *Astron. J.*, **129**, 1616.

Sokolovsky, K., and Lebedev, A. 2005, in *12th Young Scientists' Conference on Astronomy and Space Physics*, ed. A. Simon and A. Golovin, Kyiv Univ. Press, Kyiv, 79.

Soszyński, I., *et al.* 2002, *Acta Astron.*, **52**, 369.

Soszyński, I., *et al.* 2003, *Acta Astron.*, **53**, 93.

Soszyński, I., *et al.* 2008a, *Acta Astron.*, **58**, 293.

Soszyński, I., *et al.* 2008b, *Acta Astron.*, **58**, 163.

Soszyński, I., *et al.* 2009, *Acta Astron.*, **59**, 1.

Soubiran, C., Le Campion, J. -F., Cayrel de Strobel, G., and Caillo, A. 2010, *Astron. Astrophys.*, **515**, A111.

Stanek, K. Z., and Udalski, A. 1999, arXiv:astro-ph/9909346.

Stauffer, J. R., Hartmann, L. W., Burnham, J. N., and Jones, B. F. 1985, *Astrophys. J.*, **289**, 247.

Stauffer, J. R., Jones, B. F., Backman, D., Hartmann, L. W., Barrado y Navascués, D., Pinsonneault, M. H., Terndrup, D. M., and Muench, A. A. 2003, *Astron. J.*, **126**, 833.

Steer, I., and Madore, B. F. 2010, "NED-D: A Master List of Redshift-Independent Extragalactic Distances," (http://nedwww.ipac.caltech.edu/Library/Distances/), NASA/IPAC Extragalactic Database (NED), California Inst. of Tech., and The Observatories, Carnegie Inst. of Washington, Pasadena, CA.

Stetson, P. B. 1987, *Publ. Astron. Soc. Pacific*, **99**, 191.

Straižys, V., and Laugalys, V. 2009, *Baltic Astron.*, **18**, 141.

Taylor, B. J. 2008, *Astron. J.*, **136**, 1388.

Taylor, B. J., and Joner, M. D. 1985, *Astron. J.*, **90**, 479.

Templeton, M. R. 2009, in *The Biggest, Baddest, Coolest Stars*, ed. D. G. Luttermoser, B. J. Smith, and R. E. Stencel, Astron. Soc. Pacific Conf. Ser., 412, Astron. Soc. Pacific, San Francisco, 187.

Turner, D. G. 1979, *Publ. Astron. Soc. Pacific*, **91**, 642.

Turner, D. G. 2010a, *Astrophys. Space Sci.*, **326**, 219.

Turner, D. G. 2011, arXiv:1102.0347.

Turner, D. G., Majaess, D. J., Lane, D. J., Szabados, L., Kovtyukh, V. V., Usenko, I. A., and Berdnikov, L. N. 2009, in *Stellar Pulsation: Challenges for Theory and Observation*, AIP Conf. Ser., 1170, Amer. Inst. Physics, New York, 108.

Udalski, A. 2009, in *The Variable Universe: A Celebration of Bohdan Paczyński*, ed. K. Z. Stanek, Astron. Soc. Pacific Conf. Ser., 403, Astron. Soc. Pacific, San Francisco, 110.

Udalski A., Soszyński, I., Szymański, M., Kubiak, M., Pietrzyński, G., Woźniak, P., and Zebrun, K. 1999, *Acta Astron.*, **49**, 223.

Udalski, A., Wyrzykowski, L., Pietrzyński, G., Szewczyk, O., Szymański, M., Kubiak, M., Soszyński, I., and Zebrun, K. 2001, *Acta Astron.*, **51**, 221.

van Altena, W. F., *et al.* 1997, *Astrophys. J., Lett. Ed.*, 486, L123.

van Leeuwen, F. 1999, *Astron. Astrophys.*, **341**, L71.

van Leeuwen, F. 2007, *Astron. Astrophys.*, **474**, 653.

van Leeuwen, F. 2009a, *Astron. Astrophys.*, **497**, 209.

van Leeuwen, F. 2009b, *Astron. Astrophys.*, **500**, 505.

Vilardell, F., Jordi, C., and Ribas, I. 2007, *Astron. Astrophys.*, **473**, 847.

Watson, C., Henden, A. A., and Price, A. 2010, VizieR Online Data Catalog, 1, 2027.

Zacharias, N., Monet, D. G., Levine, S. E., Urban, S. E., Gaume, R., and Wycoff, G. L. 2004, *Bull. Amer. Astron. Soc.*, **36**, 1418.

Zhang, X. -B., Zhang, R. -X., and Li, Z. -P. 2005, *Chinese J. Astron. Astrophys.*, **5**, 579.

Table 1. Distances to benchmark open clusters.

Cluster	*HIP (M97)*	*HIP (R99)*	*HIP (V99)*	*HIP (V09)*	*JHK_s*	*HST*
M67	—	—	—	—	815 ± 40 pc	—
Hyades	—	—	—	46.45 ± 0.50 pc	47 ± 2 pc	48.3 ± 2.0 pc
Praesepe	177.0 ± 10.3 pc	180.5 ± 10.7 pc	180 pc	181.6 ± 6.0 pc	183 ± 8 pc	—
Pleiades	116.3 ± 3.3 pc	118.2 ± 3.2 pc	125 pc	120.2 ± 1.9 pc	138 ± 6 pc	134.6 ± 3.1 pc
α Persei	184.2 ± 7.8 pc	190.5 ± 7.2 pc	170 pc	172.4 ± 2.7 pc	171 ± 8 pc	—
Coma Ber.*	88.2 ± 1.7 pc	87.0 ± 1.6 pc	86 pc	86.7 ± 0.9 pc	85 ± 6 pc	—
Blanco 1	252.5 ± 31.1 pc	263 ± 31 pc	190 pc	207 ± 12 pc	240 ± 10 pc	—
IC 2391*	147.5 ± 5.4 pc	146.0 ± 4.7 pc	140 pc	144.9 ± 2.5 pc	134 ± 13 pc	—
IC 2602*	146.8 ± 4.7 pc	152 ± 3.7 pc	155 pc	148.6 ± 2.0 pc	147 ± 14 pc	—
NGC 2451*	—	188.7 ± 6.8 pc	220 pc	183.5 ± 3.7 pc	189 ± 15 pc	—

Notes: Hipparcos (HIP) distances from Mermilliod et al. (1997, M97), Robichon et al. (1999a, R99), van Leeuwen (1999, V99), and van Leeuwen (2009a, V09). HST distances to the Hyades and Pleiades from van Altena eta al. (1997) and Soderblom et al. (2005). JHK_s results from this study. Clusters highlighted by an asterisk were more difficult to assess (JHK_s). Iron abundances and age estimates for the clusters are tabulated in Mermilliod et al. (1997), and van Leeuwen (1999).

Table 2. New photometry for cluster δ Scuti stars.

Star	*Cluster*	*CMD position (Figure 2)*	*V*	*V–Ic*
EX Cnc	M67	BS	10.90	0.30
EW Cnc	M67	BS	12.24	0.30
HD 23156	Pleiades	MS	8.23	0.28
HD 23194	Pleiades	MS	8.08	0.20
HD 23567	Pleiades	MS	8.29	0.41
HD 23607	Pleiades	MS	8.25	0.27
HD 23628	Pleiades	MS, BR	7.69	0.24
HD 23643	Pleiades	MS, BR	7.79	0.16

Notes: magnitudes are means of observations acquired from the AAVSO's BSM, NOFS, TASS (Droege et al. 2006), and Mendoza (1967). The identifiers are as follows: stars occupying the blue straggler region (BS), binary / rapid rotator sequence (BR), and main-sequence (MS) of the color-magnitude diagram (Figure 2).

Table 3. A comparison of δ Sct pulsation modes.

Star	*Cluster*	*n*(W_{VI})	*n*	*Source*
EX Cnc	M67	> 3	3	Z05
EW Cnc	M67	1 or 0	0	Z05
HD 23156	Pleiades	1	0	F06
HD 23194	Pleiades	> 3	4	F06
HD 23567	Pleiades	1 or 2	0	F06
HD 23607	Pleiades	1	0	F06
HD 23628	Pleiades	1	0	F06
HD 23643	Pleiades	1 or 0	0	F06
HD 73175	Praesepe	> 3	3	P98
HD 73450	Praesepe	1	1	P98
HD 73575	Praesepe	≥ 3	3/?	P98
HD 73576	Praesepe	≥ 3	3	P98
HD 73763	Praesepe	> 3	3/?	P98
HD 74028	Praesepe	≥ 3	3	P98

Notes: pulsation modes (primary signal, order n) inferred for M67, Pleiades, and Praesepe δ Scuti stars from the Wesenheit template (Figure 4, n(W_{VI})) and sources in the literature (n). Sources are Zhang et al. (2005, Z05), Fox Machado et al. (2006, F06), and Pena et al. (1998, P98).

Table 4. δ Scuti stars in benchmark open clusters.

Star	*Cluster*	*CMD position (Figure 2)*	*n* (W_{VI})	*VI Photometry*
SAO 38754	α Persei	MS	1	TASS, S85
HD 20919	α Persei	MS, BR:	2 or 3	TASS
HD 21553	α Persei	MS	0	TASS
HD 23156	Pleiades	MS	1	Table 2
HD 23194	Pleiades	MS	> 3	Table 2
HD 23567	Pleiades	MS	1 or 2	Table 2
HD 23607	Pleiades	MS	1	Table 2
HD 23628	Pleiades	MS, BR	1	Table 2
HD 23643	Pleiades	MS, BR	1 or 0	Table 2
HD 27397	Hyades	EV	1 or 2	T85
HD 27459	Hyades	EV	1	J06
HD 27628	Hyades	sat./EV:	1	J06
HD 28024	Hyades	sat./EV:	1 or 0	J06
HD 28052	Hyades	sat./EV:	0	J06
HD 28319	Hyades	sat./EV:	> 3	J06
HD 30780	Hyades	sat.	> 3	J06
HD 73175	Praesepe	MS/EV	> 3	TASS, ME67
HD 73345	Praesepe	MS/EV	> 3	TASS, ME67
HD 73450	Praesepe	MS	1	TASS, ME67
HD 73575	Praesepe	EV	≥ 3	TASS, ME67
HD 73576	Praesepe	MS/EV, BR	≥ 3	TASS, ME67
HD 73712	Praesepe	EV	1 or 2	TASS, ME67
HD 73729	Praesepe	MS/EV, BR	2 or 3	TASS, ME67
HD 73746	Praesepe	MS	1	TASS, ME67
HD 73763	Praesepe	MS/EV	> 3	TASS, ME67
HD 73798	Praesepe	MS/EV	1	TASS, ME67
HD 73819	Praesepe	EV	0	TASS, ME67
HD 73890	Praesepe	MS/EV, BR	> 3	TASS, ME67
HD 74028	Praesepe	MS/EV	≥ 3	TASS, ME67
HD 74050	Praesepe	MS/EV	3	TASS, ME67
EX Cnc	M67	BS	> 3	Table 2
EW Cnc	M67	BS	1 or 0	Table 2

Notes: δ Sct cluster list compiled primarily from Li and Michel (1999) and references therein. The identifiers are as follows: stars occupying the blue straggler region (BS), binary/rapid rotator sequence (BR), evolved region (EV), and main-sequence (MS) of the color-magnitude diagram (Figure 2); Pulsation modes (primary signal, order n) inferred for the δ Scuti stars from the VI Wesenheit template (Figure 4). Hyades members may feature saturated (sat.) 2MASS photometry owing to their proximity (Table 1). There are concerns regarding the photometric zero-point for bright δ Scuti stars sampled in the all-sky surveys (Henden and Sallman 2007). References for the photometry are Mendoza (1967, ME67), Taylor and Joner (1985, T85), Stauffer et al. (1985, S85), and Joner et al. (2006, J06).

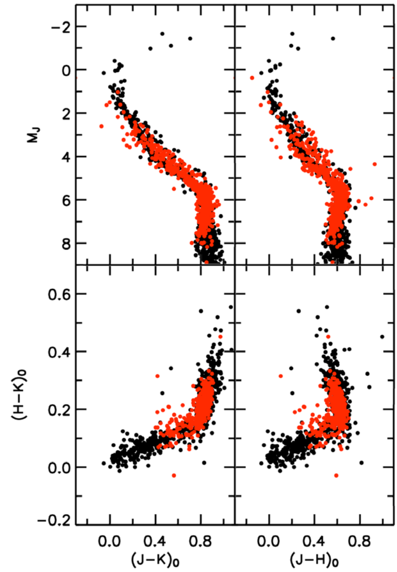

Figure 1. Deep 2MASS *JHK*$_s$ color-magnitude and color-color diagrams for the calibration (red dots) and Praesepe star cluster (black dots). Likely members of the Praesepe were selected on the basis of proper motions (NOMAD). The resulting parameters are $E(J–K_s) = 0.025 \pm 0.015$ and $d = 183 \pm 8$ pc.

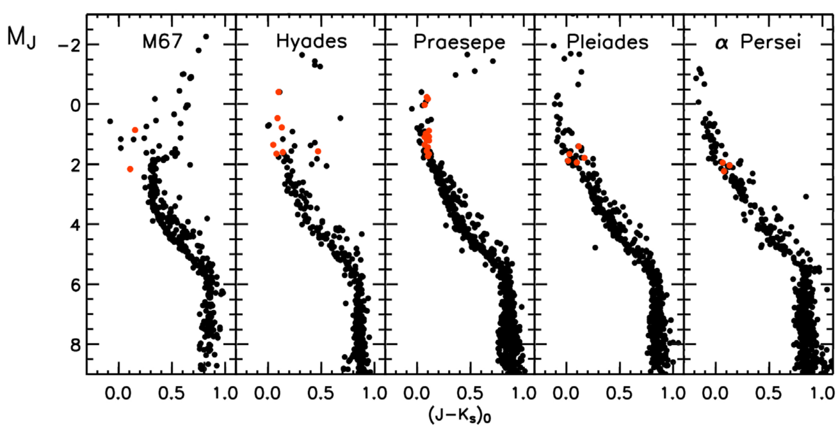

Figure 2. Deep 2MASS *JHK*$_s$ color-magnitude diagrams for M67, Hyades, Praesepe, Pleiades, and α Persei star clusters. The clusters feature a common ZAMS morphology in the infrared. The δ Scuti stars examined in section 3 (red dots) may be evolved (Hyades/Praesepe), blue stragglers (M67), or occupy the binary/rapid rotator sequence (Pleiades).

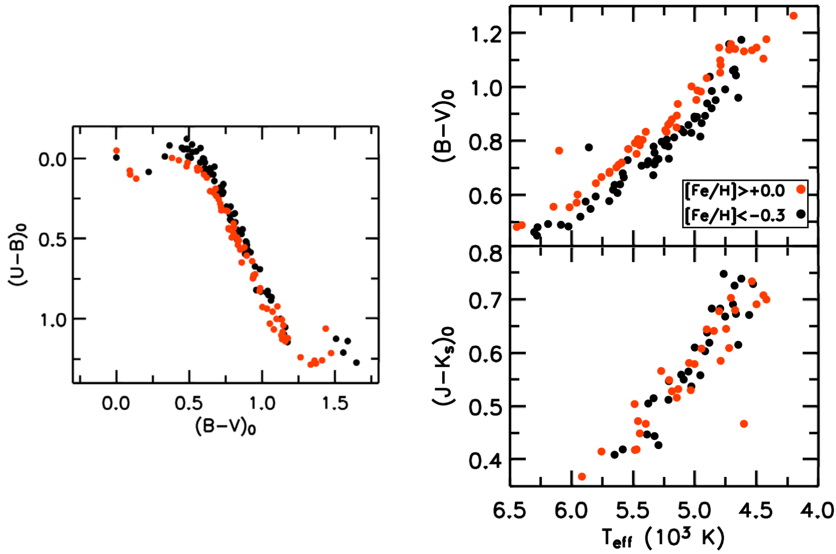

Figure 3. Semi-empirical color-T_e – [Fe/H] correlation for calibration stars (Figure 1) featured in PASTEL. Red and black dots indicate metal-rich and metal-poor stars accordingly. *B–V* and *U–B* color indices appear sensitive to metallicity, whereas *J–K*$_s$ is comparatively unaffected by changes in iron abundance (see text).

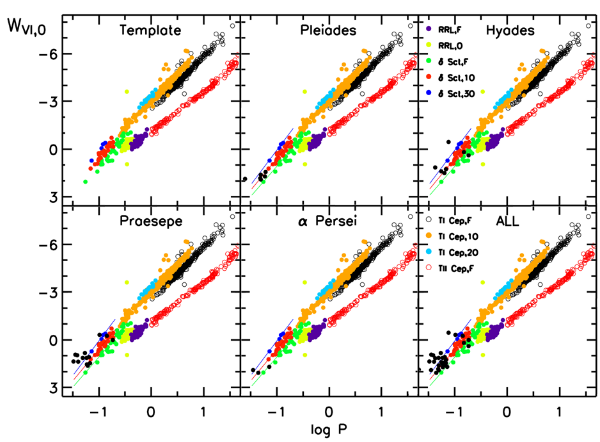

Figure 4. A calibrated universal *VI* Wesenheit template constructed from data presented in Majaess *et al.* (2010) and the latest OGLE*III* observations (e.g. Poleski *et al.* 2010). The cluster δ Scuti stars are displayed as black dots. Wesenheit magnitudes were computed via Equation 1 using the *JHK*$_s$ established cluster distances and *VI* photometry highlighted in Tables 1 and 4 accordingly. First-order constraints on the inferred pulsation modes (n) are listed in Tables 3 and 4.

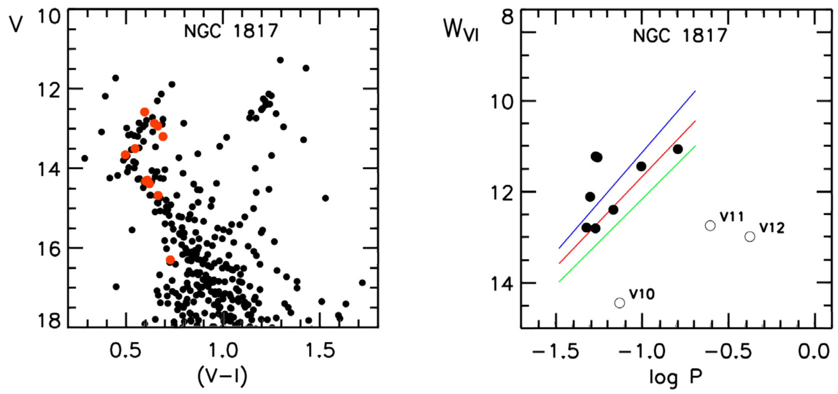

Figure 5, Left, a *preliminary VI* color-magnitude diagram for the open cluster NGC 1817 compiled from ARO observations. A subsample of Arentoft *et al.* 2005 list of δ Scuti stars are highlighted by red dots. Right, the δ Scuti stars are featured in a Wesenheit diagram where green, red, and blue ridges correspond to $n = 0, 1, 3$ pulsators accordingly (right to left). The offset from the absolute Wesenheit magnitudes (Figure 4) yields d $\simeq$ 1.7 kpc, assuming the variables define the n $\geq$ 1 boundary (see section 3.3).

Call for Papers

Aaron Price
AAVSO Headquarters, 49 Bay State Road, Cambridge, MA 02138; aaronp@aavso.org

The AAVSO and Citizen Sky invite you to contribute an article to a special issue of *JAAVSO* with a focus on ε Aurigae, similar objects, and development of new observing techniques of bright stars. All articles must present new material and conclusions in a scholarly manner and will be peer-reviewed by professionals and other experts in the field.

Sample topics span the range of the scientific method and may include: analysis of personal observations, analysis of data from the AAVSO International Database, development of an innovative observation technique or technology, review papers, historical investigation, public outreach strategies, and so forth.

We also encourage papers on scientific objects similar to ε Aurigae, such as objects that eclipse and exist in dusty environments. Please feel free to e-mail the editor of the Journal for advice as to whether a particular topic is acceptable.

Assistance is available for those new to writing scholarly, refereed publications. Presentations and videos describing how to structure papers, conduct literature reviews, format figures, and so on are available at the AAVSO's web site. Upon request, we can also assign a professional liaison to look over your drafts and make suggestions. If this is desired, please make such a request as early in your paper's development as possible.

Authors—Anyone may submit articles to *JAAVSO*. Membership in the AAVSO or participation in the Citizen Sky project is not required. Publication is free for this special issue, thanks to support from the National Science Foundation. Please note in your cover letter that this submission is for the special issue on ε Aurigae.

Submission guidelines, sample articles, a suggested article outline, and videos about authoring scientific publications are all available via the AAVSO web site at http://www.aavso.org/jaavso-call-papers .

Deadlines—The issue is scheduled for publication on December 15, 2012. We highly encourage authors to submit by March 1, 2012, to insure sufficient time for the referee and revision process. Upon request, papers that contain timely content may be published in electronic form prior to December 15.

Contact aavso@aavso.org with any questions.

Index to Volume 39

Author

Subject

NOTES